

ADA 083436

12 LEVEL III

AD-E430 391

AD

CONTRACT REPORT ARBRL-CR-00413

POST-TEST BLAST RESPONSE ANALYSES  
OF DICE THROW VEHICLES

Prepared by

Kaman AviDyne  
A Division of Kaman Sciences Corporation  
83 Second Avenue  
Burlington, MA 01803

January 1980

DTIC  
ELECTE  
APR 23 1980  
S D  
B



US ARMY ARMAMENT RESEARCH AND DEVELOPMENT COMMAND  
BALLISTIC RESEARCH LABORATORY  
ABERDEEN PROVING GROUND, MARYLAND

Approved for public release; distribution unlimited.

DMG FILE COPY

80 3 27 025

Destroy this report when it is no longer needed.  
Do not return it to the originator.

Secondary distribution of this report by originating  
or sponsoring activity is prohibited.

Additional copies of this report may be obtained  
from the National Technical Information Service,  
U.S. Department of Commerce, Springfield, Virginia  
22151.

The findings in this report are not to be construed as  
an official Department of the Army position, unless  
so designated by other authorized documents.

*The use of trade names or manufacturers' names in this report  
does not constitute endorsement of any commercial product.*

## UNCLASSIFIED

SECURITY CLASSIFICATION OF THIS PAGE (When Data Entered)

REPORT DOCUMENTATION PAGE		READ INSTRUCTIONS BEFORE COMPLETING FORM
1. REPORT NUMBER CONTRACT REPORT ARBRL-CR-00413	2. GOVT ACCESSION NO. AD-A083 436	3. RECIPIENT'S CATALOG NUMBER
4. TITLE (and Subtitle) POST-TEST BLAST RESPONSE ANALYSES OF DICE THROW VEHICLES	5. TYPE OF REPORT & PERIOD COVERED Final Report 26 Jul 77 - 1 Mar 78	
7. AUTHOR(s) Kenneth R. Wetmore	6. PERFORMING ORG. REPORT NUMBER KA TR-150	
9. PERFORMING ORGANIZATION NAME AND ADDRESS Kaman AviDyne A Division of Kaman Sciences Corporation 83 Second Avenue Burlington, MA 01803	10. PROGRAM ELEMENT, PROJECT, TASK AREA & WORK UNIT NUMBERS	
11. CONTROLLING OFFICE NAME AND ADDRESS US Army Armament Research & Development Command US Army Ballistic Research Laboratory (DRDAR-BL) Aberdeen Proving Ground, MD 21005	12. REPORT DATE JANUARY 1980	
14. MONITORING AGENCY NAME & ADDRESS (if different from Controlling Office)	13. NUMBER OF PAGES 123	
	15. SECURITY CLASS. (of this report) UNCLASSIFIED	
	16a. DECLASSIFICATION/DOWNGRADING SCHEDULE	
16. DISTRIBUTION STATEMENT (of this Report) Approved for public release; distribution unlimited.		
17. DISTRIBUTION STATEMENT (of the abstract entered in Block 20, if different from Report)		
18. SUPPLEMENTARY NOTES This research was sponsored by the U.S. Army Project DA No. 1L162118AH75, AMCMC Code 632306.11.H7200, Nuclear Weapons Effects for Army Applications, Blast and Shock.		
19. KEY WORDS (Continue on reverse side if necessary and identify by block number) DICE-THROW Test Blast Response Vehicles		
20. ABSTRACT (Continue on reverse side if necessary and identify by block number) This report summarizes the results of a blast response study of select truck configurations fielded in the DICE THROW test. Using the TRUCK computer code, the response time-histories of four different Army wheeled vehicle systems exposed to both blast overpressure and dynamic pressure loadings were obtained. Important motions of the total systems subsequent to blast wave interception, particularly vehicle overturning, are plotted.		

FOREWORD

This work was performed for Ballistic Research Laboratory under Contract Number DAAD05-74-C-0744 by Kaman AviDyne, Burlington, Mass., a division of Kaman Sciences Corporation. The technical monitor for BRL was Dr. W. Don Allison. Mr. Kenneth R. Wetmore was the project leader and principal investigator of the study which was performed in the Structural Mechanics Group, headed by Mr. E. S. Criscione, of Kaman AviDyne.

The author is indebted to Messrs. R. Raley, G. Teel, N. Ethridge and Dr. W. Shuman, Jr. of BRL, and to Mr. J. Endicott of MTD, APG for providing data relevant to the analyses reported herein. The assistance of Dr. J. Ray Ruetenik and Mr. William N. Lee of Kaman AviDyne in configuring the DICE THROW experimental pressure time-history data to the TRUCK computer code aerodynamic loading requirements is also gratefully acknowledged.

DTIC  
SELECTED  
APR 23 1980

ACCESSION for			
NTIS	White Section <input checked="" type="checkbox"/>		
DDC	Buff Section <input type="checkbox"/>		
UNANNOUNCED <input type="checkbox"/>			
JUSTIFICATION			
BY			
DISTRIBUTION/AVAILABILITY CODES			
DISP.	AVAIL.	ADM.	SPECIAL
A			

## FOREWORD

This work was performed for Ballistic Research Laboratory under Contract Number DAAD05-74-C-0744 by Kaman AviDyne, Burlington, Mass., a division of Kaman Sciences Corporation. The technical monitor for BRL was Dr. W. Don Allison. Mr. Kenneth R. Wetmore was the project leader and principal investigator of the study which was performed in the Structural Mechanics Group, headed by Mr. E. S. Criscione, of Kaman AviDyne.

The author is indebted to Messrs. R. Raley, G. Teel, N. Ethridge and Dr. W. Shuman, Jr. of BRL, and to Mr. J. Endicott of MTD, APG for providing data relevant to the analyses reported herein. The assistance of Dr. J. Ray Ruetenik and Mr. William N. Lee of Kaman AviDyne in configuring the DICE THROW experimental pressure time-history data to the TRUCK computer code aerodynamic loading requirements is also gratefully acknowledged.

DTIC  
ELECTE  
S APR 23 1980 D  
B

ACCESSION for	
NTIS	White Section <input checked="" type="checkbox"/>
DDC	Buff Section <input type="checkbox"/>
UNANNOUNCED <input type="checkbox"/>	
JUSTIFICATION _____	
BY _____	
DISTRIBUTION/AVAILABILITY CODES	
Dist. Avail. and/or Special	
A	

## TABLE OF CONTENTS

	<u>Page</u>
FOREWORD . . . . .	3
LIST OF ILLUSTRATIONS. . . . .	7
1. INTRODUCTION. . . . .	9
2. VEHICLE SYSTEM CONFIGURATIONS . . . . .	11
2.1 Introduction . . . . .	11
2.2 M35A2 Truck Configurations . . . . .	11
2.3 M38A1 Jeep Configuration . . . . .	13
3. TRUCK COMPUTER CODE . . . . .	15
3.1 Introduction . . . . .	15
3.2 Capabilities of the Code . . . . .	15
3.3 Input Data Requirements. . . . .	16
4. VEHICLE SYSTEM MECHANICAL MODELS. . . . .	19
4.1 Introduction . . . . .	19
4.2 M35A2 Truck Configurations . . . . .	19
4.3 M38A1 Jeep Configuration . . . . .	23
5. VEHICLE SYSTEM AERODYNAMIC MODELS . . . . .	25
5.1 Introduction . . . . .	25
5.2 M35A2 Truck Configurations . . . . .	25
5.3 M38A1 Jeep Configuration . . . . .	26
6. VEHICLE SYSTEM AERODYNAMIC LOADS. . . . .	27
6.1 Introduction . . . . .	27
6.2 DICE THROW Experimental Overpressure Data. . . . .	27
6.3 Analytical Overpressure and Dynamic Pressure Data. . . . .	27
7. TRUCK RESPONSE ANALYSES RESULTS . . . . .	41
7.1 Introduction . . . . .	41
7.2 TRUCK Response Analysis Parameters . . . . .	41
7.3 M38A1 Jeep Response Results. . . . .	41
7.4 M35A2 Truck Response Results . . . . .	48

TABLE OF CONTENTS (CONT'D)

	<u>Page</u>
APPENDIX A    INPUT DATA LIST FOR TRUCK CODE - M35A2 TRUCK, EMPTY . . . . .	73
APPENDIX B    INPUT DATA LIST FOR TRUCK CODE - M35A2 TRUCK, LOADED, WITH CANVAS . . . . .	81
APPENDIX C    INPUT DATA LIST FOR TRUCK CODE - M35A2 TRUCK, WITH S280 SHELTER . . . . .	89
APPENDIX D    INPUT DATA LIST FOR TRUCK CODE - M38A1 JEEP . . . .	97
APPENDIX E    INPUT DATA LIST FOR TRUCK CODE - M35A2 TRUCK, LOADED, WITHOUT CANVAS. . . . .	105
DISTRIBUTION LIST. . . . .	113

LIST OF ILLUSTRATIONS

<u>Figure</u>		<u>Page</u>
1.	M35A2 Truck . . . . .	12
2.	M38A1 Jeep. . . . .	14
3.	Schematic of S280 Shelter in M35A2 Truck. . . . .	21
4.	Schematic of Concrete Blocks in M35A2 Truck . . . . .	22
5.	Experimental Overpressure Time-History at Gage Station 324-2 . . . . .	28
6.	Experimental Overpressure Time-History at Gage Station 324-3 . . . . .	29
7.	Experimental Overpressure Time-History at Gage Station 322-3 . . . . .	30
8.	Experimental Overpressure Time-History at Gage Station 322-2 . . . . .	31
9.	Experimental Overpressure Time-History at Gage Station 223 . . . . .	32
10.	C.G. Margin Time-History for M38A1 Jeep Subjected to 12.9 psi Incident Overpressure (88.9 kPa). . . . .	42
11.	Roll Angle Time-History for M38A1 Jeep Subjected to 12.9 psi Incident Overpressure (88.9 kPa). . . . .	43
12.	Lateral C.G. Displacement Time-History for M38A1 Jeep Subjected to 12.9 psi Incident Overpressure (88.9 kPa)	44
13.	C.G. Margin Time-History for M38A1 Jeep Subjected to 21.9 psi Incident Overpressure (151.0 kPa) . . . . .	45
14.	Roll Angle Time-History for M38A1 Jeep Subjected to 21.9 psi Incident Overpressure (151.0 kPa) . . . . .	46
15.	Lateral C.G. Displacement Time-History for M38A1 Jeep Subjected to 21.9 psi Incident Overpressure (151.0 kPa)	47
16.	C.G. Margin Time-History for M35A2 Empty Truck Subjected to 13.9 psi Incident Overpressure (95.8 kPa)	49
17.	Roll Angle Time-History for M35A2 Empty Truck Subjected to 13.9 psi Incident Overpressure (95.8 kPa) . . . . .	50
18.	Lateral C.G. Displacement Time-History for M35A2 Empty Truck Subjected to 13.9 psi Incident Overpressure (95.8 kPa) . . . . .	51
19.	C.G. Margin Time-History for M35A2 Empty Truck Subjected to 21.6 psi Incident Overpressure (148.9 kPa)	52
20.	Roll Angle Time-History for M35A2 Empty Truck Subjected to 21.6 psi Incident Overpressure (148.9 kPa) . . . . .	53
21.	Lateral C.G. Displacement Time-History for M35A2 Empty Truck Subjected to 21.6 psi Incident Overpressure (148.9 kPa) . . . . .	54

LIST OF ILLUSTRATIONS (CONT'D)

<u>Figure</u>		<u>Page</u>
22.	C.G. Margin Time-History for Restrained M35A2 Loaded Truck Subjected to 12.9 psi Incident Overpressure (88.9 kPa) . . . . .	56
23.	Roll Angle Time-History for Restrained M35A2 Loaded Truck Subjected to 12.9 psi Incident Overpressure (88.9 kPa) . . . . .	57
24.	Lateral C.G. Displacement Time-History for Restrained M35A2 Loaded Truck Subjected to 12.9 psi Incident Overpressure (88.9 kPa) . . . . .	58
25.	C.G. Margin Time-History for Unrestrained M35A2 Loaded Truck Subjected to 12.9 psi Incident Overpressure (88.9 kPa) . . . . .	59
26.	Roll Angle Time-History for Unrestrained M35A2 Loaded Truck Subjected to 12.9 psi Incident Overpressure (88.9 kPa) . . . . .	60
27.	Lateral C.G. Displacement Time-History for Unrestrained M35A2 Loaded Truck Subjected to 12.9 psi Incident Overpressure (88.9 kPa) . . . . .	61
28.	C.G. Margin Time-History for Restrained M35A2 Loaded Truck Subjected to 21.9 psi Incident Overpressure (151.0 kPa) . . . . .	63
29.	Roll Angle Time-History for Restrained M35A2 Loaded Truck Subjected to 21.9 psi Incident Overpressure (151.0 kPa) . . . . .	64
30.	Lateral C.G. Displacement Time-History for Restrained M35A2 Loaded Truck Subjected to 21.9 psi Incident Overpressure (151.0 kPa) . . . . .	65
31.	C.G. Margin Time-History for Unrestrained M35A2 Loaded Truck Subjected to 21.9 psi Incident Overpressure (151.0 kPa) . . . . .	66
32.	Roll Angle Time-History for Unrestrained M35A2 Loaded Truck Subjected to 21.9 psi Incident Overpressure (151.0 kPa) . . . . .	67
33.	Lateral C.G. Displacement Time-History for Unrestrained M35A2 Loaded Truck Subjected to 21.9 psi Incident Overpressure (151.0 kPa) . . . . .	68
34.	C.G. Margin Time-History for M35A2 Truck Carrying S-280 Shelter . . . . .	69
35.	Roll Angle Time-History for M35A2 Truck Carrying S-280 Shelter . . . . .	70
36.	Lateral C.G. Displacement Time-History for M35A2 Truck Carrying S-280 Shelter . . . . .	71

## SECTION 1

### INTRODUCTION

The response of tracked and wheeled vehicles to blast waves in a tactical nuclear warfare scenario is of considerable interest to military planners. In order to predict such response, Kaman AviDyne previously developed for the U.S. Army Ballistic Research Laboratory a complex computer program called TRUCK.

The TRUCK program, Reference 1, was originally developed to analyze the blast response of either a soft- or hard-mounted communications shelter on a truck, including either soft- or hard-mounted equipment racks within the shelter. As such, both gross motions of the truck, including vehicle overturning, and motions of the shelter and its internal equipment relative to the vehicle body are considered in the program response through inclusion of the necessary multiple degrees of freedom. For less complex dynamic models involving a smaller number of degrees of freedom, the code retains its inherent ability to predict blast-induced system response but with a reduction both in modeling requirements and computer running time.

In the study presently being reported, the TRUCK program was applied to the analysis of four different Army wheeled vehicle systems exposed to blast loading in the DICE THROW field test. During this event, which took place on 6 October 1976 at the White Sands Missile Range, New Mexico, the Ballistic Research Laboratory conducted projects concerned with determining the response of communication systems and a number of vehicles to the blast loading. Additionally, the Ballistic Research Laboratory performed measurements to document the air blast phenomena, and the measured pressure time histories were the basis of the aerodynamic loadings employed in the TRUCK analyses. Three of the vehicle systems studied were different load configurations of a 2 1/2-ton M35A2 cargo truck while the fourth system examined was a 1/4-ton M38A1 utility truck, commonly referred to as a jeep.

Three of the four wheeled vehicle systems were analyzed for two different incident pressure levels and two different vehicle restraint conditions in order to simulate the actual conditions experienced by the systems in DICE THROW. The fourth vehicle system was analyzed only at one incident pressure level and one restraint condition.

---

Reference 1. Hobbs, N.P., et al, TRUCK-A Digital Computer Program for Calculating the Response of Army Vehicles to Blast Waves, Kaman AviDyne TR-136, March, 1977.

In Section 2, a discussion of the various vehicle and loading configurations analyzed in this study is presented. A brief overview of the TRUCK computer code capabilities and input data requirements is included in Section 3. Sections 4 and 5 describe the mechanical and aerodynamic models, respectively, developed for the various vehicle system configurations analyzed. The aerodynamic loads employed in the TRUCK response runs for the various vehicle systems are included in Section 6, and Section 7 presents the results of the TRUCK analyses. Finally, Appendices A to E contain the TRUCK code input data listings for the system configurations analyzed.

## SECTION 2

### VEHICLE SYSTEM CONFIGURATIONS

#### 2.1 Introduction

As stated in Section 1, blast response analyses of four different Army wheeled vehicle systems exposed to blast in the DICE THROW field test were conducted in the presently reported study. Three of these wheeled vehicle systems were basically M35A2 cargo trucks with different load configurations, while the fourth vehicle was an M38A1 utility truck often referred to as an M38A1 jeep.

#### 2.2 M35A2 Truck Configurations

The configurations of the truck systems to be analyzed were specified in References 2 and 3 as (1) an M35A2C truck with an S-280 communications shelter tied down in the cargo body, (2) an M35 truck with stake sides but no load in the cargo body, and (3) an M35 truck with canvas top raised over the cargo body and loaded with concrete blocks to simulate cargo. All three configurations were specified as including no winch on the vehicle.

Figure 1, which was used as a guide in formulating the computer models, is an unaltered copy of an original drawing of the 2 1/2-ton, M35A2 cargo truck and shows the basic truck dimensions. Attempts at differentiating between the major characteristics and dimensions of the M35, M35A2 and M35A2C truck versions were, as a whole, unsuccessful and the minor dimensional differences which were determined were considered to be relatively unimportant. Consequently, the primary configuration of the M35A2 truck without winch, as dimensioned in Figure 1, was employed as a base for configuring the three truck versions to be analyzed.

The major components of the M35A2 truck are the cab, the engine, the cargo body, the frame or chassis which supports those three components, and the running gear. Of these major components, only the cab and the cargo body can be reconfigured.

The top of the cab above the doors is a supported canvas structure which is removable, and the cab windshield may be either erect or folded down onto the top of the engine hood when the cab top is removed. The cargo body bed is solid structure at the front and sides and extends vertically approximately 14 inches (.36m) above the cargo bed floor. The rear of the cargo bed may be either open or closed, depending upon

---

Reference 2. Contract "Scope of Work" Statement.

Reference 3. Wheeled vehicle and shelter physical data contained in private communication from Noel Ethridge of BRL in Spring, 1977.

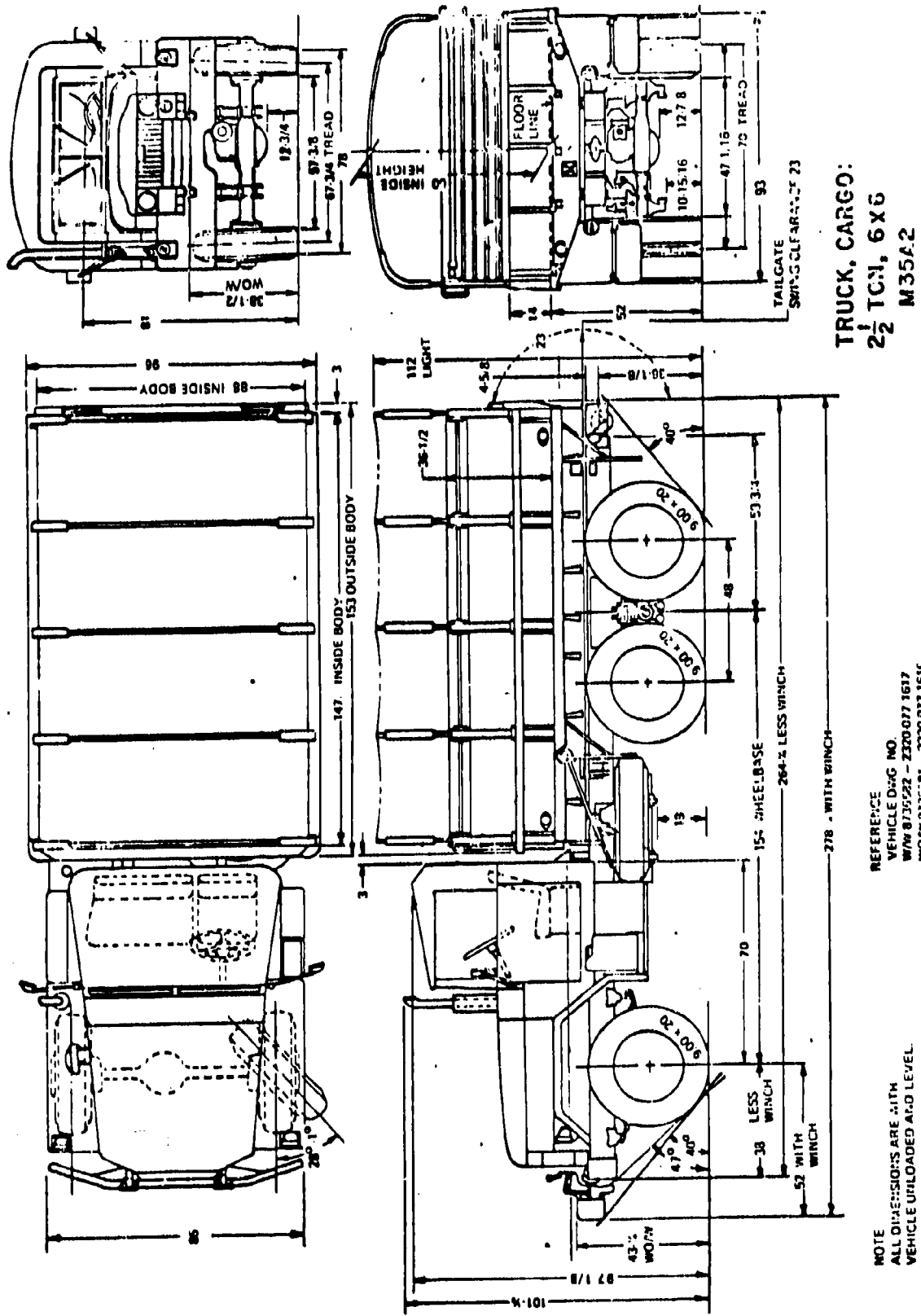


FIGURE 1. M35A2 TRUCK

**TRUCK, CARGO:**  
**2 1/2 TON, 6 X 6**  
**M35A2**

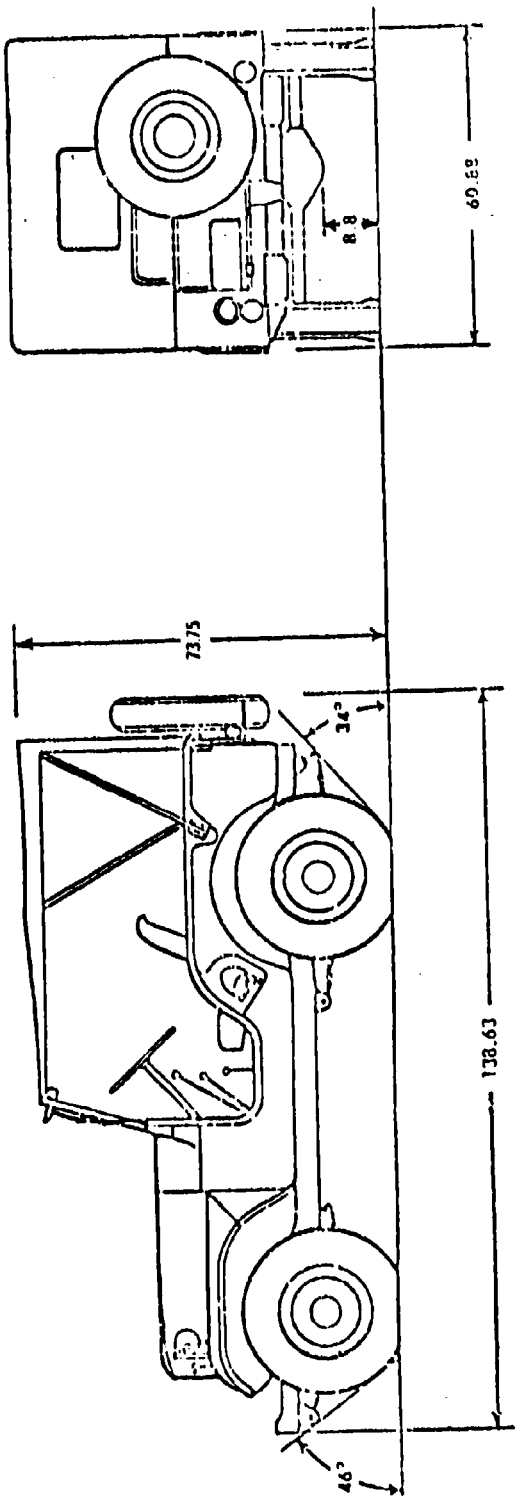
whether the movable tailgate is down or up. Although not clearly indicated in Figure 1, the cargo body may be reconfigured with stake sides such that both the front and sides of the truck are enclosed by gapped longitudinal slats attached to vertical stakes which extend to a height of approximately 36 1/2 inches (.93m) above the cargo bed floor. Additionally, with the insertion of bowed support frames above the stake sides, a canvas top may be added which completely encloses the cargo body on the front and sides and leaves only a small opening at the rear of the truck.

As analyzed in this study, then, all three of the previously mentioned truck configurations from the top of the cab door and the top of the cargo body bed downward, which represents the unchangeable portions of the vehicle, were identical and as shown in Figure 1. Additionally, for all three configurations the cab side windows were open, the windshield was erect, and the cargo body tailgate was in an up position. For configuration (1), the only addition to this base configuration was an S-280 shelter tied down in the cargo bed. No canvas top on the cab was included in configuration (1). Configuration (2) included the canvas top on the cab, no load in the cargo body bed, but the slatted stake sides were erected on the cargo body. Configuration (3) also included the canvas top on the cab, a 5300 pound (2404 kg) load of concrete blocks and supporting timbers rested on the cargo bed floor, and the canvas top was erected to enclose the cargo body.

### 2.3 M38A1 Jeep Configuration

Unlike the three different M35A2 truck configurations requiring analysis, only one basic configuration of the M38A1 jeep was analyzed. As specified in Reference 2, the basic configuration to be examined was the jeep empty, with no canvas.

The specification of jeep empty indicated that no cargo was onboard the vehicle and the specification of no canvas indicated that neither the removable canvas top nor the removable canvas side curtains were on the vehicle. Figure 2 portrays the 1/4-ton M38A1 jeep with canvas top erected but without the side curtains. The basic configuration of the jeep so analyzed, then, was as shown in Figure 2 but with the canvas top removed from the vehicle. The possibility that the windshield was folded down onto the hood, achievable only in the no canvas condition, in the DICE THROW field test is of negligible importance as will be indicated later in the report.



NOTE: DIMENSIONS IN INCHES

FIGURE 2. M38A1 JEEP

## SECTION 3

### TRUCK COMPUTER CODE

#### 3.1 Introduction

The computer code which was employed to analyze the response of the vehicles discussed in Section 2 to blast exposure in DICE THROW was the TRUCK computer code. Within this section, only an overview of the capabilities and input requirements of the code will be presented. Reference 1, Kaman AviDyne's report on the development of TRUCK, should be referred to for explicit details of the program.

#### 3.2 Capabilities of the Code

The TRUCK code was formulated basically to have the capability of analyzing the response of a truck-mounted communications shelter exposed to a blast wave. In its simplest concept, therefore, consideration had to be given to items such as the non-linearity of the vehicle suspension system and the complex tire-ground interaction effects. Required consideration of the possibility of either or both of the shelter and its internal equipment racks being soft-mounted instead of rigidly attached added to the program development complexity. Additional consideration of all or part of the vehicle lifting off the ground or even overturning, as well as consideration of both the diffraction and drag loading phases of an arbitrarily oriented blast wave, further increased the program scope.

As finally developed, the code has the capability of analyzing the response to an arbitrarily oriented blast wave of either a hard- or soft-mounted shelter, with either hard- or soft-mounted internal racks, on a wheeled or tracked vehicle, with a non-linear suspension system, and parked on a possibly inclined surface. The large number of degrees of freedom included within the program permit examination of large displacements and rotations of the vehicle including overturning, as well as individual motions of the vehicle axles, the shelter, and the internal shelter racks, relative to the vehicle body. Bottoming and rebounding of the suspension system springs are included in the code, and the tire-ground interaction modeling permits the tire to leave the ground, to recontact the ground, to slide along the ground, and to stop sliding.

Options within the code permit repression of various degrees of freedom when analyzing problems of lesser complexity than those indicated above. The truck and jeep configurations analyzed in this study, for example, did not require consideration of all the degrees of freedom available within the code. This point may best be illustrated by describing certain of the input data requirements as they applied to the study.

### 3.3 Input Data Requirements

The majority of the input data required by the TRUCK code may be characterized, in general, as mass data, spring data, tire-ground data, aerodynamic model data, and aerodynamic load data. The present discussion will be restricted to a general analysis of the TRUCK input data requirements, since following sections of the report discuss in more detail specific modeling procedures relevant to the input data requirements of this study.

The mass data require specification of the individual values of the mass, center of gravity location, and mass moments of inertia for all of the following items which may be individually suspended: the vehicle body, the vehicle axle assemblies (axle assembly includes axle, wheels and tires, springs and shock absorbers), the shelter, and the internal shelter equipment racks. For truck configuration (1), the M35A2 truck carrying the S-280 shelter, the shelter internal racks were rigidly attached to the shelter and the shelter itself was rigidly attached to the truck cargo bed floor. Therefore, both the shelter and the internal racks were included as part of the vehicle body mass, leaving only the vehicle body and the axle assemblies as the individually suspended masses requiring input data definition. For truck configuration (2), the M35A2 truck with stake sides but with no load, again the vehicle body and the axle assemblies were the only masses requiring definition. The M35A2 truck with canvas top and loaded with concrete blocks, truck configuration (3), also required only vehicle body and axle assembly mass data input since the concrete blocks were not spring mounted and were included as part of the vehicle body mass. Similarly, since the M38A1 jeep carried no cargo, only the vehicle body and the axle assemblies required individual mass identification.

The spring data portion of the input data defines the characteristics of the spring systems which couple the aforementioned individually suspended mass items. As previously indicated, all of the four vehicle systems analyzed required specification only of the individually suspended vehicle body and axle assembly masses, and correspondingly only the spring systems linking these masses required definition. It should be noted that the term spring system is used in the general sense and includes both actual springs as well as shock absorbers. In specifying the characteristics of the spring system, the locations of the attachment points of each of the springs are required to define the line of action of the spring force. Additionally, data defining the non-linear spring force-displacement and damping force-velocity curves for both the compression and rebound phases of each spring are required.

The tire-ground data required by TRUCK are those data which define the interaction between the vehicle's tires and the ground. For each tire on the vehicle, the program requires information on the tire location on the vehicle, the tire radius, and the coefficient of sliding friction

between the tire and surface upon which it rests. Additionally, the non-linear force-normal displacement and force-tangential displacement data as well as the radial and tangential tire damping coefficients must be provided. Since the three truck systems analyzed involved the same M35A2 vehicle, all of the tire-ground input data were identical for all three truck configurations but differed from the M38A1 jeep data.

The TRUCK input data defining the blast loading on the vehicle are a combination of the aerodynamic model data and the aerodynamic load data. The aerodynamic model data require that the vehicle system to be analyzed be broken down into a finite number of rectangular boxes comprising the total aerodynamic model of the system. Each rectangular box in turn establishes a specific geometry relevant to both the diffraction loading of the incident blast wave and the drag loading associated with the material velocity behind the shock front. The aerodynamic load data are necessary to define the time-history of the blast loading to be applied to the aerodynamic model and are comprised of the blast overpressure time-history and the material velocity time-history. Since all of the aerodynamic models and some of the aerodynamic load data were different for each of the four vehicle system configurations analyzed in this study, further discussion of these data will be deferred to later sections of the report.

SECTION 4  
VEHICLE SYSTEM MECHANICAL MODELS

4.1 Introduction

As indicated in the previous section, the majority of the TRUCK code input data may be generally grouped into mass data, spring data, tire-ground interaction data, aerodynamic model data, and aerodynamic load data. The first three of these data groups may be more specifically characterized as mechanical model data relevant to the physical features of a vehicle system. The aerodynamic model and load data development will be subsequently discussed in Sections 5 and 6 respectively, while the remainder of this section will be exclusively devoted to the mechanical model development of the four primary vehicle system configurations analyzed in this study.

Appendices A to D should be referred to for specific values of relevant mechanical model data.

4.2 M35A2 Truck Configurations

As indicated in Section 3, the only portions of all three truck system configurations which normally would have required separate mass modeling to satisfy the input data requirements were the vehicle body and the vehicle running gear, since none of the cargos carried were independently suspended. However, since the running gear were identical for all three truck configurations due to the assumed commonality of the primary vehicles, only the vehicle bodies required different models in order to account for the differences in the cargo configurations.

It should be noted that the TRUCK code inherently assumes that any system to be modeled is laterally symmetrical. Hence, in modeling the vehicle systems for this study, any asymmetries of the vehicle or cargo were ignored, and the lateral c.g. location of each mass was assumed to lie in a vertical plane passing through the mid-points of the vehicle axles.

References 3 and 4 were used to first establish the mass, c.g. location, and mass moments of inertia about the c.g. of an empty M35A2 truck with stale sides but without running gear. These values then were used as the vehicle body mass data for the no-load truck configuration. For the truck configuration involving the S-280 shelter

Reference 4. "Preliminary Target Description Data for the Calculation of the Response of a Truck-Shelter-Rack System Exposed to a Blast Wave, and Proposed Test Procedures for Obtaining Such Data" prepared by R-Associates for BRL under Contract No. DAAD05-74-C-0754.

rigidly mounted in the vehicle cargo body (Figure 3), the mass, c.g. location, and mass moments of inertia about the shelter c.g. were established from data contained in Reference 3. The shelter mass and c.g. were then combined with the vehicle body mass and c.g. for the no-load truck configuration to obtain a combined truck-shelter mass and center of gravity. Mass moments of inertia about the combined c.g. were then calculated to complete the vehicle body mass data for the combined truck-shelter system. For the truck configuration involving the truck cargo body loaded with concrete blocks and covered with the canvas top, a procedure similar to the above was employed to obtain a set of combined truck-load mass data.

The configuration of the concrete blocks carried in the truck cargo body was as portrayed in Figure 4, based on information provided by Reference 5, and the configuration of the canvas covering the cargo body was estimated from Figure 1. Individual mass data for both the concrete blocks and the canvas top were then calculated and combined, as previously indicated, with the no-load vehicle body mass data to obtain a complete set of combined truck-load mass data.

The M35A2 vehicle running gear is comprised of a single front axle assembly and a dual rear axle assembly. The front axle assembly consists of an axle attached to a single wheel on each side of the vehicle, while the dual rear axle assembly, a bogie arrangement, consists of two axles, each attached to dual wheels on either side of the vehicle. The front suspension system on each side of the vehicle is comprised of a leaf-type spring and a shock absorber, each item attached to both the chassis and to the front axle. The rear suspension system on each side of the vehicle contains no shock absorbers per se, but does have one leaf-type spring attached at each end to one of the dual rear axles and at its mid-point to the vehicle chassis.

The separate mass data for each of the three M35A2 wheel-axle combinations were established from the data contained in References 3 and 4. The spring and shock absorber attachment point locations were given in Reference 4, and Reference 6 was used to establish the spring and shock absorber response characteristics. Since the same vehicle running gear were modeled for all three truck configurations, the mass and spring input data remained constant.

Due to the commonality of the running gear on all three configurations, the tire-ground interaction modeling was the same for all three configurations except for the coefficient of sliding friction between the vehicle tires and the ground. Although all of the trucks were assumed to be sitting on level ground in the DICE THROW field test,

---

Reference 5. Telephone conversation with Mr. R. Raley of BRL on August 2, 1977.

Reference 6. "Determination of Physical Characteristics of a Wheeled Vehicle," USATECOM Project No. 9-CO-150-000, Test Record No. TU-W-162, Materiel Testing Directorate, U.S. Army Aberdeen Proving Ground, 16 September 1977.

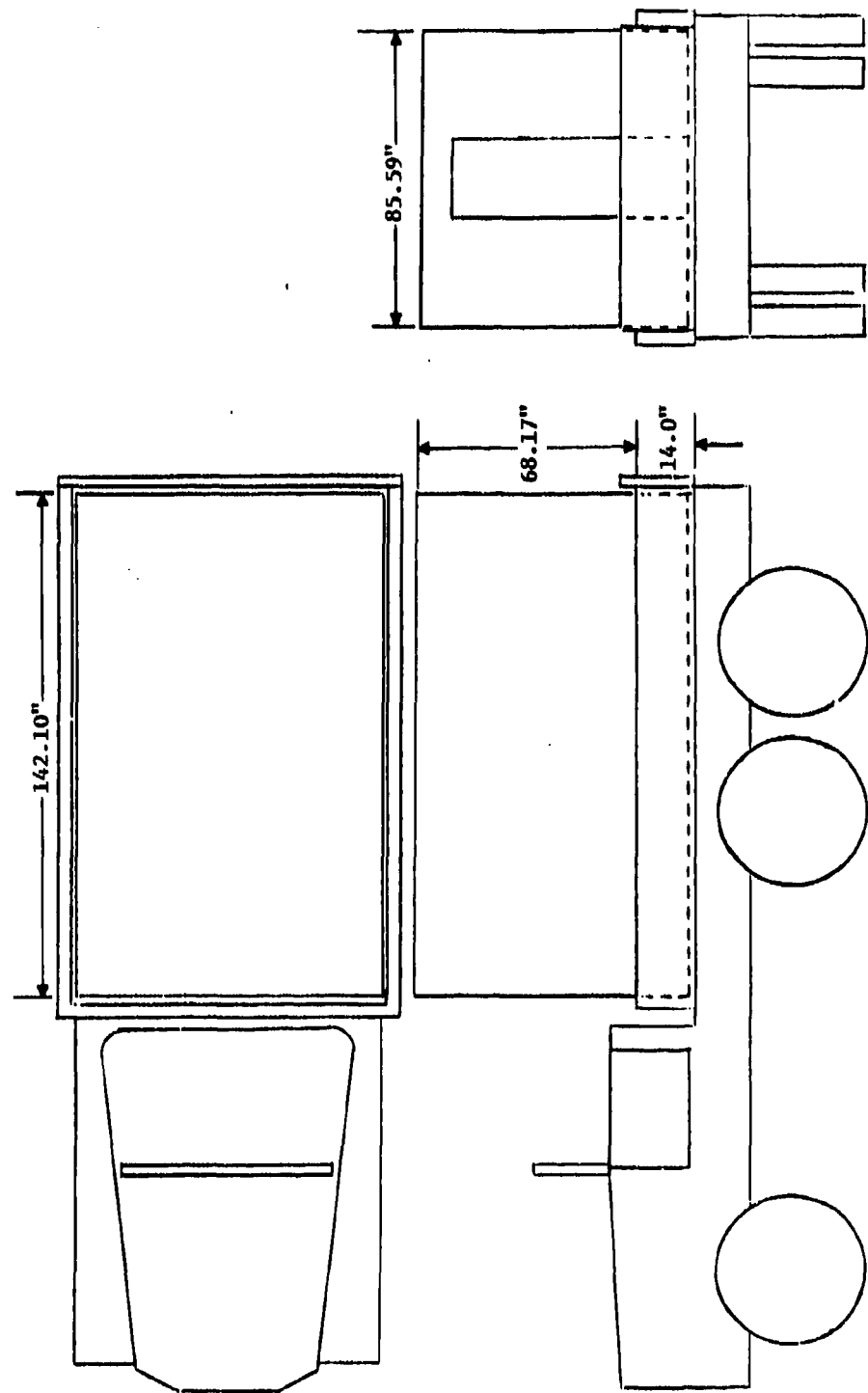


FIGURE 3. SCHEMATIC OF S280 SHELTER IN H35A2 TRUCK

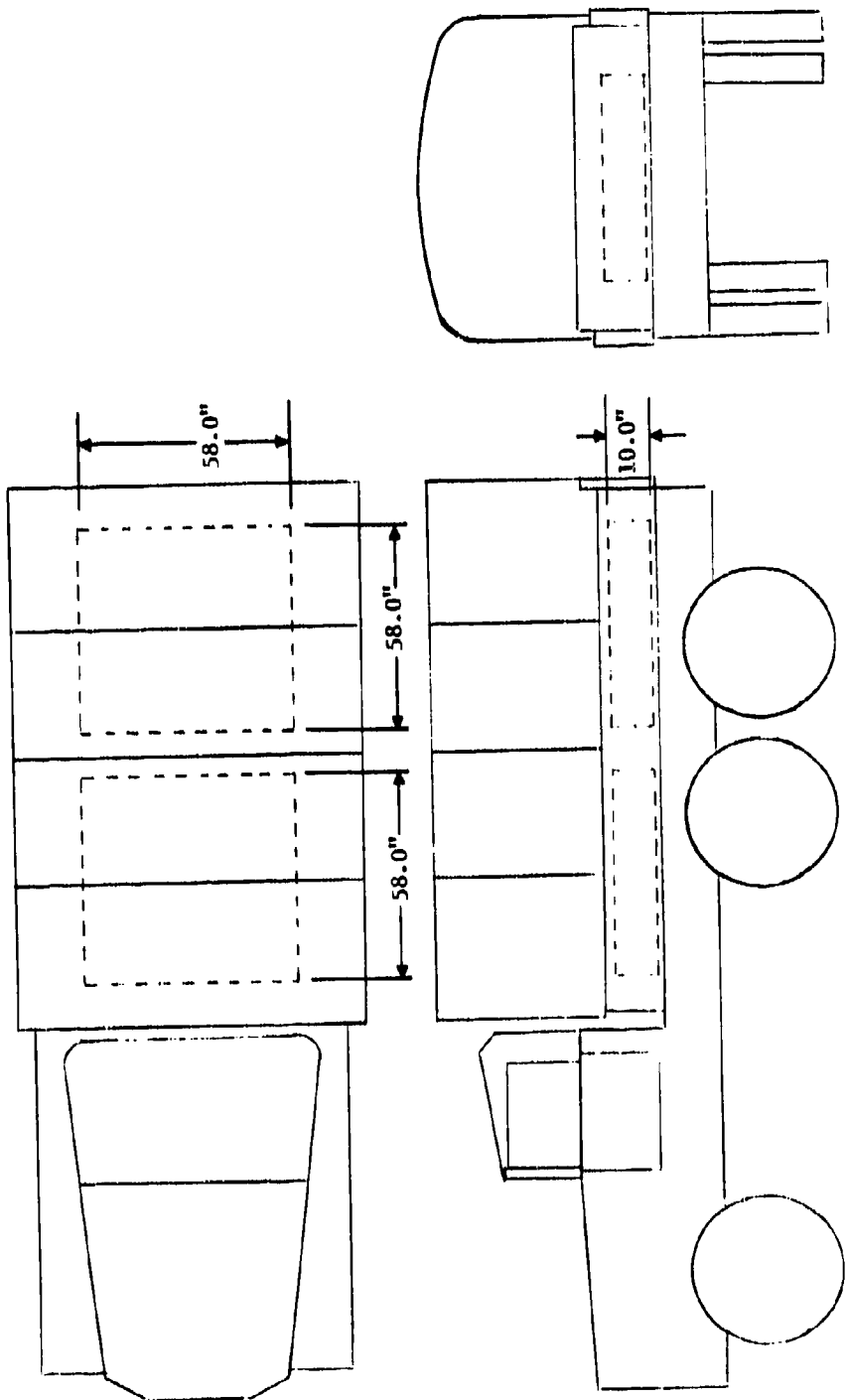


FIGURE 4. SCHEMATIC OF CONCRETE BLOCKS IN M35A2 TRUCK

different restraint conditions were imposed on two of the three truck configurations. Since the truck carrying the S-280 shelter was unrestrained from sliding, a coefficient of sliding friction of 0.8, from Reference 4, was used in the TRUCK code input for this vehicle. For each of the remaining two truck configurations, two vehicles of the same configuration but with different sliding restraints were fielded in the test event at each pressure level. For each of these two configurations, one vehicle was unrestrained from normal sliding motion and the second vehicle was restrained from sliding by concrete curbs placed against the tires on the leeward side of the vehicle. Each unrestrained vehicle was modeled with a coefficient of sliding friction of 0.8, and the restrained vehicles were modeled with a coefficient of 1000, thus effectively restricting the sliding of the truck. The remainder of the data required by the tire-ground interaction modeling for all three truck configurations were established from the data contained in Reference 4.

#### 4.3 M38A1 Jeep Configuration

The one M38A1 jeep configuration modeled was the empty, no canvas configuration previously discussed in Section 2. Separate mass models for both the vehicle body and the vehicle running gear were established from the data presented in References 3, 4 and 7.

The M38A1 running gear consists of single front and rear axle assemblies, with each axle attached to a single wheel on each side of the vehicle. The front and rear suspension systems of the jeep are similar in that each suspension system on each side of the vehicle is comprised of both a leaf-type spring and a shock absorber, and the attachment points on the vehicle for these items were obtained from Reference 4. The response characteristics of the jeep front and rear springs and shock absorbers required for the TRUCK input were taken from Reference 4, since MTD test data on the jeep springs and shocks were not available as they were for the M35A2 truck.

The tire-ground interaction modeling necessary to satisfy the TRUCK input data requirements for the jeep followed the same general pattern established for the M35A2 truck configurations, even though the tire size for the two vehicles differed. At each pressure level analyzed, two jeeps of the same configuration were fielded in DICE THROW, one restrained and one unrestrained against sliding. Coefficients of sliding friction of 1000 and 0.8, as used for the M35A2 trucks, were also used for the jeep to represent the different restraint conditions, and the vehicles again were assumed to be sitting on level ground in the field test. The remainder of the tire-ground interaction model data were also established from information contained in Reference 4.

---

Reference 7. "Measurement of Weight, Center-of-Gravity, and Moment-of-Inertia About the Roll Axis of Test Item (Truck, Utility, 1/4-Ton, 4X4, M38A1)", USATECOM Project No. 9-CO-150-000-019, Test Record No. TU-W-155, Material Testing Directorate, U.S. Army Aberdeen Proving Ground, 10 March 1977.

SECTION 5  
VEHICLE SYSTEM AERODYNAMIC MODELS

5.1 Introduction

Aside from the mechanical modeling of a vehicle system to be analyzed by the TRUCK code, the other large body of data required in the input data requirements are the specification of the aerodynamic models and the aerodynamic loads. The present section is restricted to a discussion of the aerodynamic models developed for the vehicle analyses, since the aerodynamic loads are subsequently discussed in Section 6 of this report.

For specific values of the relevant aerodynamic models, Appendices A to D at the end of the report should be consulted.

5.2 M35A2 Truck Configurations

In the aerodynamic loading section of Reference 1, a discussion is presented of the methodology employed in the TRUCK code for simulating the diffraction pressure loading on a rectangular block as measured in shock-tube experimentation. As an extension of these shock-tube results, the code employs crude models to approximate the blast wave diffraction process wherein all aerodynamically loaded surfaces of the model to be analyzed are represented in the code input as the complete or partial faces of a set of rectangular boxes.

In order to reduce the amount of time involved in formulating the aerodynamic models and associated program input data for three different truck configurations, efforts were initially made to identify the commonality of the aerodynamically loaded surface areas amongst the three configurations. In the DICE THROW test, all three truck configurations were oriented such that the incident blast wave struck all the vehicles side on, i.e., the shock front was parallel to the assumed plane of symmetry of the vehicles. The initially loaded surfaces of all the truck configurations were then seen to be those surfaces which faced the blast, that is, the side areas of the vehicles and cargos.

As previously discussed in Section 2, the selection of the M35A2 truck as the basic vehicle for all three truck system configurations resulted in a major portion of the truck, from the top of the cab door and cargo body bed downward, being identical for all configurations. It was also pointed out previously that the truck carrying the S-280 shelter had no canvas top on the cab, whereas the canvas top was on the cab for the other two configurations. Furthermore, since the cab side windows were open and the windshield erect on all vehicles, the only difference in the side aerodynamic surface areas of the three

truck cabs was due to the side-on area of the cab canvas top. Since the combined side-on areas of the windshield and cab canvas top are small in comparison with the side areas of the remainder of the truck, it was decided to simplify the modeling by ignoring the cab top such that all three configurations, exclusive of the cargo body, would have the same aerodynamic surface area.

Each of the three truck system configurations was aerodynamically modeled to consist of three rectangular boxes. One rectangular box represented that portion of the truck forward of the cargo body, another rectangular box represented the remainder of the truck below the top of the cargo body bed, and both of these boxes were identical for all three truck-system configurations. The third rectangular box was modeled to represent the aerodynamic surfaces above the top of the cargo body bed and, hence, was different for each of the three configurations.

For the empty truck with stake sides, the third rectangular box was modeled to represent the aerodynamic surface areas of the slatted, stake sides of the cargo body. The modeling of the truck with canvas top and loaded with concrete blocks required that the third rectangular box represent only the canvas top over the cargo body since the concrete blocks contributed nothing to the aerodynamic model. The third rectangular box for the truck loaded with the S-280 shelter represented only that portion of the shelter which protruded above the top of the cargo body bed.

### 5.3 M38A1 Jeep Configuration

The aerodynamic model for the one M38A1 jeep configuration analyzed, empty with no canvas, was based on the configuration of the jeep in Figure 2 but without the portrayed canvas top. Since the jeep fielded in DICE THROW was also oriented side-on to the blast, the initially loaded surface areas of the vehicle were those areas shown in the side view of Figure 2. The side-on area of the windshield, as viewed in Figure 2, was considered negligible and, hence, the assumption of either an upright or lowered windshield was irrelevant.

The aerodynamic model of the jeep was constructed as four rectangular aerodynamic boxes. The first aerodynamic box was modeled to represent the forward portion of the vehicle ahead of the windshield. The second aerodynamic box was modeled to represent the small portion of the body between the windshield and the driver's seat. The aft portion of the body between the driver's seat and the aft end of the vehicle was represented by the third box, and the fourth box approximated the spare tire on the rear of the vehicle as a rectangular box.

## SECTION 6

### VEHICLE SYSTEM AERODYNAMIC LOADS

#### 6.1 Introduction

Section 5 of this report discusses the procedures employed in constructing the aerodynamic models for the primary vehicle-system configurations analyzed. In the present section, the derivation of the loads which were applied to these aerodynamic models are discussed. Additionally, the actual loads data which were employed in the TRUCK analyses are presented herein and are excluded from the input data listings of Appendices A to D.

#### 6.2 DICE THROW Experimental Overpressure Data

As specified in Reference 2, each of the vehicle-system configurations with the exception of the truck carrying the S-280 shelter were to be analyzed at two different pressure levels, with different sliding restraint conditions imposed at each pressure level as previously indicated. Each of the pressure levels selected by BRL corresponded to actual blast data measurements recorded in DICE THROW in the vicinity of the actual test vehicle-system configurations.

Figures 5 through 9 are time-history plots of blast static overpressure measured at various pressure gage stations in DICE THROW, as provided by BRL. The values of peak shock static overpressure indicated by BRL on Figures 5 through 8 were designated as the appropriate pressure levels for the analyses to be performed. Specific values for the durations of the positive phase of the blast overpressure portrayed in Figures 5 through 8 were also obtained from BRL (Reference 8). The correspondence of the designated pressure levels to the appropriate vehicle-system configurations as specified by BRL are presented in Table 1, together with positive phase durations and gage station numbers, for completeness. It should be noted that no values of either peak overpressure level or positive phase duration are indicated in Table 1 for the truck carrying the S-280 shelter for reasons which will be discussed subsequently.

#### 6.3 Analytical Overpressure and Dynamic Pressure Data

The aerodynamic loads normally used in a TRUCK code response analysis are blast model data self-contained within the program. For the present correlation response study, however, the aerodynamic loads which were to be applied to the aerodynamic models discussed in Section 5 were the actual loads measured in the DICE THROW test. Since the TRUCK code employs both blast overpressure and dynamic pressure time-histories in its simulation of the diffraction and drag loading regimes of blast waves, additional efforts were required to formulate dynamic pressure time-histories compatible with the experimentally-measured overpressure time-histories provided.

---

Reference 8. Telephone conversation with Mr. G. Teal of BRL on September 1, 1977.

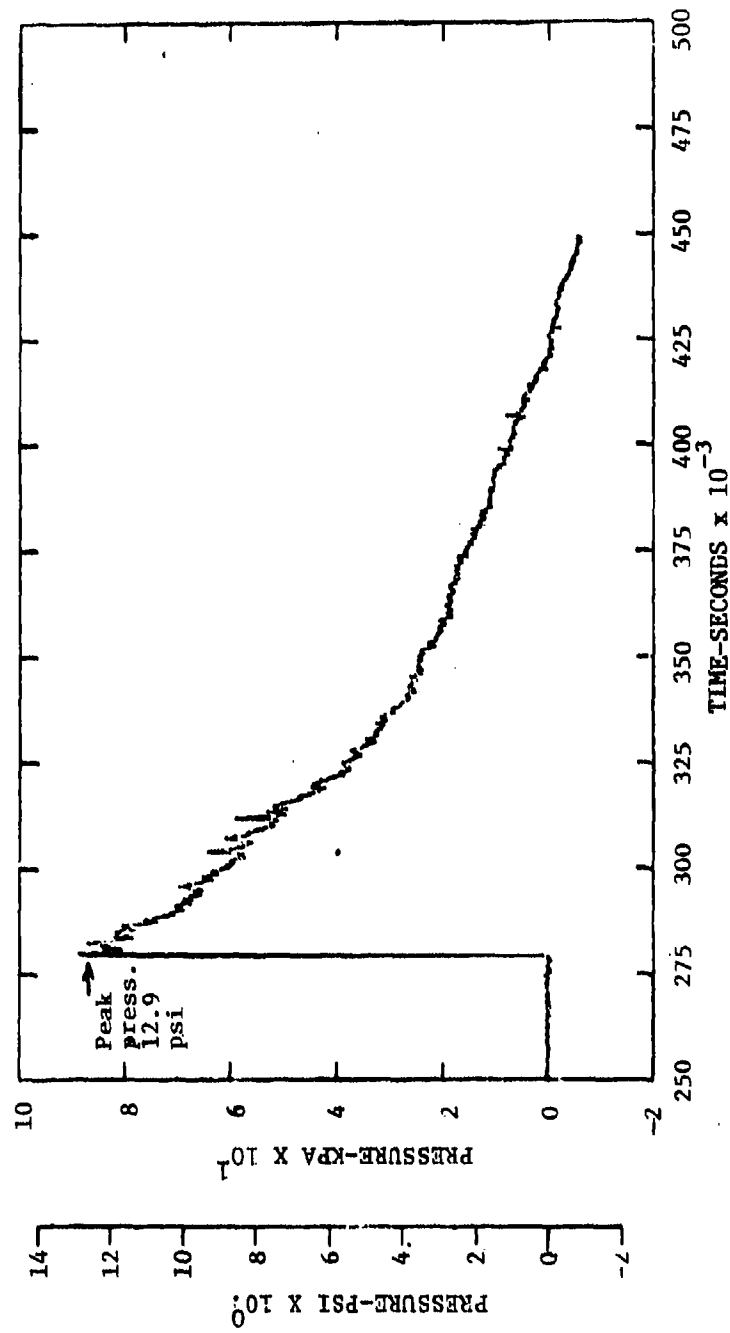


FIGURE 5. EXPERIMENTAL OVERPRESSURE TIME-HISTORY AT GAGE STATION 324-2

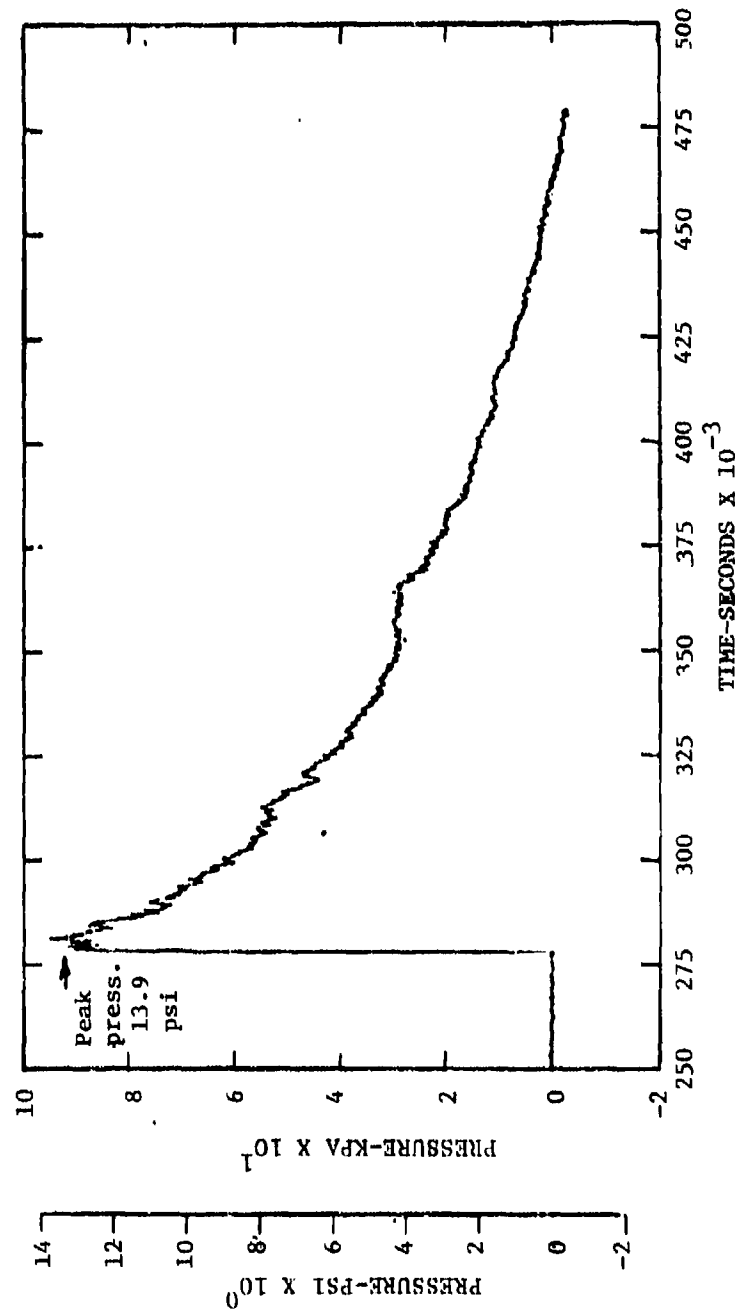


FIGURE 6. EXPERIMENTAL OVERPRESSURE TIME-HISTORY AT GAGE STATION 324-3

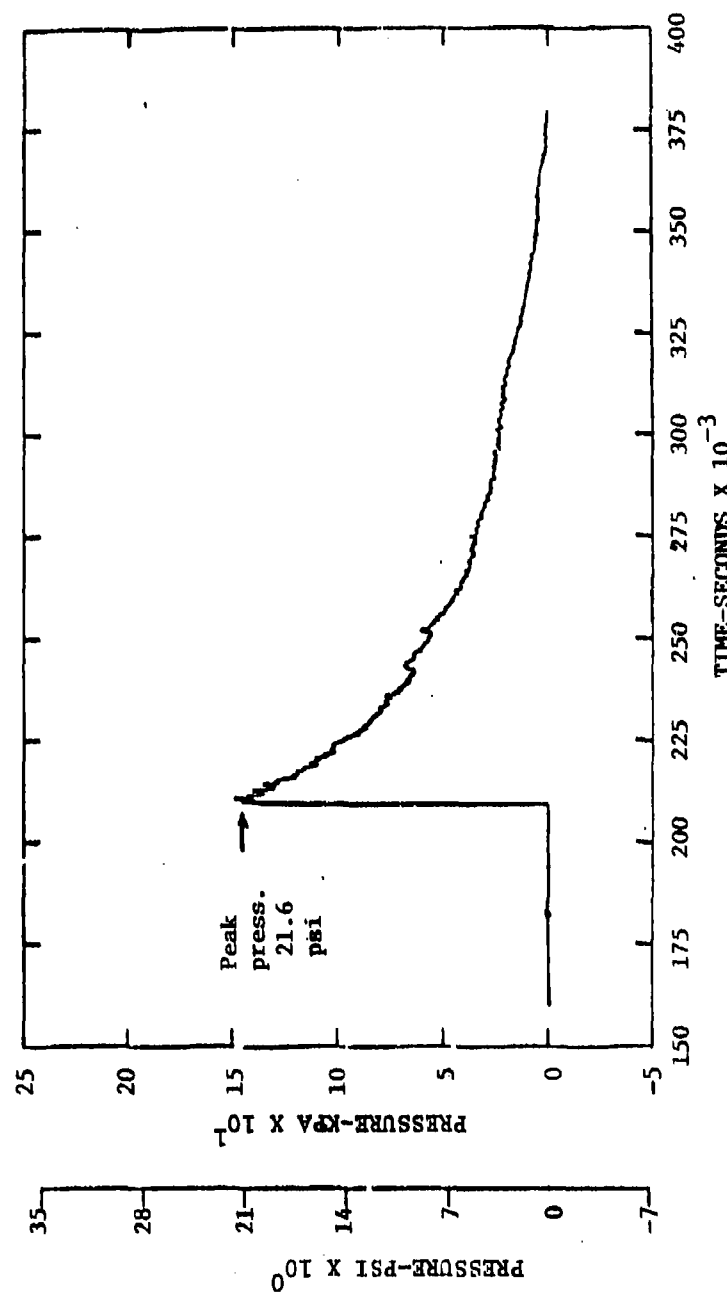


FIGURE 7. EXPERIMENTAL OVERPRESSURE TIME-HISTORY AT GAGE STATION 322-3

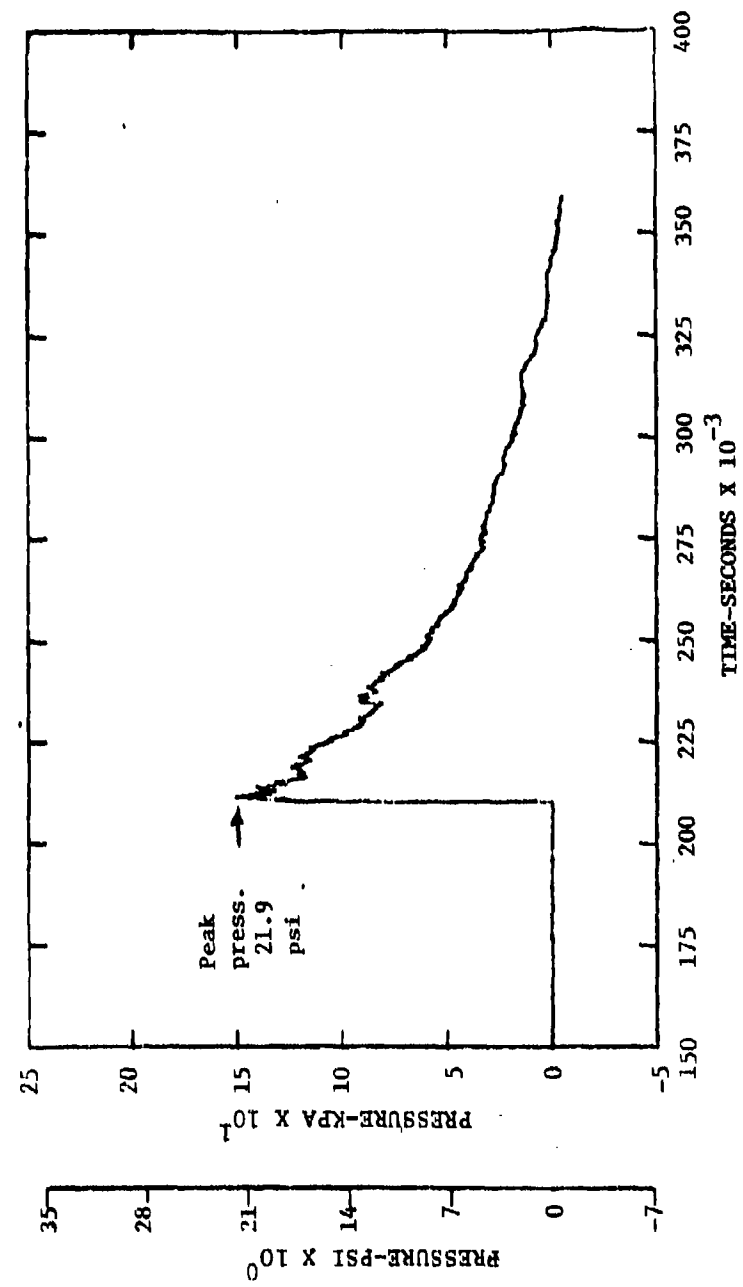


FIGURE 8. EXPERIMENTAL OVERPRESSURE TIME-HISTORY AT GAGE STATION 322-2

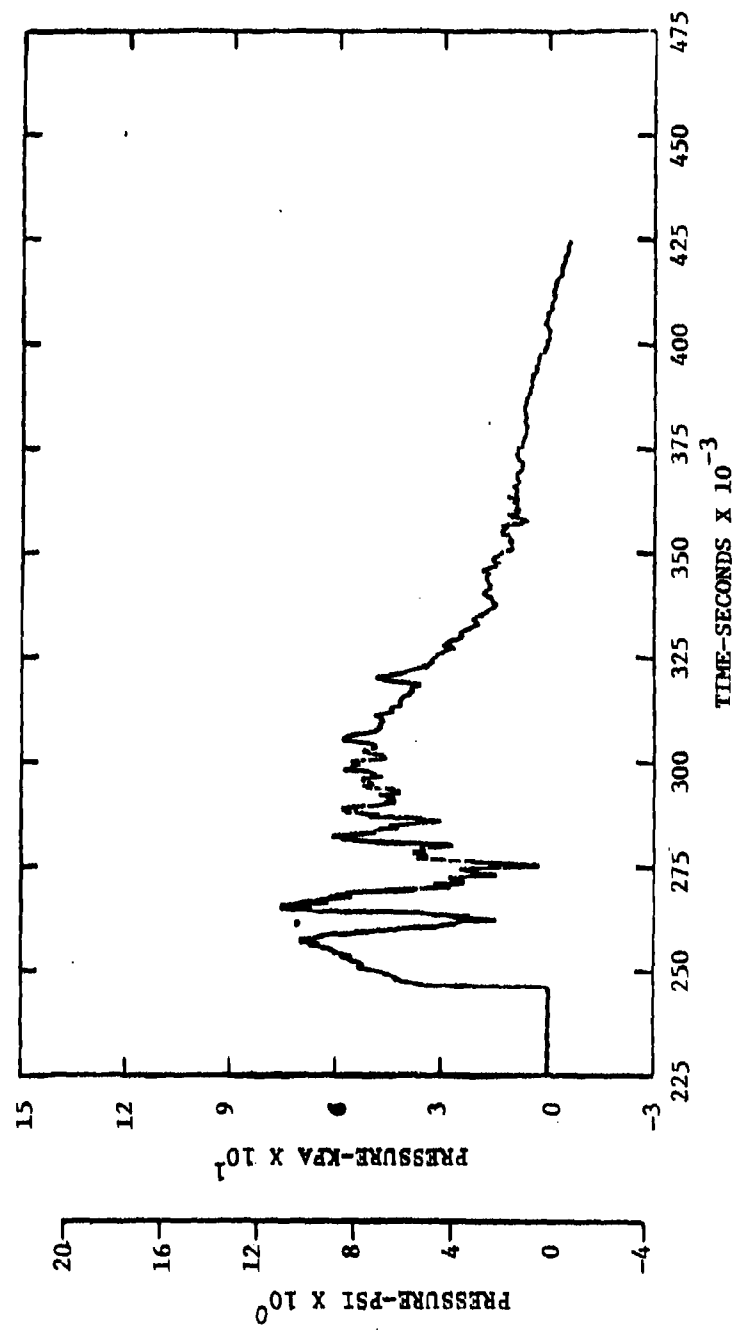


FIGURE 9. EXPERIMENTAL OVERPRESSURE TIME-HISTORY AT GAGE STATION 223

TABLE 1  
PEAK OVERPRESSURE LEVELS FOR SYSTEM CONFIGURATIONS

System Configuration	Peak Overpressure Level psi (kPa)	Positive Phase Duration (Ref. 8) msec.	Gage Station Number
M35A2 truck with S-280 Shelter	13.9 (95.8)	—	223
M35A2 truck, empty, with stake sides	21.6 (148.9)	184	324-3
M35A2 truck, empty, with stake sides	21.6 (148.9)	170	322-3
M35A2 truck, loaded with concrete blocks, with canvas top	12.9 (88.9)	141	324-2
M35A2 truck, loaded with concrete blocks, with canvas top	21.9 (151.0)	131	322-2
M38A1 jeep, empty, with no canvas	12.9 (88.9)	141	324-2
M38A1 jeep, empty, with no canvas	21.9 (151.0)	131	322-2

The general procedure used in formulating the required dynamic pressure time-history data was based on a slight modification of the methodology contained in Reference 9. Reference 9 presents an analytical method which was formulated for computing the pressure, density, and material velocity behind a spherical blast wave, produced by TNT or Pentolite, based on experimental measurements of overpressure recorded at a number of gage locations. Part of the methodology in Reference 9 involves the use of a constructed cross plot of pressure, density, and material velocity behind the shock front, and two key parameters established from the peak overpressure at the shock front, the ambient pressure ahead of the shock front, and the specific value of interest of the overpressure behind the shock.

For each of the overpressure traces of Figures 5 through 8, an arbitrary number of overpressure values were first read from a smooth curve drawn through the data as recorded. Since the ambient pressure was readily established and the peak overpressure was already specified, it was then possible to calculate the two key parameters, corresponding to each selected overpressure value, which were required to enter the cross plot of Reference 9. Interpolation of the plotted values of density and material velocity behind the shock provided the appropriate data necessary to formulate values of dynamic pressure corresponding to the selected values of overpressure. At the shock front, a more accurate value of dynamic pressure than that obtained from the plot of Reference 9 was independently calculated from normal shock equations. The dynamic pressure data were then plotted against the times after shock arrival obtained from the original overpressure traces corresponding to the initially chosen values of overpressure, and smooth curves were drawn through the data to eliminate any minor computational errors. The final list of discrete values of overpressure and dynamic pressure which were used in the TRUCK code response analyses to represent the blast wave positive phase duration for each of the specified pressure levels in Figures 5 through 8 are presented in Tables 2 through 5.

Table 6 presents the discrete values of overpressure and dynamic pressure which were used in the TRUCK code to represent the assumed overpressure and dynamic pressure time-histories corresponding to Gage Station No. 223.

As can be seen from Figure 9, the recorded static overpressure time-history trace for Station No. 223 was extremely erratic and ill-defined. Since neither the maximum overpressure value at the shock front nor the positive phase duration could be ascertained from Figure 9 with any degree of confidence, it was impossible to fair a smooth curve through the experimental overpressure trace. After reviewing all the available overpressure, both static and total, time-histories recorded along the DICE THROW blast line 2, it was decided that the only feasible way to obtain a realistic static overpressure time-history curve for Station No. 223 would be through interpolation of the static overpressure data measured at other blast line 2 pressure gage stations, based on ground range location of the gages. Consequently, after considerable cross-plotting

Reference 9. Ruetenik, J.R., and Lewis, S.D., Computation of Blast Properties for Spherical TNT or Pentolite From Measured Pressure Histories, AFFDL-TR-66-47, October 1966.

TABLE 2  
AERODYNAMIC LOADS - 12.9 PSI PRESSURE LEVEL

Time after shock-wave arrival msec.	Overpressure psi (kPa)	Dynamic Pressure psi (kPa)
0.0	12.9 (88.9)	4.12 (28.41)
20.0	8.75 (60.33)	2.53 (17.44)
40.0	6.11 (42.13)	1.48 (10.20)
50.0	5.07 (34.96)	1.15 (7.93)
60.0	4.18 (28.82)	0.89 (6.14)
70.0	3.40 (23.44)	0.68 (4.69)
80.0	2.74 (18.89)	0.52 (3.59)
90.0	2.16 (14.89)	0.39 (2.69)
100.0	1.64 (11.31)	0.29 (2.00)
120.0	0.78 (5.38)	0.16 (1.10)
141.0	0.0 (0.0)	0.065 (0.45)
160.0	0.0 (0.0)	0.0 (0.0)

TABLE 3  
AERODYNAMIC LOADS - 13.9 PSI PRESSURE LEVEL

Time after shock-wave arrival msec.	Overpressure psi (kPa)	Dynamic Pressure psi (kPa)	
		(psi)	(kPa)
0.0	13.9 (95.84)	4.74 (32.68)	
10.0	11.02 (75.98)	3.80 (26.20)	
20.0	9.28 (63.98)	3.01 (20.75)	
30.0	7.87 (54.26)	2.29 (15.79)	
40.0	6.70 (46.19)	1.77 (12.20)	
50.0	5.75 (39.64)	1.41 (9.72)	
60.0	4.94 (34.06)	1.14 (7.86)	
70.0	4.22 (29.10)	0.94 (6.48)	
80.0	3.58 (24.68)	0.78 (5.38)	
100.0	2.50 (17.24)	0.52 (3.59)	
120.0	1.68 (11.58)	0.33 (2.28)	
140.0	1.04 (7.17)	0.19 (1.31)	
184.0	0.0 (0.0)	0.070 (0.48)	
230.0	0.0 (0.0)	0.0 (0.0)	

TABLE 4  
AERODYNAMIC LOADS - 21.6 PSI PRESSURE LEVEL.

Time after shock-wave arrival usec.	Overpressure psi (kPa)	Dynamic Pressure psi (kPa)
0.0	21.6 (148.93)	10.64 (73.36)
10.0	16.40(113.07)	7.74 (53.37)
20.0	12.77(88.05)	5.60 (38.61)
30.0	10.00(68.95)	4.03 (27.79)
40.0	7.95(54.81)	2.92 (20.13)
50.0	6.40(44.13)	2.10 (14.48)
60.0	5.28(36.40)	1.58 (10.89)
70.0	4.40(30.34)	1.30 (8.96)
80.0	3.73(25.72)	1.07 (7.38)
100.0	2.58(17.79)	0.72 (4.96)
120.0	1.63(11.24)	0.47 (3.24)
145.0	0.72(4.96)	0.23 (1.59)
170.0	0.0 (0.0)	0.10 (0.69)
190.0	0.0 (0.0)	0.0 (0.0)

TABLE 5  
AERODYNAMIC LOADS - 21.9 PSI PRESSURE LEVEL

Time after shock-wave arrival sec.	Overpressure psi (kPa)	Dynamic Pressure psi (kPa)
0.0	21.9 (151.00)	10.90 (75.15)
10.0	16.60 (114.45)	8.60 (59.29)
20.0	13.17 (90.80)	6.20 (42.75)
30.0	10.40 (71.71)	4.27 (29.44)
40.0	8.26 (56.95)	3.16 (21.79)
50.0	6.60 (45.51)	2.24 (15.44)
60.0	5.27 (36.34)	1.57 (10.82)
70.0	4.15 (28.61)	1.17 (8.07)
80.0	3.18 (21.93)	0.88 (6.07)
100.0	1.60 (11.03)	0.43 (2.96)
115.0	0.74 (5.10)	0.21 (1.45)
131.0	0.0 (0.0)	0.10 (0.69)
150.0	0.0 (0.0)	0.0 (0.0)

TABLE 6  
AERODYNAMIC LOADS - GAGE STATION NO. 223

Time after shock-wave arrival msec.	Overpressure psi (kPa)	Dynamic Pressure psi (kPa)
0.0	12.064 (83.18)	3.634 (25.06)
20.0	9.25 (63.78)	2.48 (17.10)
40.0	6.78 (46.75)	1.65 (11.38)
60.0	4.88 (33.65)	1.08 (7.45)
80.0	3.52 (24.27)	0.69 (4.76)
100.0	2.38 (16.41)	0.43 (2.96)
120.0	1.44 (9.93)	0.26 (1.79)
140.0	0.72 (4.96)	0.14 (0.97)
160.0	0.24 (1.65)	0.07 (0.48)
175.0	0.0 (0.0)	0.04 (0.28)
200.0	0.0 (0.0)	0.0 (0.0)

of the data pertinent to the various pressure gage stations of blast line 2, a static overpressure time-history curve for Station No. 223 was formulated.

Once the formulation of an acceptable curve of static overpressure time-history for Station No. 223 was accomplished, it was a simple task to formulate the required compatible dynamic pressure time-history data. The procedure followed was identical to that previously described for Figures 5 through 8 and, as indicated previously, the resultant discrete values of both overpressure and dynamic pressure used in the TRUCK analysis of the truck-shelter system are tabulated in Table 6.

SECTION 7  
TRUCK RESPONSE ANALYSES RESULTS

7.1 Introduction

TRUCK response analyses of the three different M35A2 truck system configurations and the one M38A1 jeep configuration were conducted, based on the models and loads discussed in the previous sections of this report. The results of these analyses are presented herein.

7.2 TRUCK Response Analysis Parameters

For each of the four vehicle system configurations analyzed, three TRUCK program output parameters were plotted: total system roll angle, c.g. margin, and lateral c.g. displacement. The response time-histories of these three parameters, when viewed as an entity, portray the important motions of the total system subsequent to blast wave interception, particularly with respect to vehicle overturning.

The total system roll angle is measured about a longitudinal axis through the total system c.g. and, for the systems analyzed herein where the pitch and yaw angles are relatively small, the roll axis is essentially parallel to the ground. The lateral c.g. displacement is measured along a horizontal axis whose origin is at the original pre-blast position of the total system c.g. and, for vehicles sliding on level ground, the axis is parallel to the ground. The c.g. margin is a measurement of the minimum distance between the total system c.g. and the edge of the footprint defined by the projections onto a horizontal plane, through the total system c.g., of the vehicle front and rear tire positions. A zero c.g. margin is in most cases an indication of vehicle overturning, particularly if the slope of the c.g. margin versus response time curve is relatively steep.

Since the same three response parameter time-histories are presented and discussed for all of the vehicle systems analyzed, the order of presentation will be uniformly maintained as c.g. margin time-history, roll angle time-history, and lateral c.g. displacement time-history. Hence, in referring to Figures A-C for a particular vehicle system, it should be tacitly understood, unless noted to the contrary, that Figure A portrays c.g. margin response, Figure B portrays roll angle response, and Figure C portrays lateral c.g. displacement response. On each response plot, zero response time corresponds to the instant at which the blast wave initially intercepts any portion of the vehicle system model.

7.3 M38A1 Jeep Response Results

Figures 10-12 illustrate the analytical response of the M38A1 jeep subjected to the DICE THROW blast wave peak overpressure level of 12.9 psi (88.9kPa), and Figures 13-15 illustrate the corresponding analytical response of the jeep when subjected to the 21.9 psi (151.0 kPa) peak overpressure level.

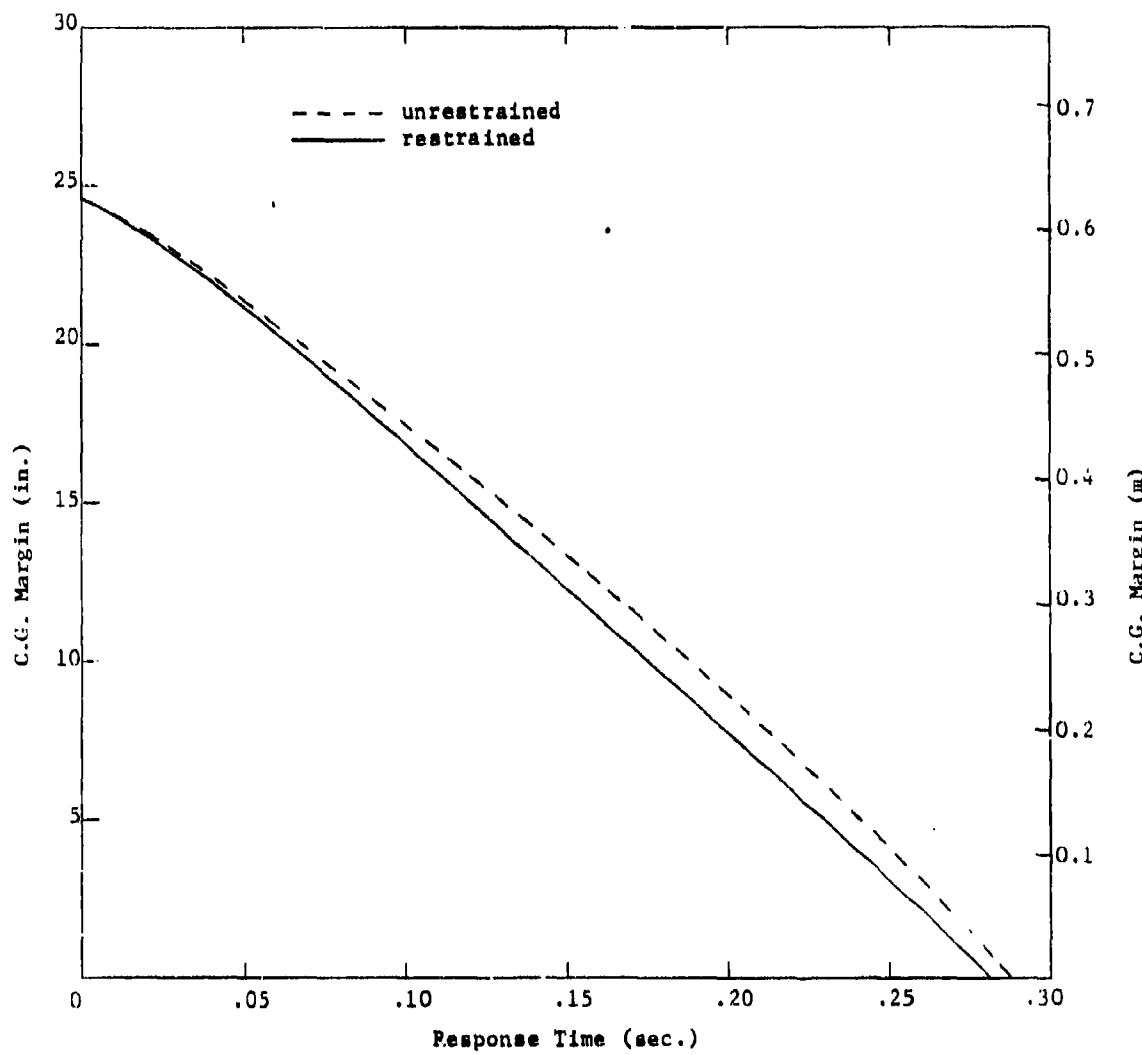


FIGURE 10. C.G. MARGIN TIME-HISTORY FOR M38A1 JEEP SUBJECTED TO 12.9  
PSI INCIDENT OVERPRESSURE (88.9 kPa)

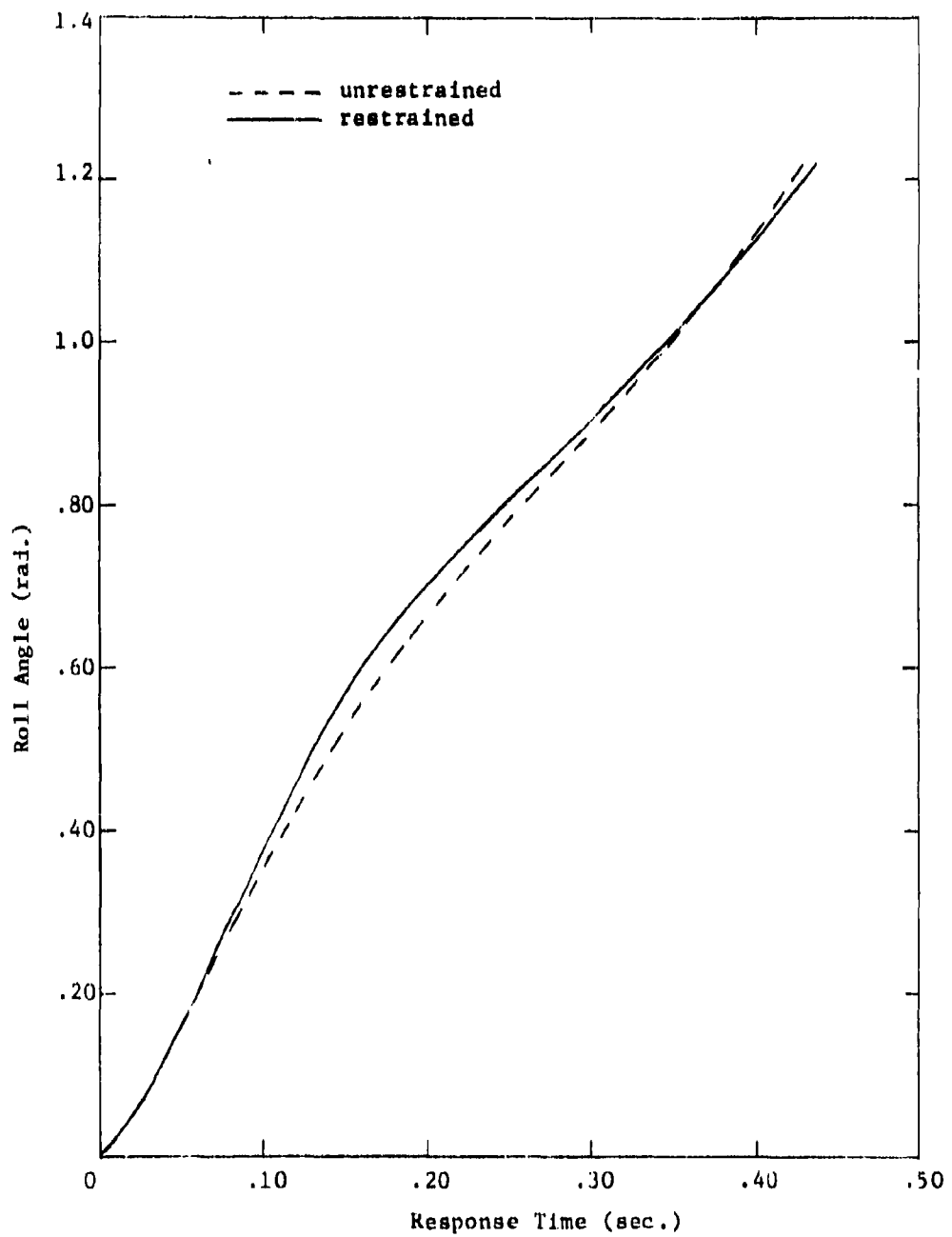


FIGURE 11. ROLL ANGLE TIME-HISTORY FOR M38A1 JEEP SUBJECTED TO 12.9 PSI INCIDENT OVERPRESSURE (88.9 kPa)

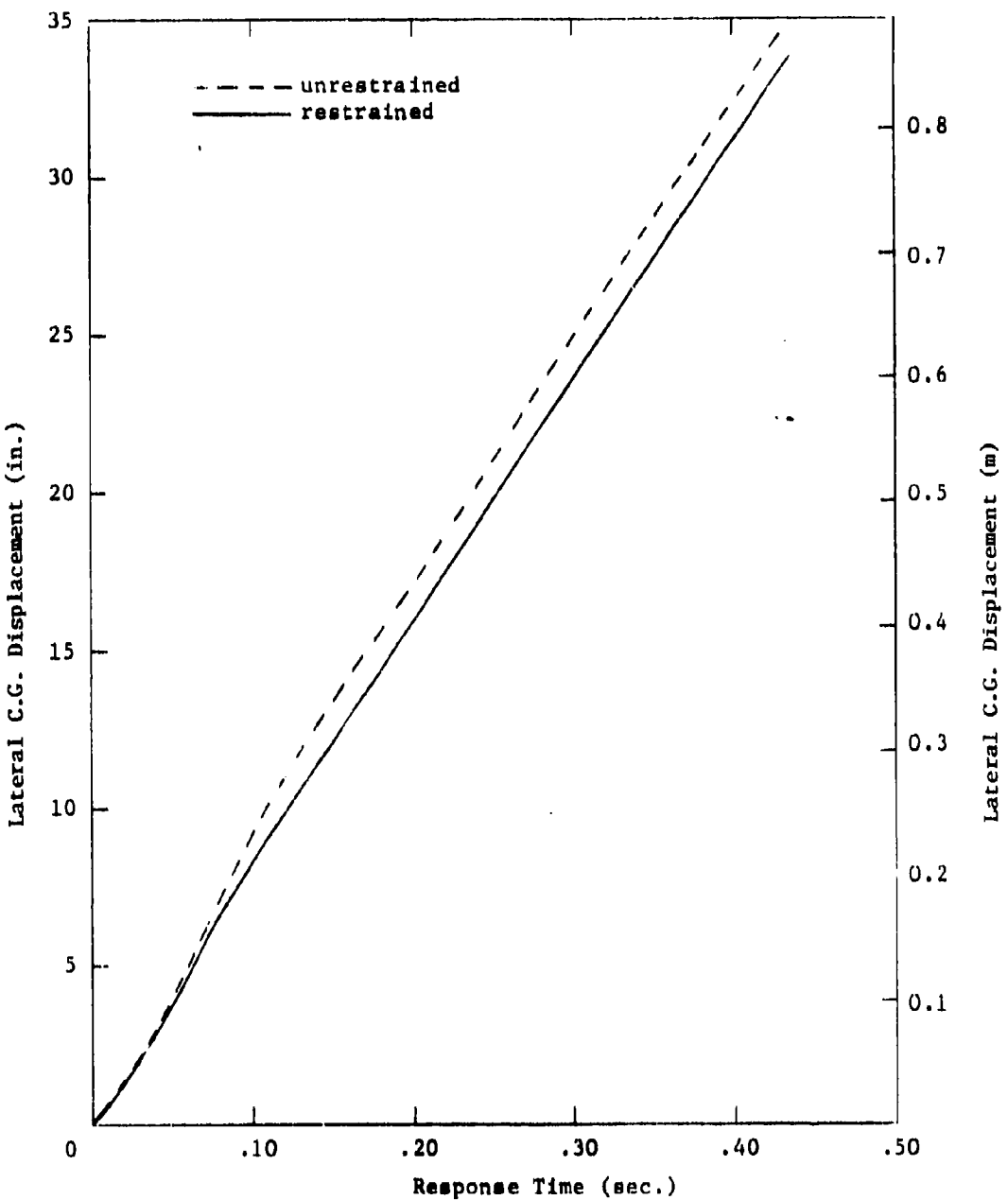


FIGURE 12. LATERAL C.G. DISPLACEMENT TIME-HISTORY FOR M38A1 JEEP SUBJECTED TO 12.9 PSI INCIDENT OVERPRESSURE (88.9 kPa)

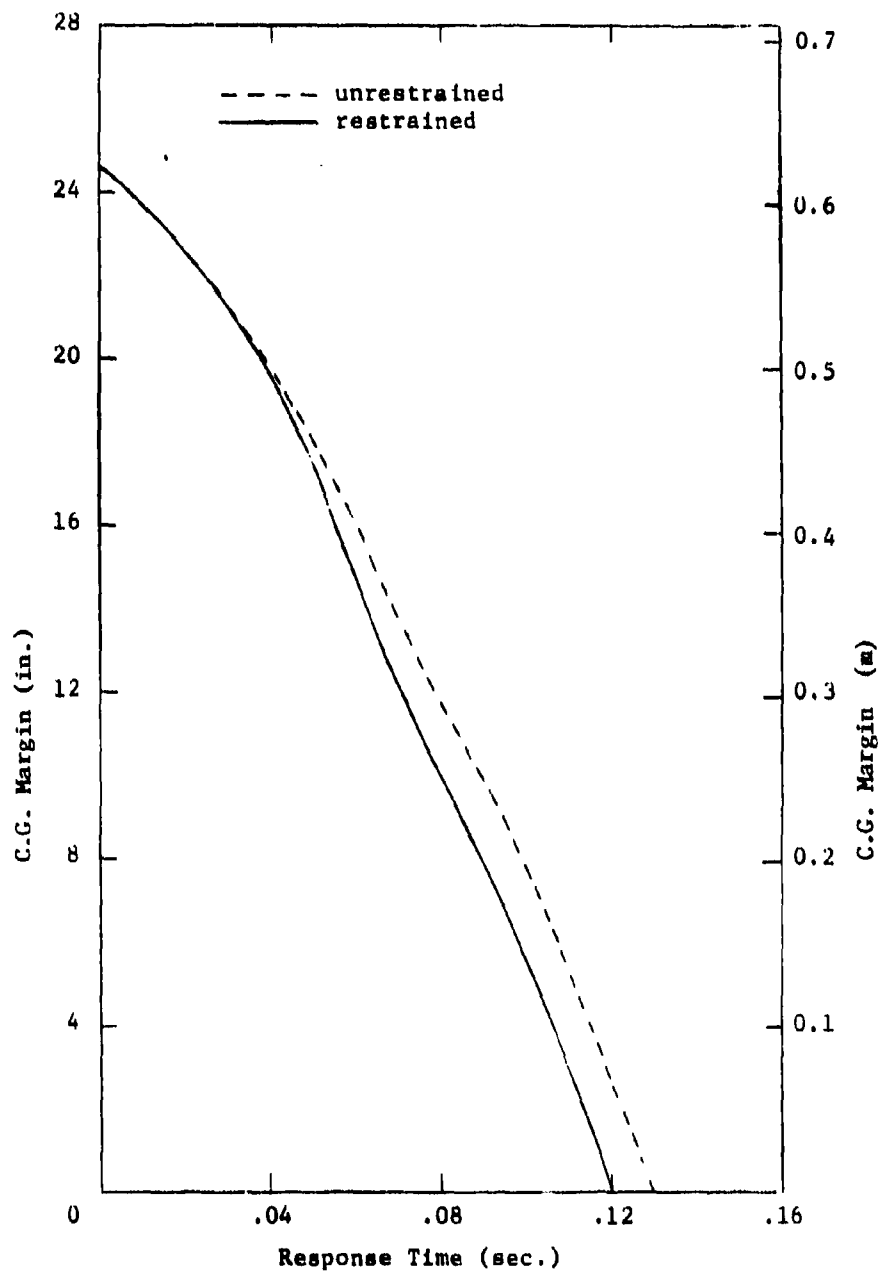


FIGURE 13. C.G. MARGIN TIME-HISTORY FOR M38A1 JEEP SUBJECTED TO 21.9 PSI INCIDENT OVERPRESSURE (151.0 kPa)

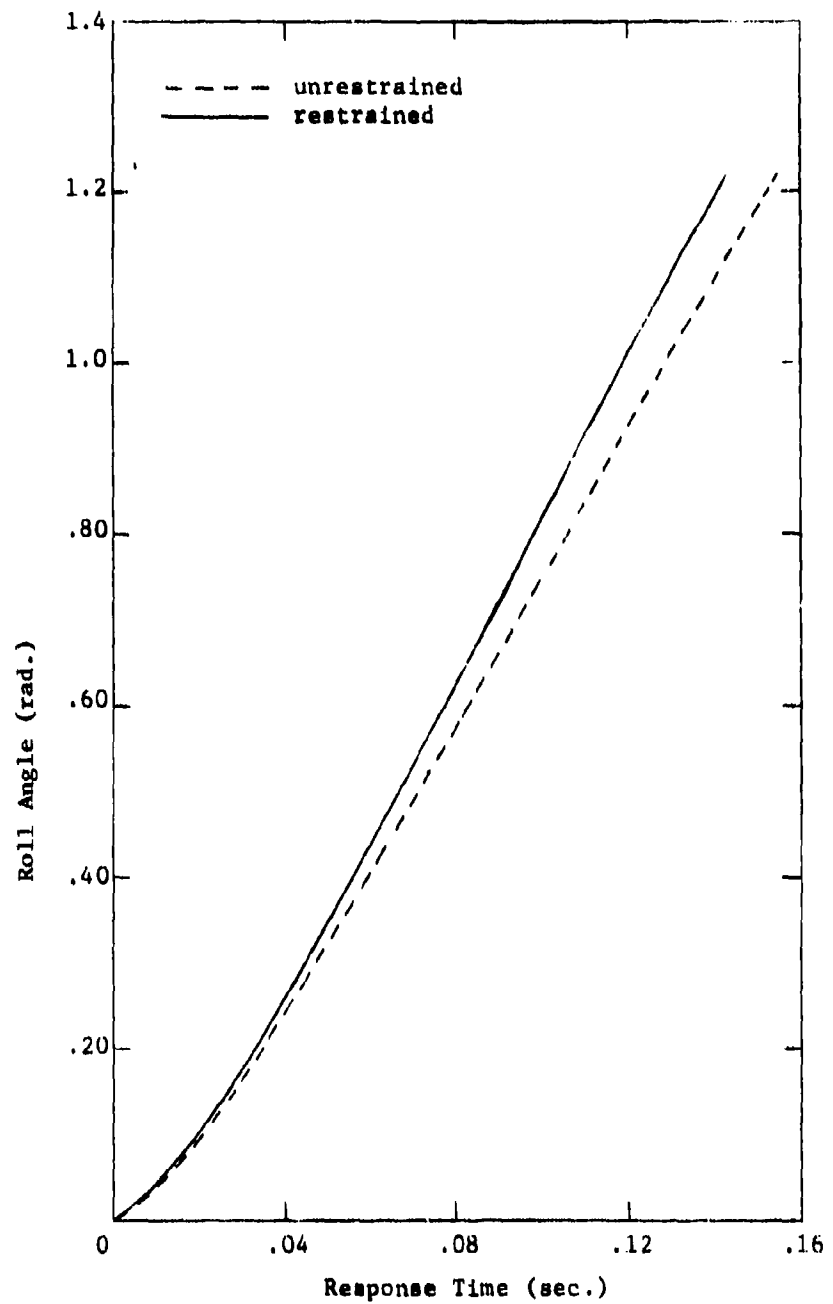


FIGURE 14. ROLL ANGLE TIME-HISTORY FOR M38A1 JEEP SUBJECTED TO 21.9 PSI INCIDENT OVERPRESSURE (151.0 kPa)

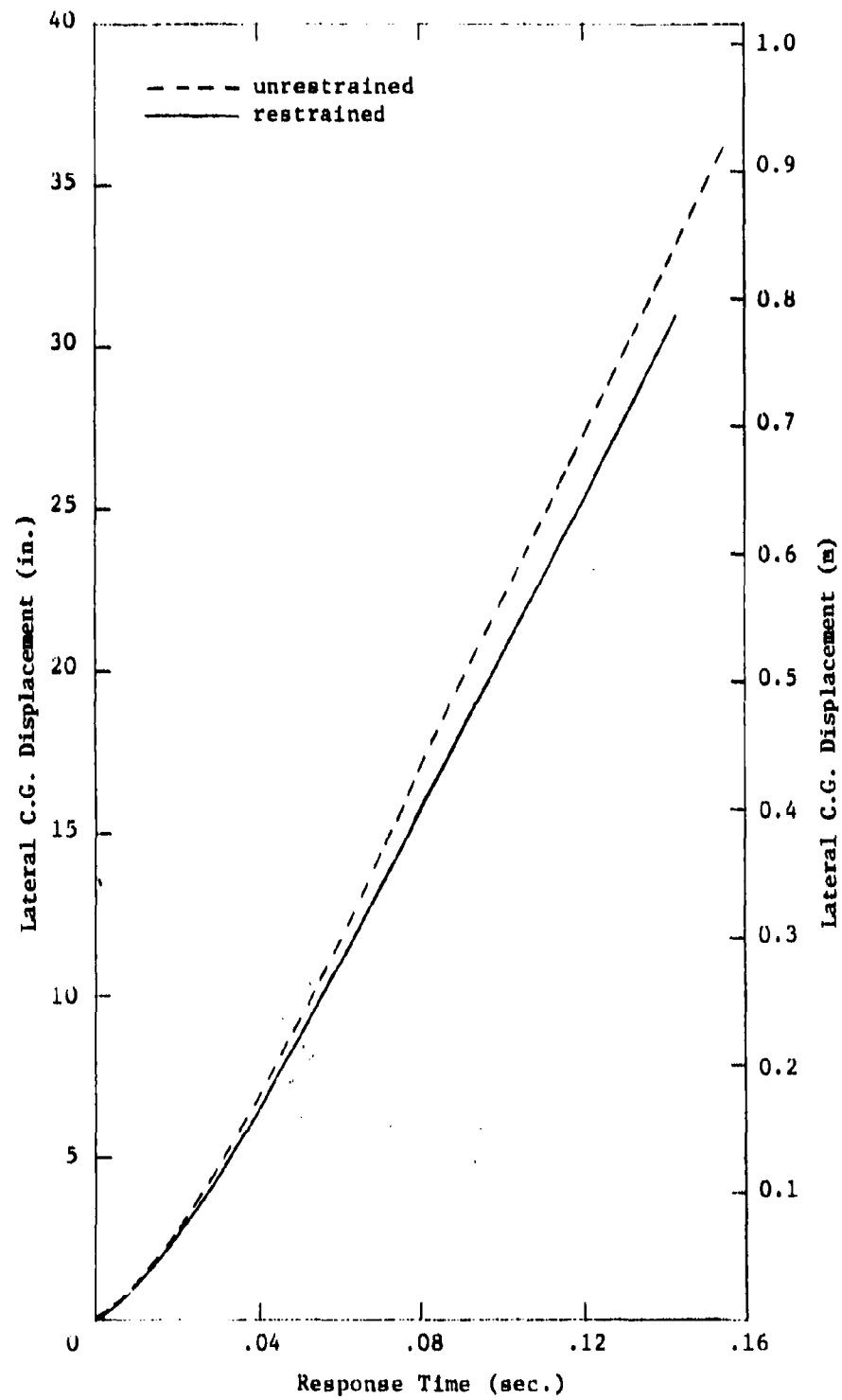


FIGURE 15. LATERAL C.G. DISPLACEMENT TIME-HISTORY FOR M38A1 JEEP  
SUBJECTED TO 21.9 PSI INCIDENT OVERPRESSURE (151.0 kPa)

For both overpressure levels analyzed, the comparative results shown for the two assumed sliding restraint conditions indicate that very little sliding motion of the total system takes place, as evidenced by the closeness of the restrained and unrestrained curves. The slopes of the c.g. margin time-history curves at zero c.g. margin indicate that overturning of the vehicle occurs at both levels of overpressure, with the system subjected to the higher overpressure overturning much earlier as would normally be expected due to the higher level of loading. For the higher overpressure level, the values of both roll angle and lateral c.g. displacement at the response time corresponding to zero c.g. margin are slightly higher than the corresponding values for the lower overpressure level.

#### 7.4 M35A2 Truck Response Results

Figures 16-18 portray the analytical response of the M35A2 empty truck subjected to the 13.9 psi (95.8 kPa) peak overpressure level, and the analytical response of the same system subjected to a peak overpressure level of 21.6 psi (148.9 kPa) is presented in Figures 19-21.

The c.g. margin time-history curves indicate that overturning of the empty truck also occurs at both overpressure levels analyzed and, again, at a much earlier response time for the higher overpressure level. Although the results presented indicate that the restrained vehicle overturns slightly faster than the unrestrained vehicle and that relatively little sliding motion takes place at either overpressure level, it is interesting to note that at the lower overpressure level the vehicle shows a slight hesitancy to overturn as evidenced by the marked change in vehicle roll rate prior to the attainment of a zero value for the c.g. margin. Again, at the higher overpressure level the values of both roll angle and lateral c.g. displacement at the response time corresponding to overturning are higher than the corresponding values for the lower overpressure level, and more so for the roll angle due to the roll rate change experienced at the lower overpressure level.

Before discussing the analysis results presented for the response of the M35A2 loaded trucks containing concrete blocks and subjected to the two DICE THROW overpressure test levels of 12.9 psi (88.9 kPa) and 21.9 psi (151.0 kPa), some background discussion is necessary since the analyses required procedures different than originally planned. As previously indicated in Sections 4 and 5, a separate mechanical model was originally formulated to represent the M35A2 loaded truck with canvas and a separate aerodynamic box was modeled to represent the covered cargo body for aerodynamic loading. The combination of these models, together with the two assumed restrained conditions, were to be used to investigate the system response at the two indicated pressure levels. It was subsequently learned, however, that during the actual DICE THROW experiment the canvas enclosures on the M35A2 loaded trucks were blown off the trucks shortly after blast wave interception and at both levels of overpressure to be analyzed. Consequently, the actual M35A2 loaded truck configurations which required analysis were systems

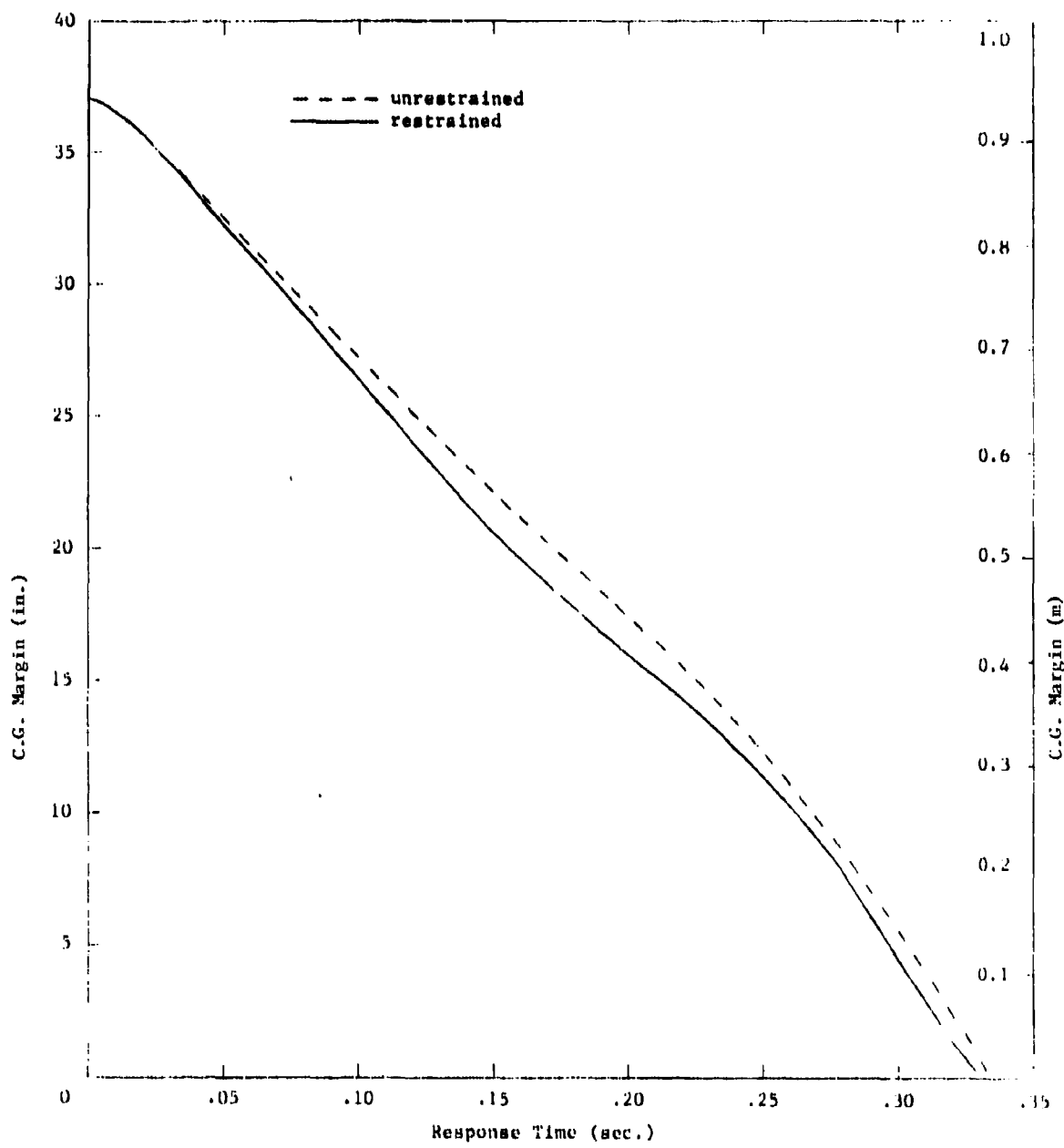


FIGURE 16. C.G. MARGIN TIME-HISTORY FOR M35A2 EMPTY TRUCK SUBJECTED TO 13.9 PSI INCIDENT OVERPRESSURE (95.8 kPa)

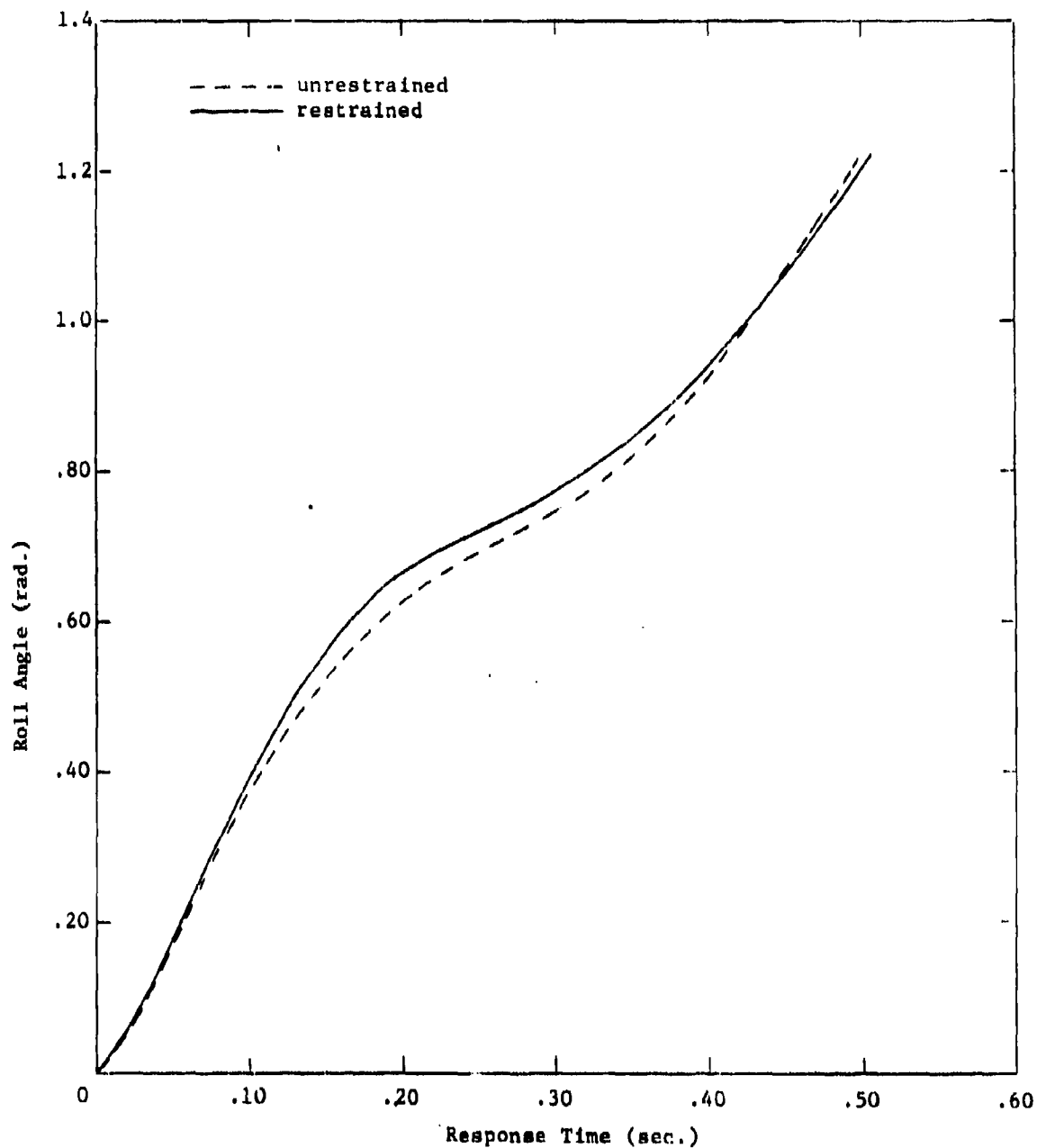


FIGURE 17. ROLL ANGLE TIME-HISTORY FOR M35A2 EMPTY TRUCK SUBJECTED TO 13.9 PSI INCIDENT OVERPRESSURE (95.8 kPa)

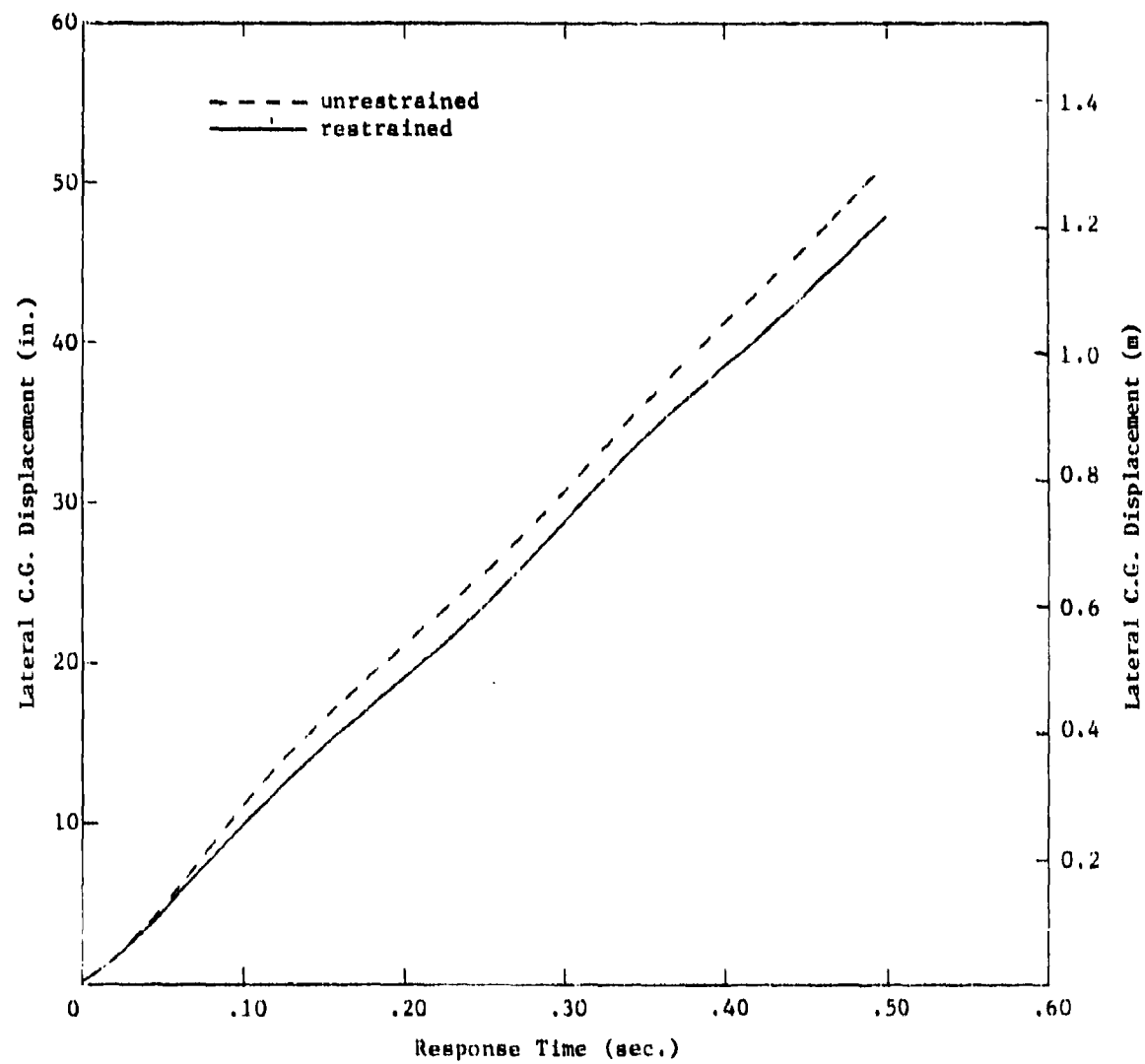


FIGURE 18. LATERAL C.G. DISPLACEMENT TIME-HISTORY FOR M35A2 EMPTY TRUCK SUBJECTED TO 13.9 PSI INCIDENT OVERPRESSURE (95.8 kPa)

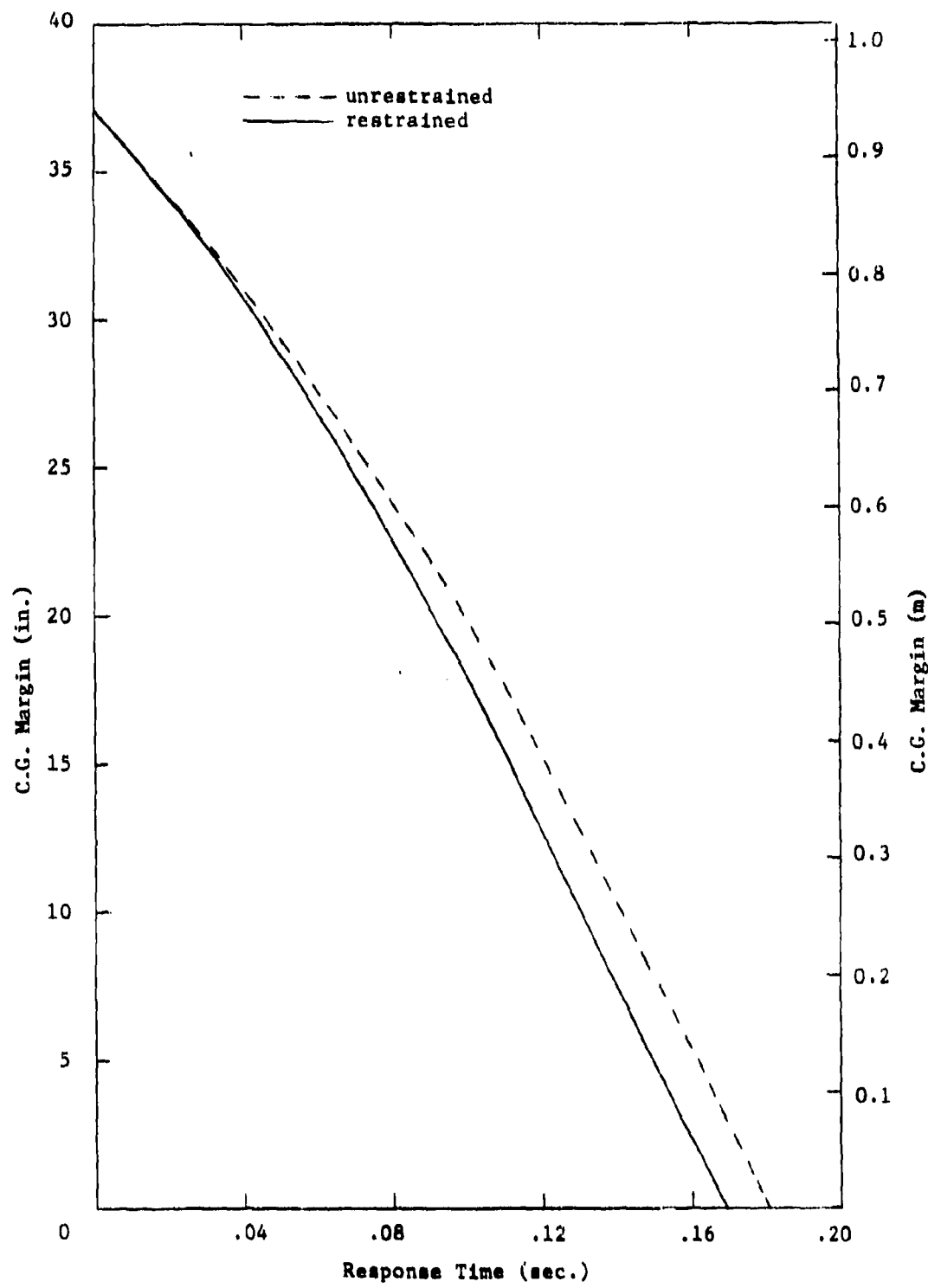


FIGURE 19. C.G. MARGIN TIME-HISTORY FOR M35A2 EMPTY TRUCK  
SUBJECTED TO 21.6 PSI INCIDENT OVERPRESSURE (148.9 kPa)

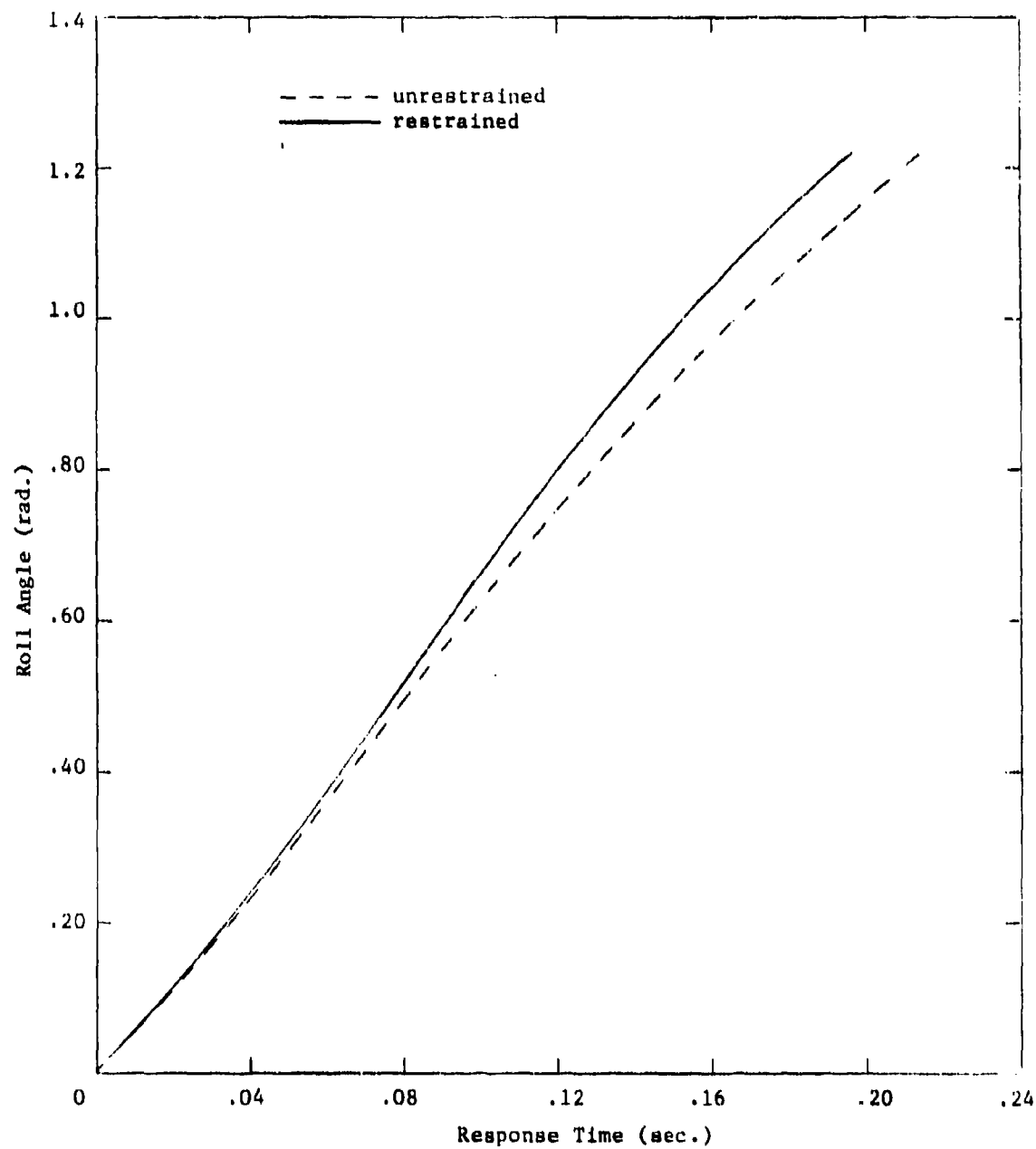


FIGURE 20. ROLL ANGLE TIME-HISTORY FOR M35A2 EMPTY TRUCK SUBJECTED TO 21.6 PSI INCIDENT OVERPRESSURE (148.9 kPa)

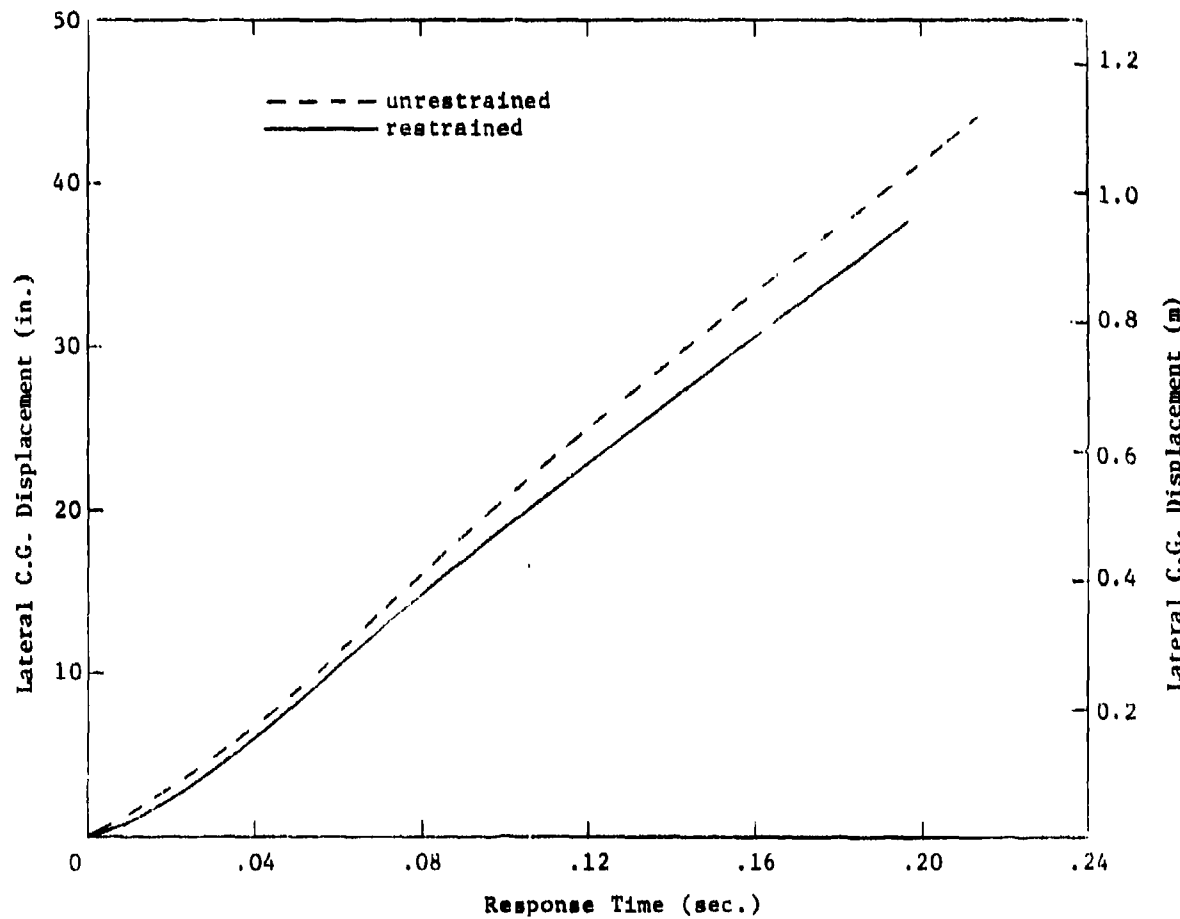


FIGURE 21. LATERAL C.G. DISPLACEMENT TIME-HISTORY FOR M35A2 EMPTY TRUCK SUBJECTED TO 21.6 PSI INCIDENT OVERPRESSURE (148.9 kPa)

which realistically underwent both mechanical and aerodynamic configuration changes during the period of system response.

Since the TRUCK code has no provision for configuration changes during response evaluation, it was apparent that the actual M35A2 loaded truck response simulation could not be properly handled by TRUCK. However, it did appear logical to expect that the actual response of the system would be between two extremes - the analytical response of a loaded truck with canvas erected during the entire response time and the response of a loaded truck without canvas during the entire response time. Accepting this premise as valid and having the canvas erect models already at hand, it was only necessary to model the loaded truck without canvas in order to proceed with the intended comparative analyses.

The formulation of the required mechanical model of an M35A2 truck loaded with concrete blocks but without canvas was relatively simple. The only effort involved was to remove the mass and inertia contributions of the cargo body canvas top from the previously constructed model with canvas top, resulting in a new total system model with modified mass, inertia, and c.g. characteristics. No additional effort was involved in aerodynamically modeling the loaded truck without canvas since, aerodynamically, that configuration was identical to the aerodynamic configuration of the M35A2 empty truck. Specific values of the relevant mechanical and aerodynamic model data for the M35A2 loaded truck without canvas are presented in Appendix E at the end of the report. Once this new model was completed, TRUCK response analyses for the loaded truck with and without canvas were conducted for both required overpressure levels and both assumed restraint conditions.

The analytical response results for the restrained M35A2 loaded truck subjected to the 12.9 psi (88.9 kPa) peak overpressure level are presented in Figures 22-24. Similarly, the results for the unrestrained vehicle subjected to the same overpressure level are shown in Figures 25-27.

For either assumed restraint condition, the plotted results show a most obvious difference in the overall system response of the two vehicles - namely, the vehicle with canvas overturns, as evidenced by the c.g. margin time-history curve going to zero, but the vehicle without canvas does not, as evidenced by the c.g. margin time-history curve returning to its original time zero value. Both the restrained and unrestrained vehicles with canvas do show a slight hesitancy to overturn, as indicated by the change in roll rate, but this hesitancy is overcome and overturning takes place. Again, as was noted in discussing both the M38A1 jeep and the M35A2 empty truck results, the overall total motions of the restrained and unrestrained loaded trucks are quite similar, indicating that very little sliding motion of the vehicles has taken place.

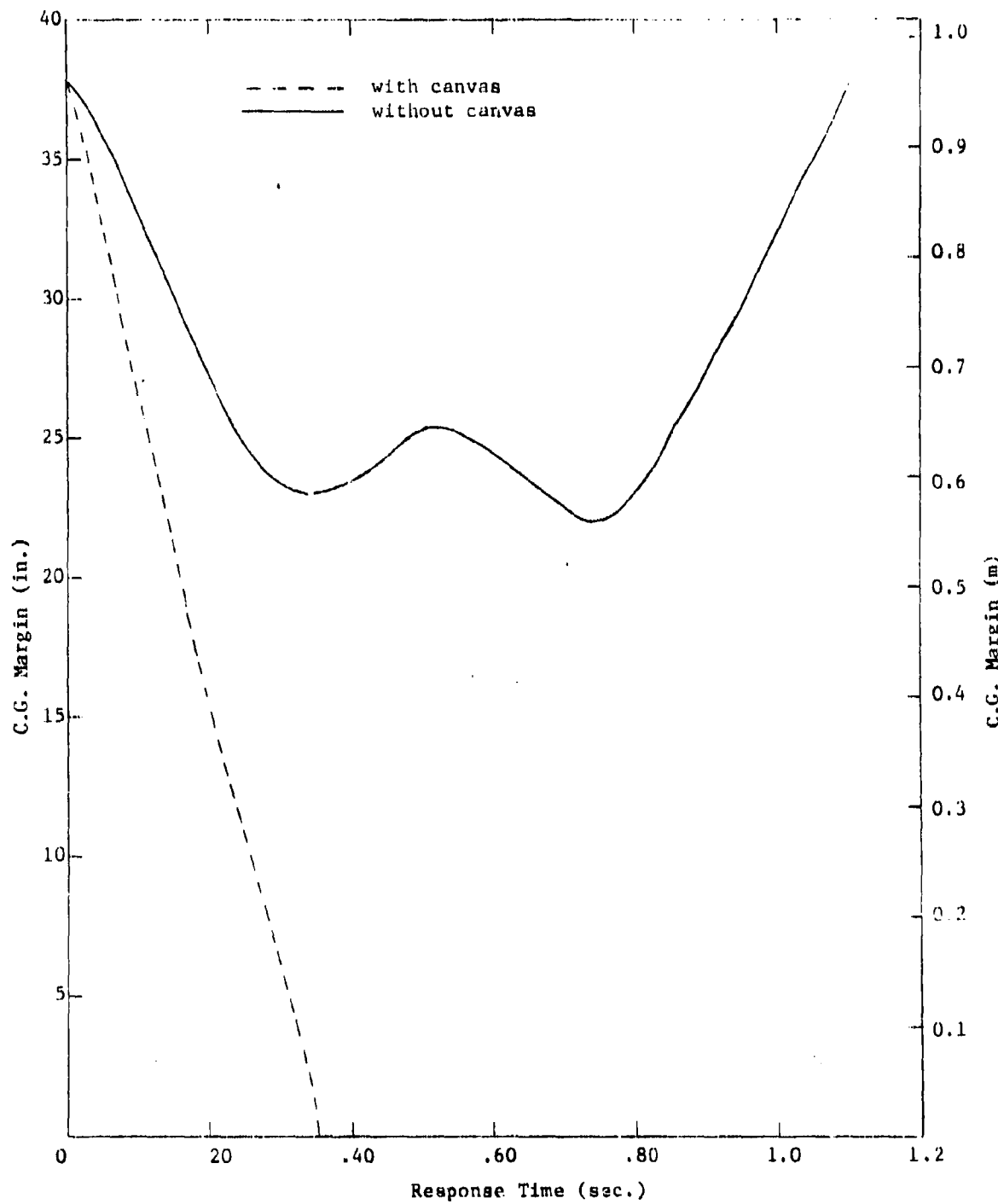


FIGURE 22. C.G. MARGIN TIME-HISTORY FOR RESTRAINED M35A2 LOADED TRUCK  
SUBJECTED TO 12.9 PSI INCIDENT OVERPRESSURE (88.9 kPa)

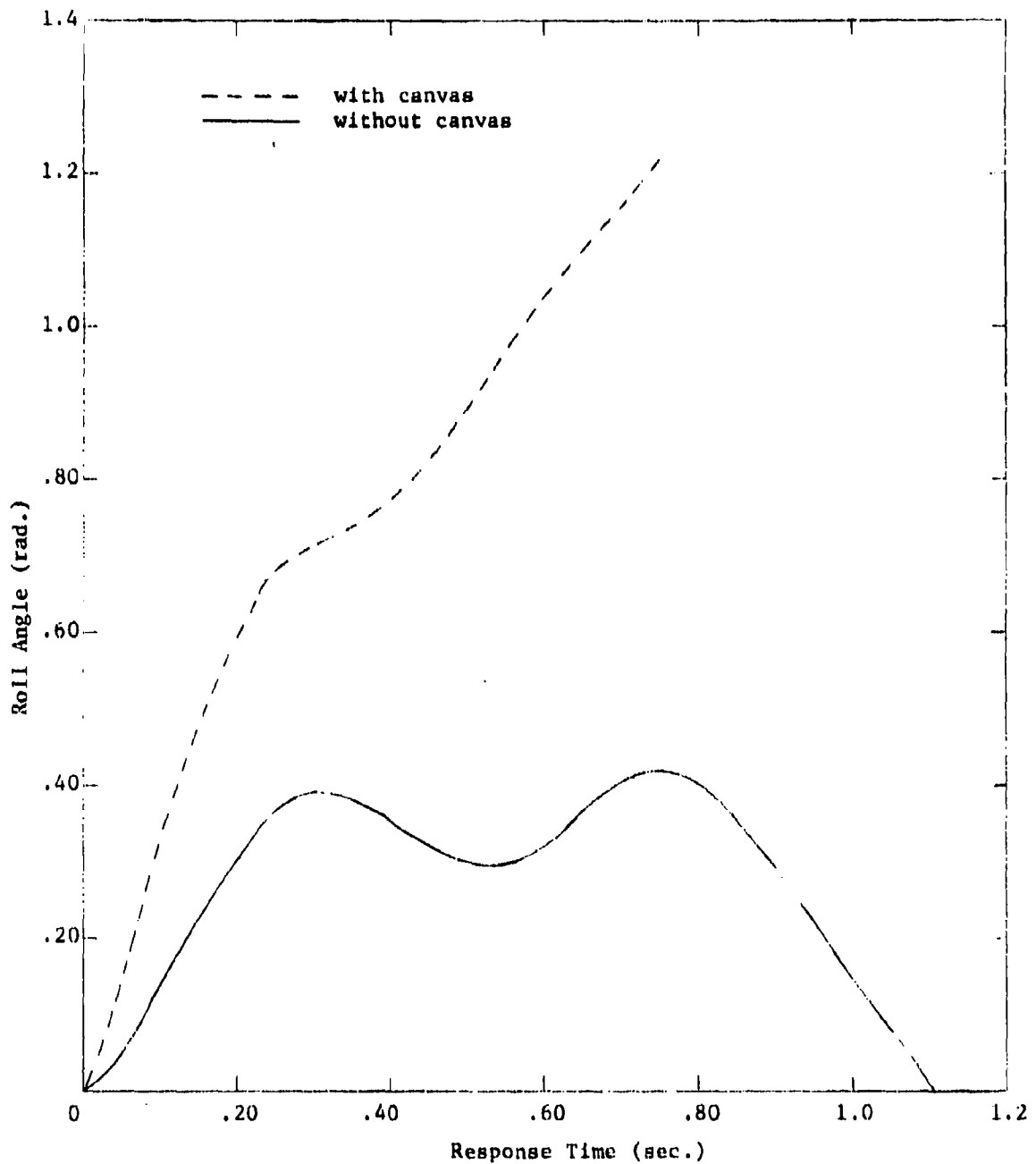


FIGURE 23. ROLL ANGLE TIME-HISTORY FOR RESTRAINED M35A2 LOADED TRUCK  
SUBJECTED TO 12.9 PSI INCIDENT OVERPRESSURE (88.9 kPa)

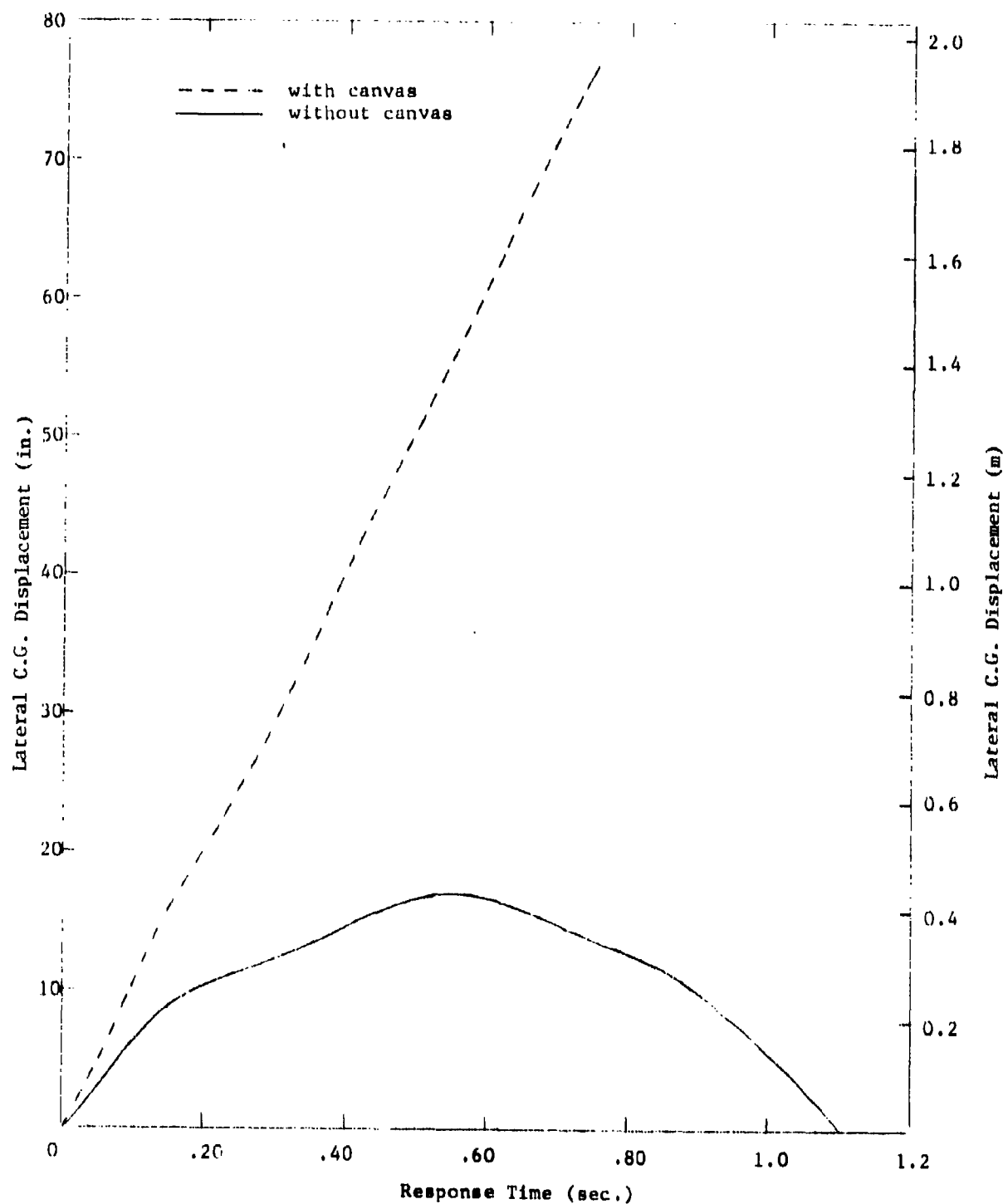


FIGURE 24. LATERAL C.G. DISPLACEMENT TIME-HISTORY FOR RESTRAINED M35A2 LOADED TRUCK SUBJECTED TO 12.9 PSI INCIDENT OVERPRESSURE (88.9 kPa)

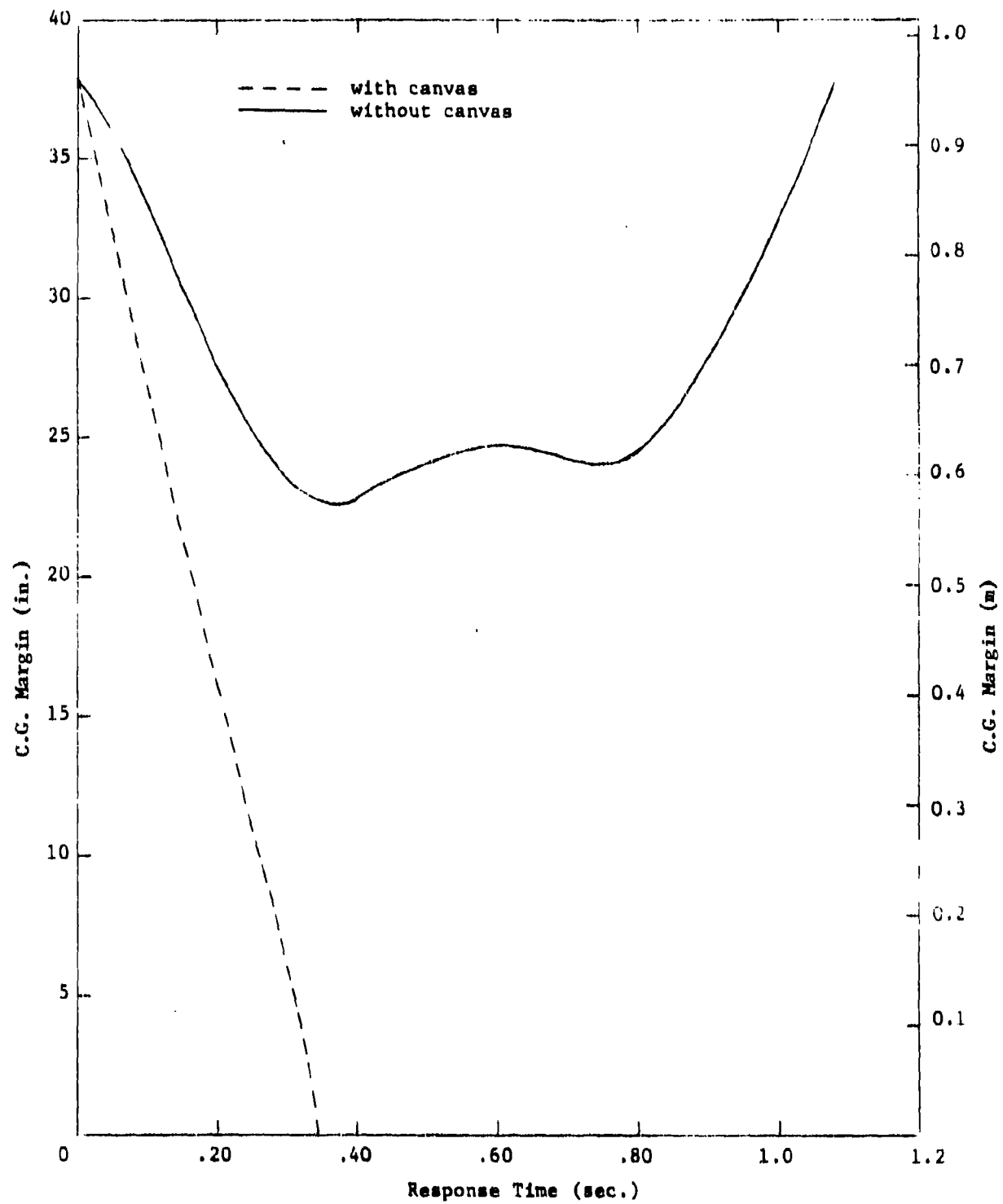


FIGURE 25. C.G. MARGIN TIME-HISTORY FOR UNRESTRAINED M35A2 LOADED TRUCK  
SUBJECTED TO 12.9 PSI INCIDENT OVERPRESSURE (88.9 kPa)

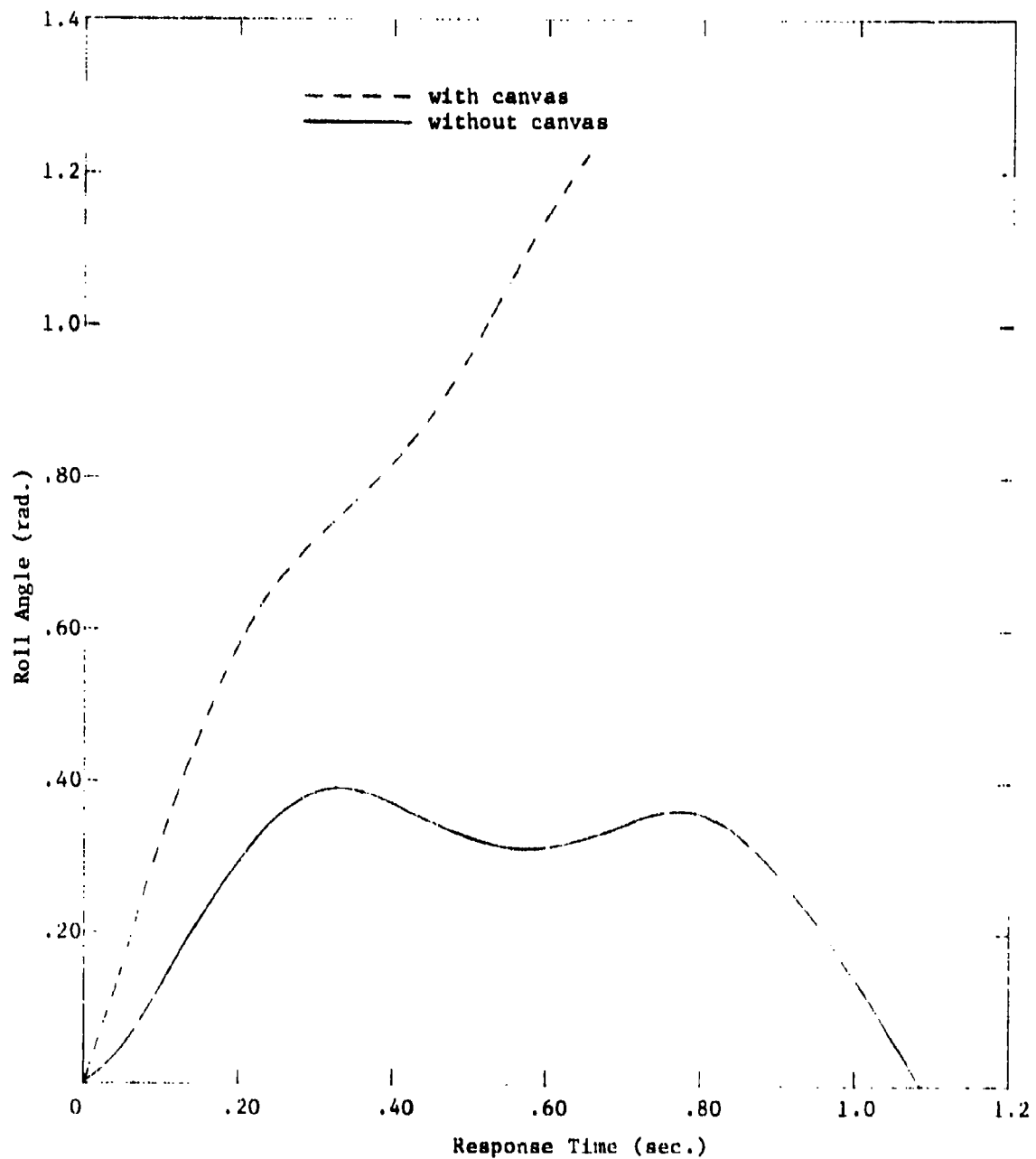


FIGURE 26. ROLL ANGLE TIME-HISTORY FOR UNRESTRAINED M35A2 LOADED TRUCK SUBJECTED TO 12.9 PSI INCIDENT OVERPRESSURE (88.9 kPa)

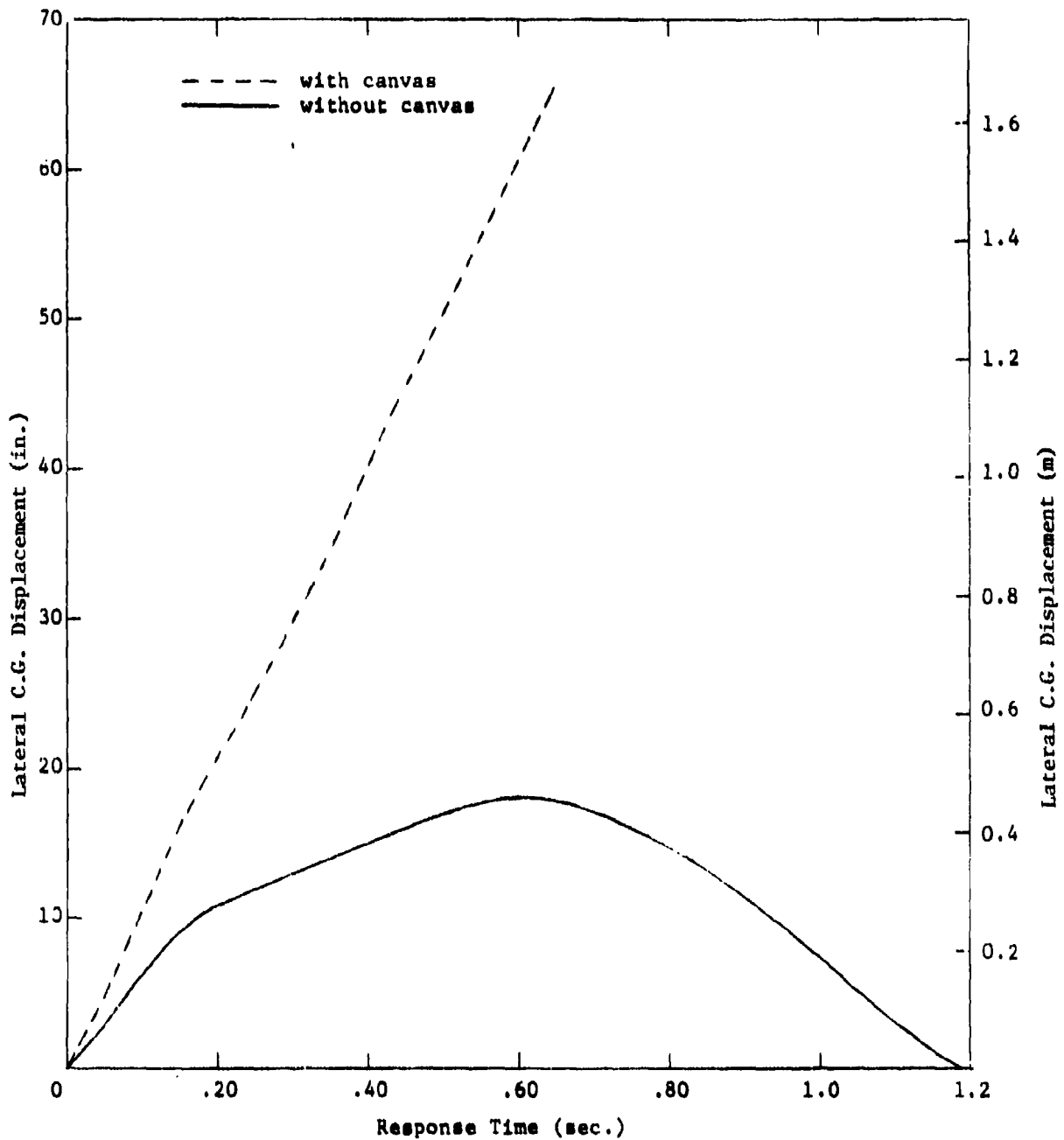


FIGURE 27. LATERAL C.G. DISPLACEMENT TIME-HISTORY FOR UNRESTRAINED M35A2 LOADED TRUCK SUBJECTED TO 12.9 PSI INCIDENT OVERPRESSURE (88.9 kPa)

For the M35A2 loaded truck subjected to the 21.9 psi (151.0 kPa) peak overpressure level, the analytical results are presented in Figures 28-30 for the restrained vehicle and in Figures 31-33 for the unrestrained vehicle. For either restraint condition, the results indicate that both the vehicle with canvas and the vehicle without canvas overturn, with a slight overturning hesitancy showing up in the roll angle time-histories of both vehicles. The same previously noted similarity in total vehicle response between the restrained and unrestrained vehicles is evident.

Based on the premise that the simulated response of the actual M35A2 loaded trucks in the DICE THROW experiment would fall somewhere between the analytical responses of a truck with canvas and a truck without canvas, the analyses conducted indicate overturning of the trucks does occur at the 21.9 psi (151.0 kPa) overpressure level but at the 12.9 psi (88.9 kPa) level a definite conclusion regarding overturning cannot be made. The assumed conditions of restraint for the vehicles have little or no bearing on these conclusions.

Figures 34-36 indicate the analytical response results for the M35A2 truck carrying the modified S-280 communications shelter. As previously mentioned in Section 4, this configuration as fielded in the DICE THROW test was unrestrained from sliding and, hence, only a coefficient of sliding friction of 0.8 was used in the TRUCK analysis. Furthermore, this particular vehicle system was subjected to only one incident overpressure level and, as indicated in Section 6, this level was estimated as 12.064 psi (83.18 kPa).

As indicated in Figure 34, the c.g. margin curve rapidly decreases to a value of zero indicating an overturning vehicle, and both Figure 35 and Figure 36 further confirm this overturning occurrence. It should be noted, however, that although Figures 34-36 indicate entirely reasonable results consistent with the assumed overpressure loading, the validity of accepting these results as indicative of the actual vehicle response is questionable due to the uncertainty of the actual overpressure time-history at Station 223 in the DICE THROW test.

A summary of the vehicle overturning predictions resulting from the TRUCK code analyses of all system configurations reported herein are presented in Table 7.

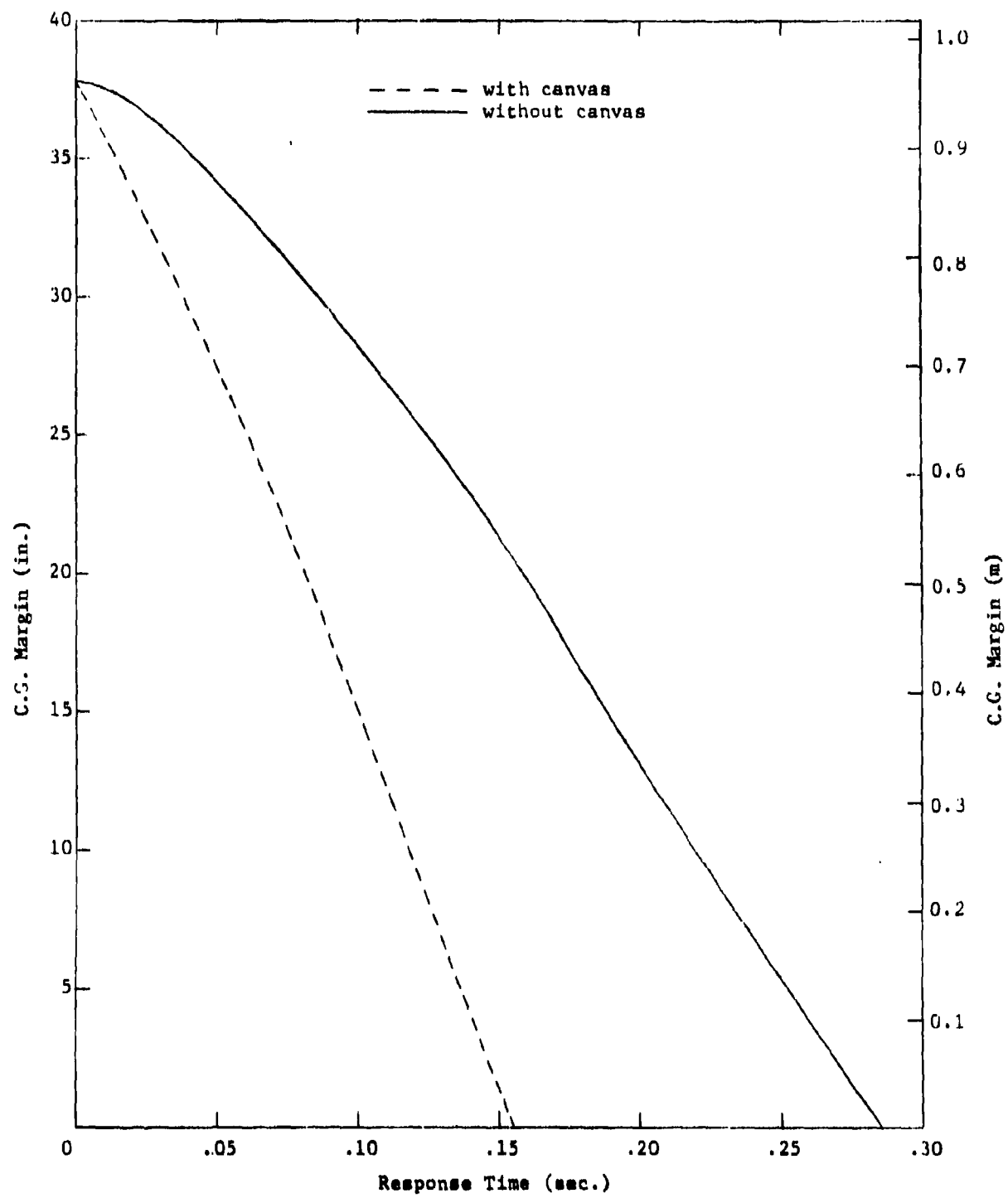


FIGURE 28. C.G. MARGIN TIME-HISTORY FOR RESTRAINED M35A2 LOADED TRUCK  
SUBJECTED TO 21.9 PSI INCIDENT OVERPRESSURE (151.0 kPa)

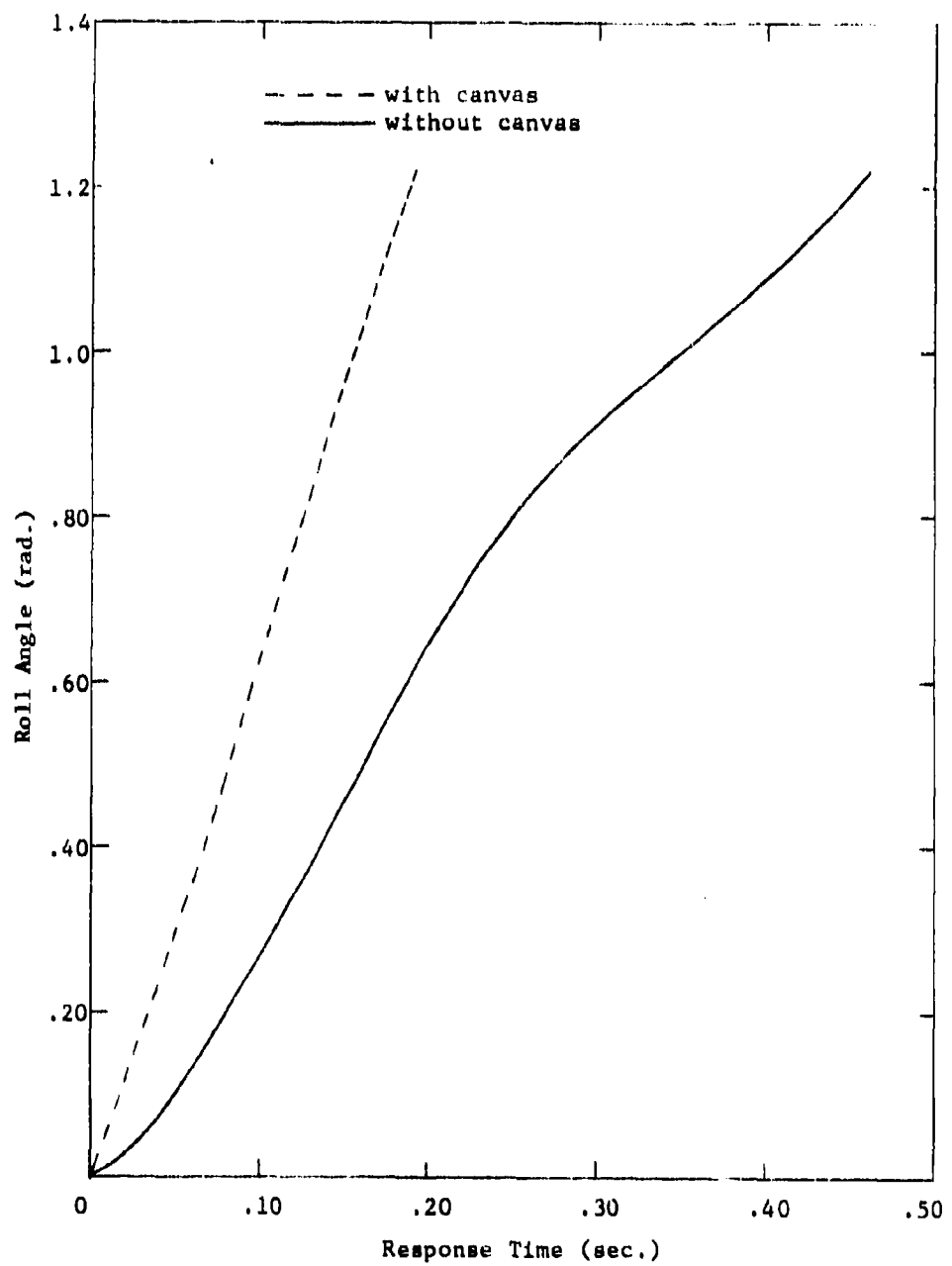


FIGURE 29. ROLL ANGLE TIME-HISTORY FOR RESTRAINED M35A2 LOADED TRUCK SUBJECTED TO 21.9 PSI INCIDENT OVERPRESSURE (151.0 kPa)

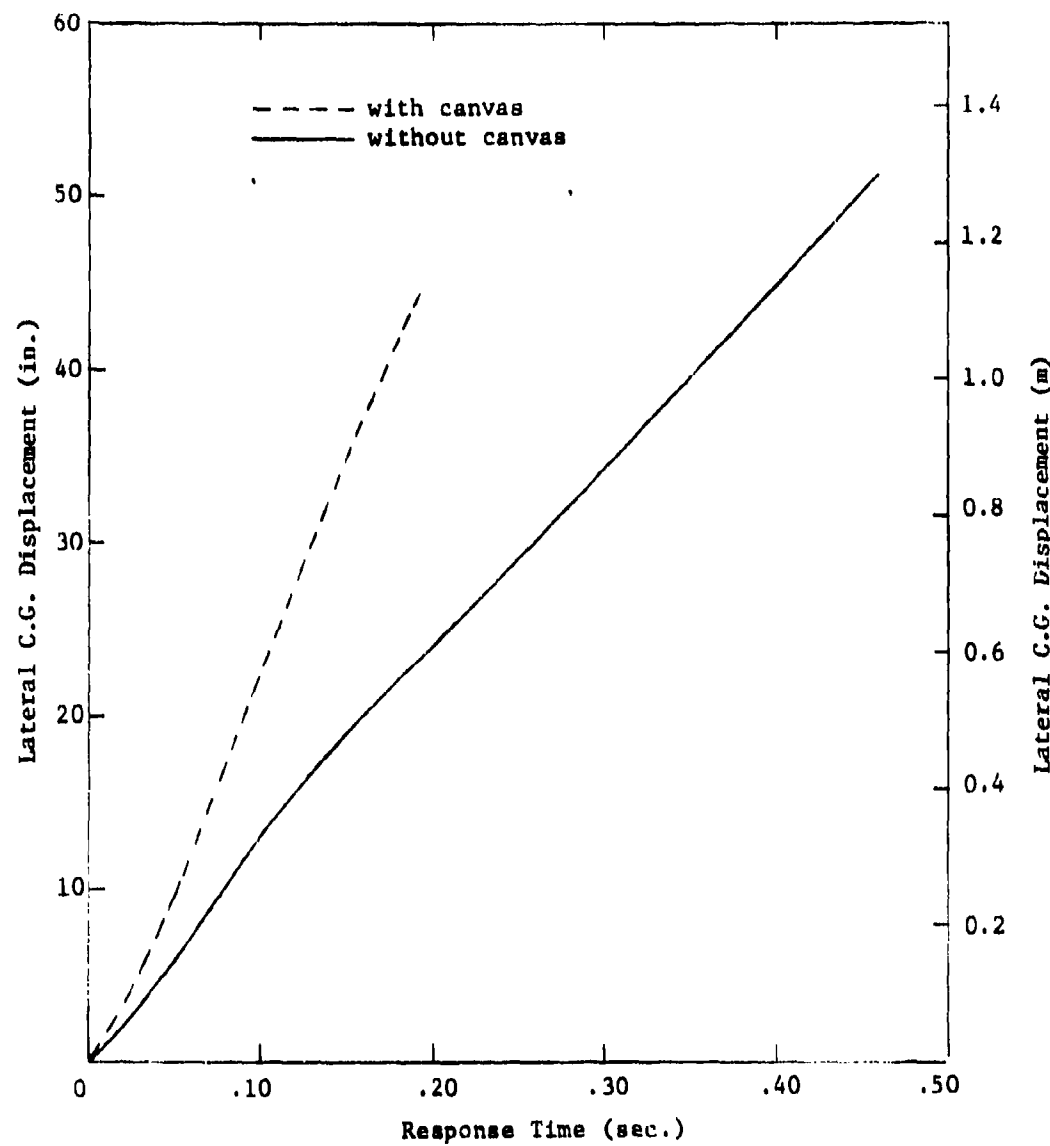


FIGURE 30. LATERAL C.G. DISPLACEMENT TIME-HISTORY FOR RESTRAINED M35A2 LOADED TRUCK SUBJECTED TO 21.9 PSI INCIDENT OVERPRESSURE (151.0 kPa)

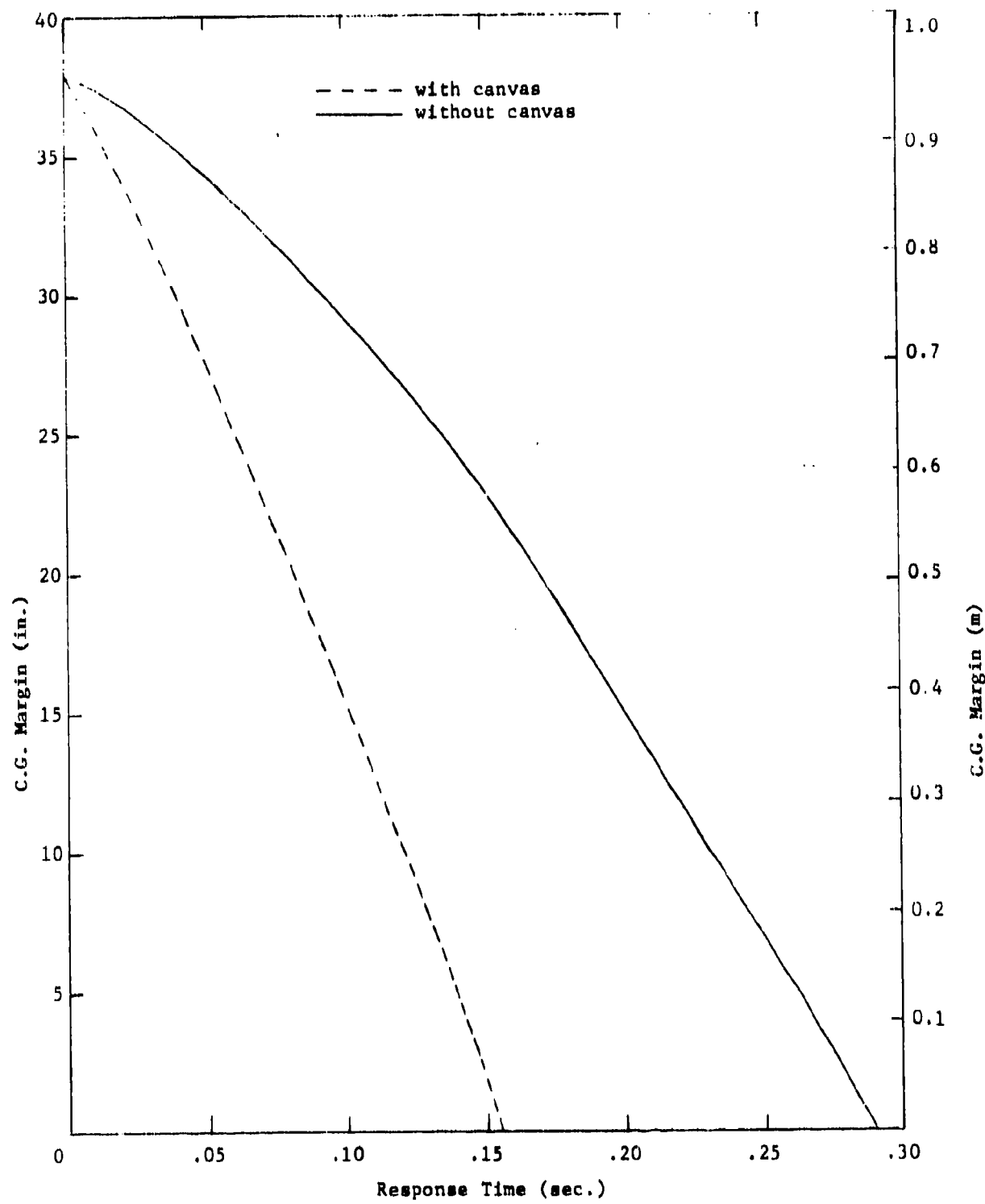


FIGURE 31. C.G. MARGIN TIME-HISTORY FOR UNRESTRAINED M35A2 LOADED TRUCK SUBJECTED TO 21.9 PSI INCIDENT OVERPRESSURE (151.0 kPa)

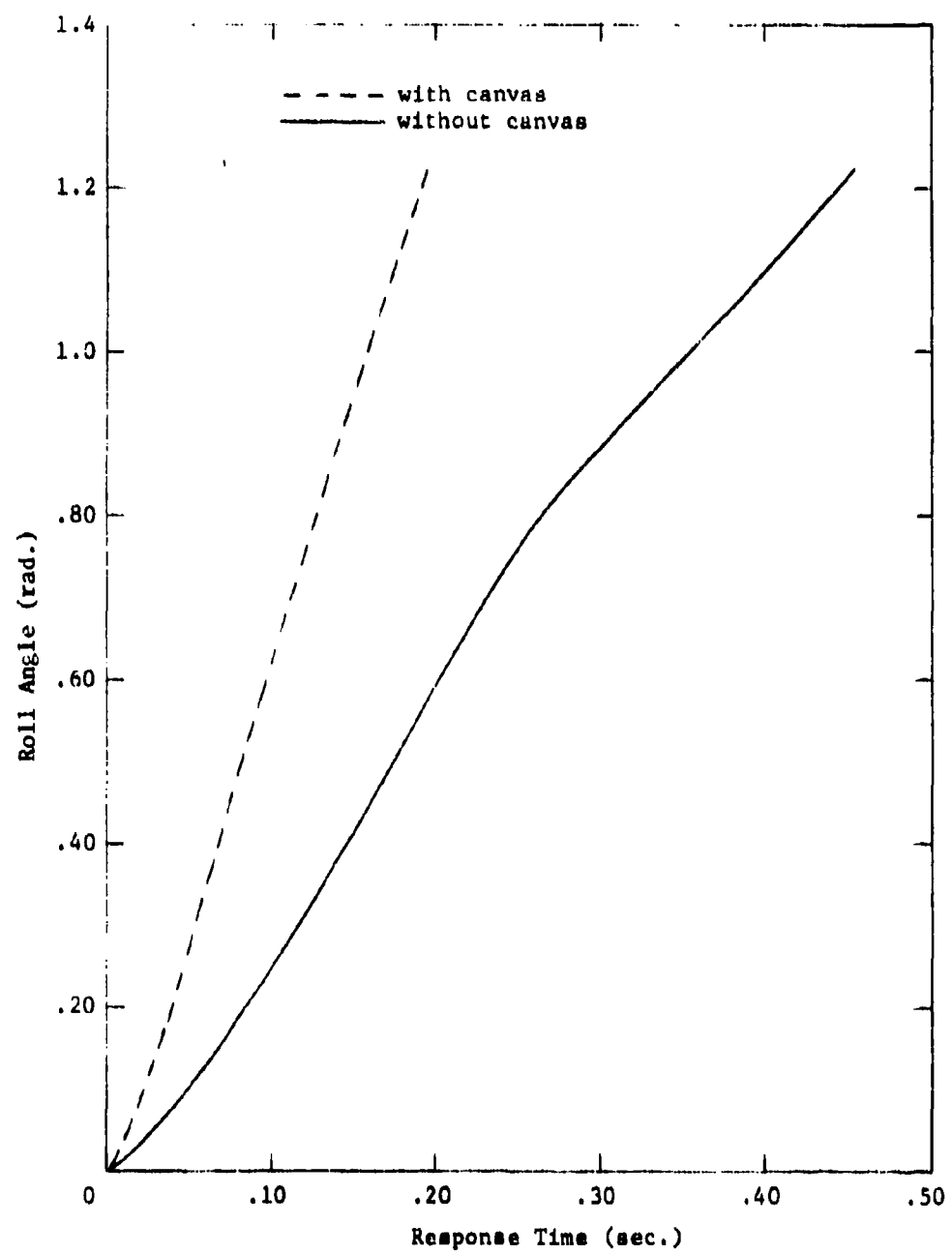


FIGURE 32. ROLL ANGLE TIME-HISTORY FOR UNRESTRAINED M35A2 LOADED TRUCK SUBJECTED TO 21.9 PSI INCIDENT OVERPRESSURE (151.0 kPa)

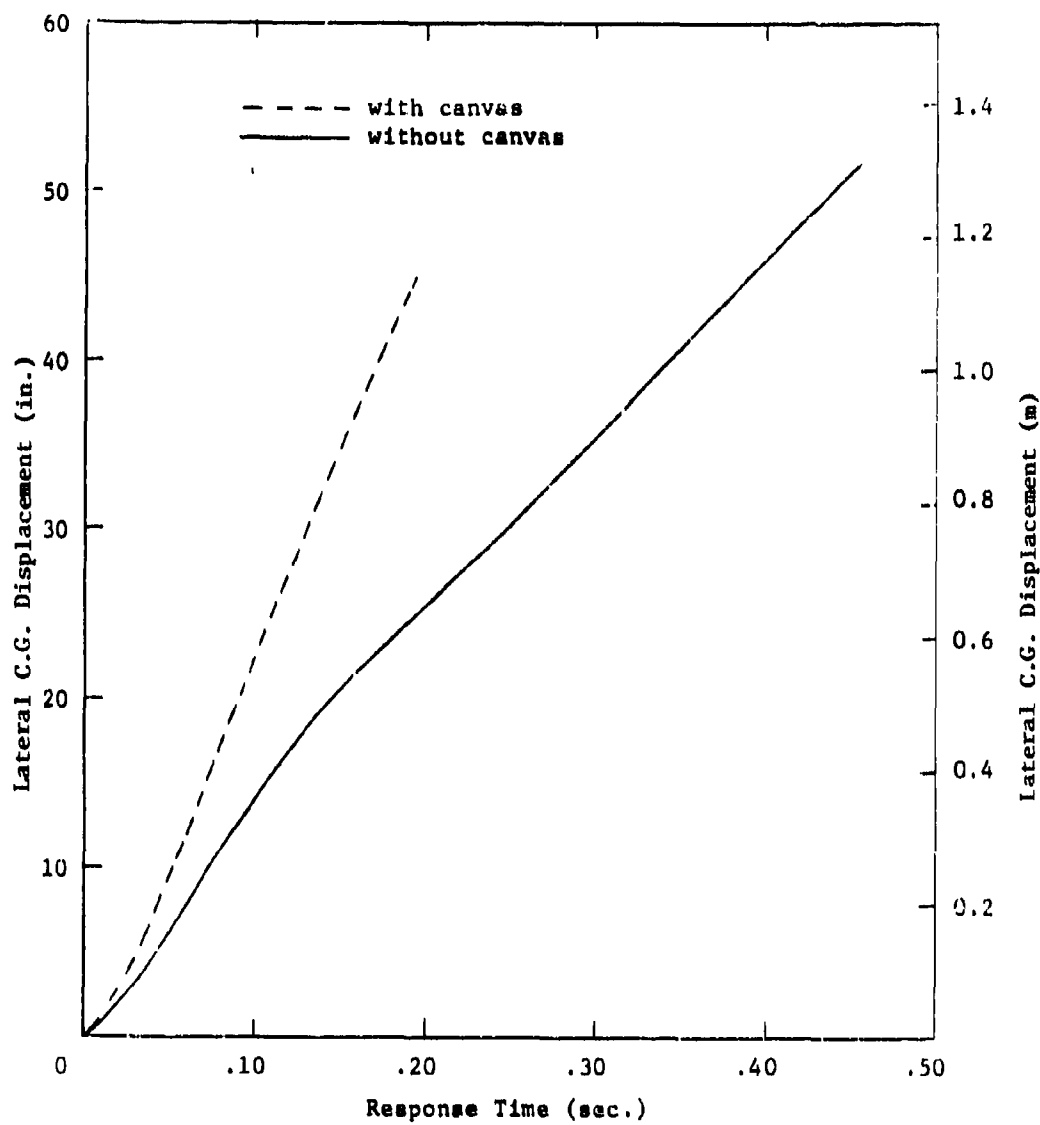


FIGURE 33. LATERAL C.G. DISPLACEMENT TIME-HISTORY FOR UNRESTRAINED M35A2 LOADED TRUCK SUBJECTED TO 21.9 PSI INCIDENT OVERPRESSURE (151.0 kPa)

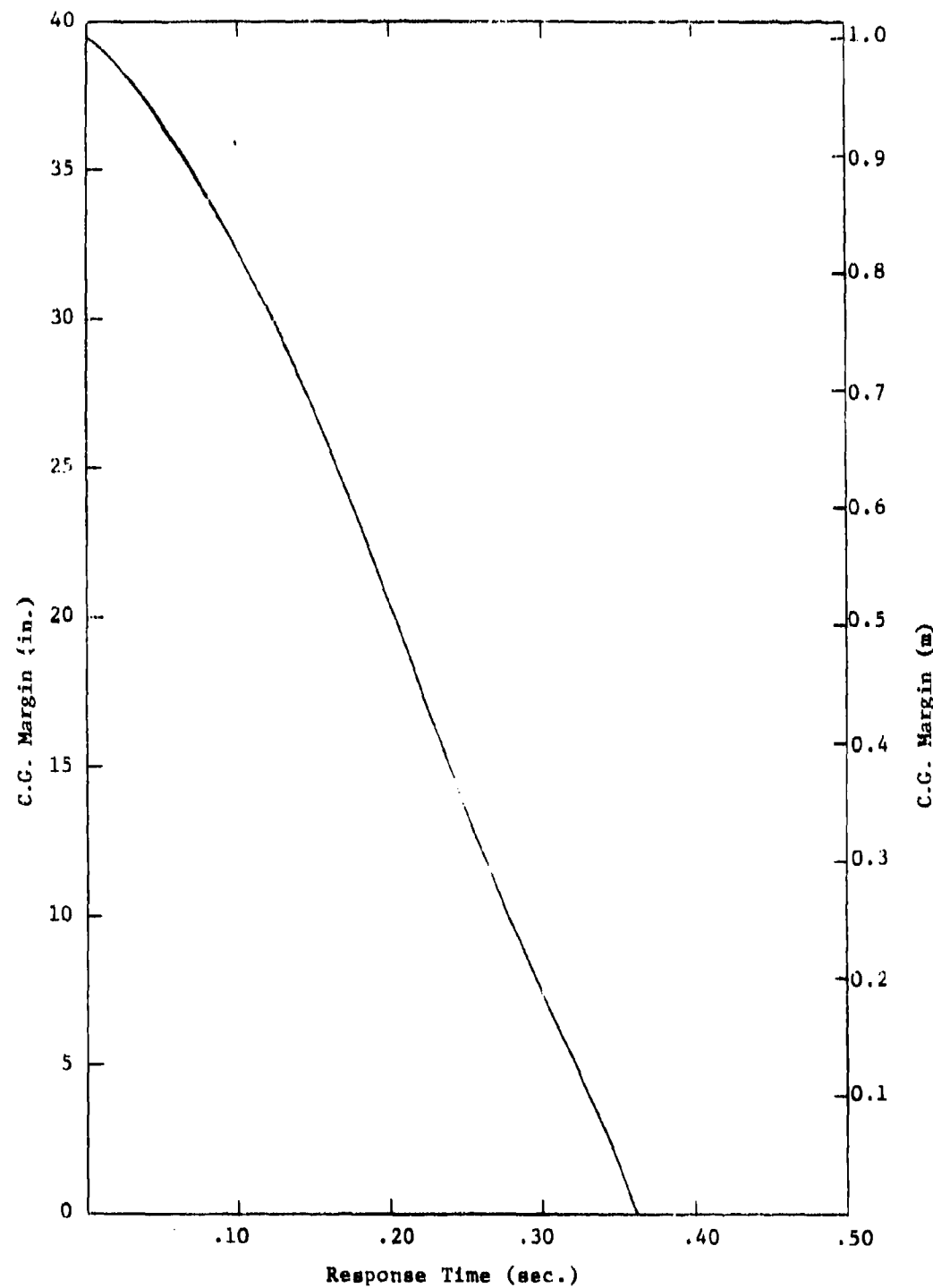


FIGURE 34. C.G. MARGIN TIME-HISTORY FOR M35A2 TRUCK CARRYING S-280 SHELTER

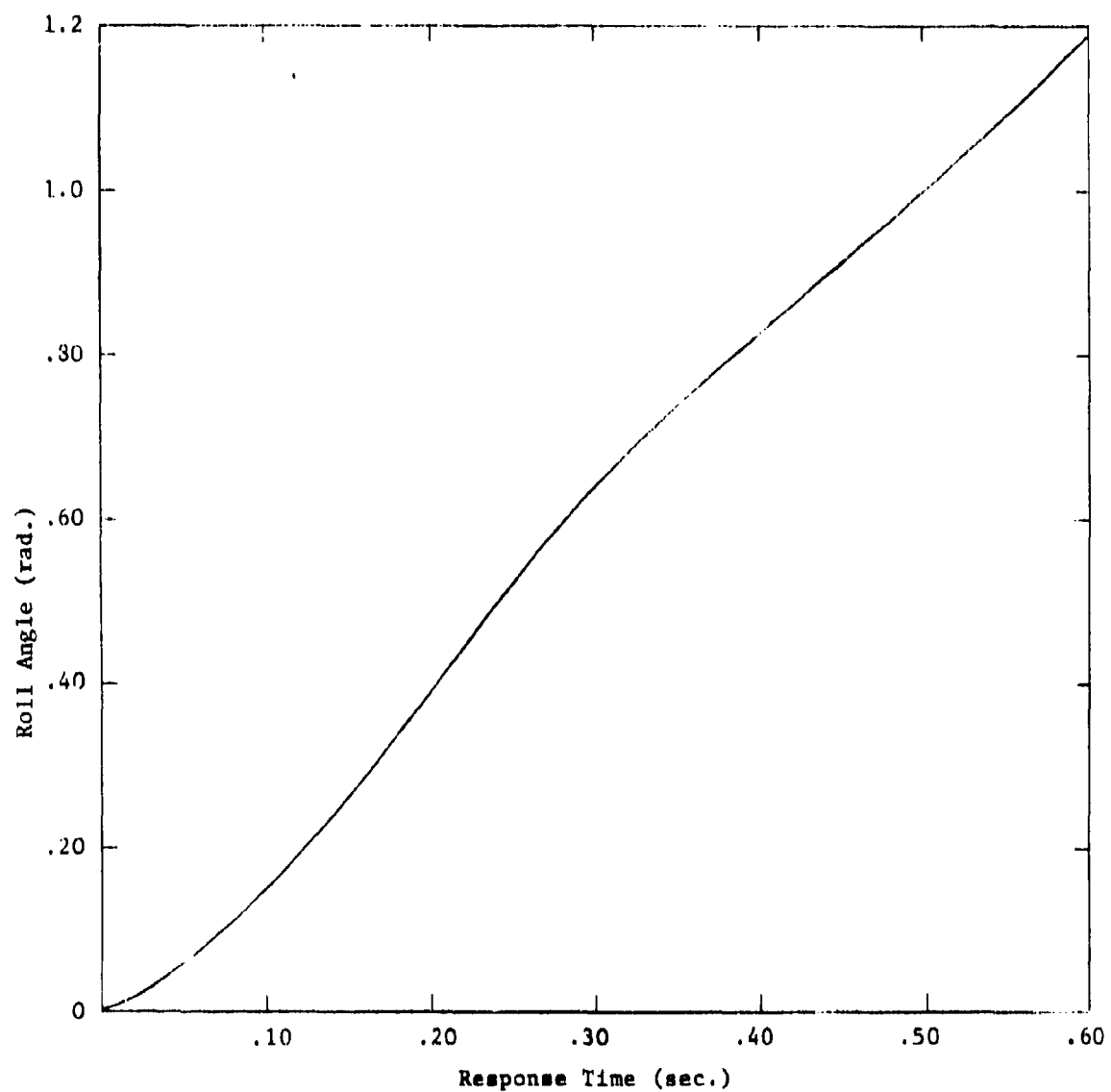


FIGURE 35. ROLL ANGLE TIME-HISTORY FOR M35A2 TRUCK CARRYING S-280 SHELTER

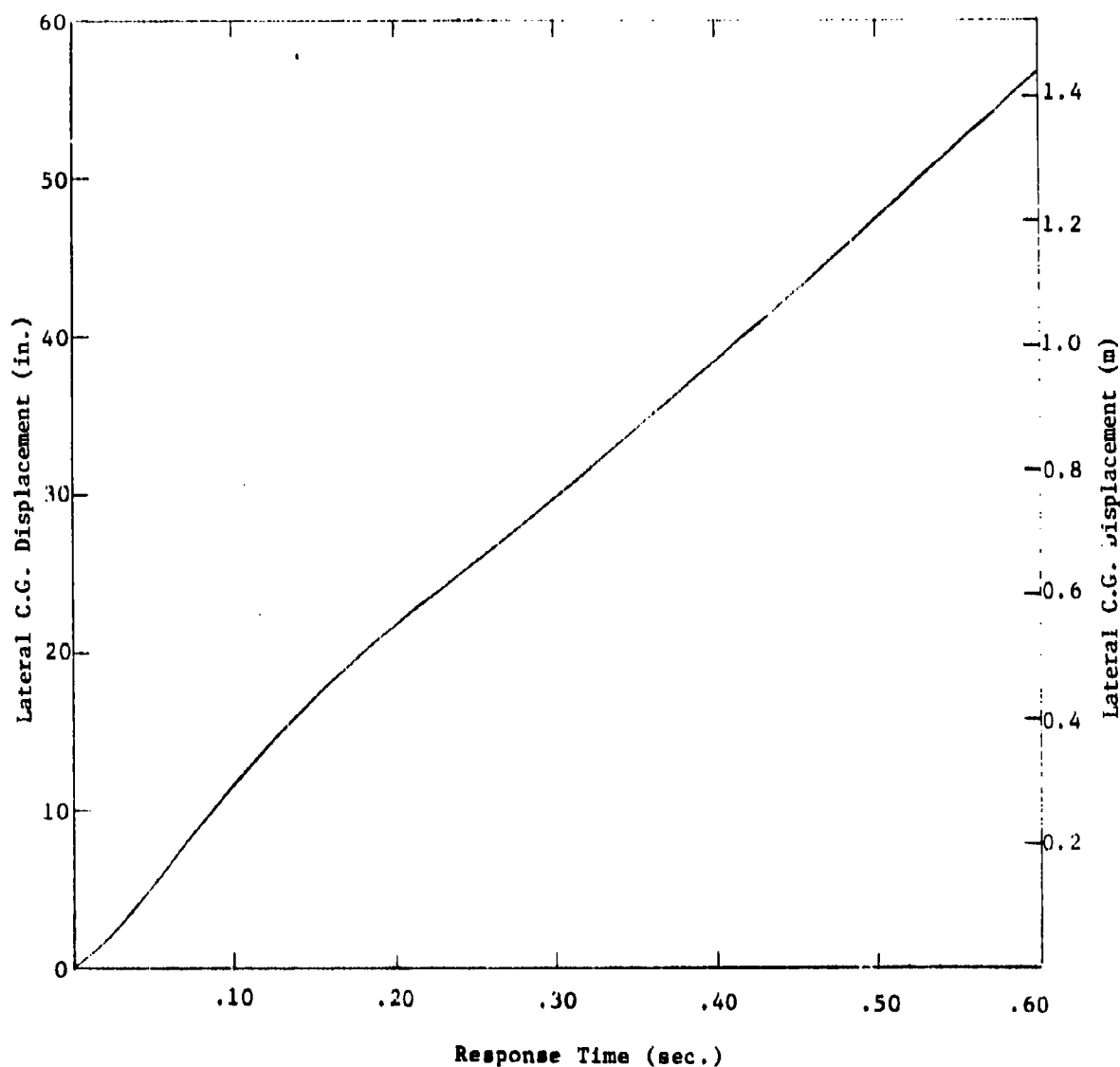


FIGURE 36. LATERAL C.G. DISPLACEMENT TIME-HISTORY FOR M35A2 TRUCK CARRYING S-280 SHELTER

TABLE 7  
SYSTEM CONFIGURATION OVERTURNING PREDICTIONS

System Configuration	Peak Overpressure psi (kPa)	Overshielding Predicted
M35A2 truck, with S-280 shelter (unrestrained)	12.064 (83.18) (assumed)	Yes
M35A2 truck, empty, with stake sides (unrestrained)	13.9 (95.8) 21.6 (148.9)	Yes Yes
M35A2 truck, empty, with stake sides (restrained)	13.9 (95.8) 21.6 (148.9)	Yes Yes
M35A2 truck, loaded with concrete blocks, with canvas top (unrestrained)	12.9 (88.9) 21.9 (151.0)	Yes Yes
M35A2 truck, loaded with concrete blocks, with canvas top (restrained)	12.9 (88.9) 21.9 (151.0)	Yes Yes
M35A2 truck, loaded with concrete blocks, without canvas top (unrestrained)	12.9 (88.9) 21.9 (151.0)	No Yes
M35A2 truck, loaded with concrete blocks, without canvas top (restrained)	12.9 (88.9) 21.9 (151.0)	No Yes
M38A1 jeep, empty, with no canvas (unrestrained)	12.9 (88.9) 21.9 (151.0)	Yes Yes
M38A1 jeep, empty, with no canvas (restrained)	12.9 (88.9) 21.9 (151.0)	Yes Yes

**APPENDIX A**

**INPUT DATA LIST FOR TRUCK CODE  
M35A2 TRUCK, EMPTY**

Gp. 1 - Identification  
M35A2 TRUCK WITH STAKE SIDES, EXPTV

Gp. 2 - Vehicle type  
0

Gp. 3 - Configuration data  
0 0 0 0 0 0 0

Gp. 4 - No. of tires on left end of each axle  
1 2 2

Gp. 5 - No. of springs on left side of each axle  
1 1 2

Gp. 7 - Masses and their locations (lbs-sec<sup>2</sup>/in, inches)  
19.45 0.0 19.69 -65.69  
19.45 0.0 1.0 0.0  
3.705 0.0 0.0 -130.0  
4.483 0.0 0.0 -178.0  
4.483 0.0 0.0

Gp. 8 - Product of inertia of mass 1 (lbs-in-sec<sup>2</sup>)  
1513.0

Gp. 9 - Mass moments of inertia (lbs-in-sec<sup>2</sup>)

11520.0.	119100.	12390.
312.0	2952.0	2844.0
93.26	3381.0	3960.0
93.26	3381.0	3960.0

Gp. 10 - Attachment points for axle springs (inches)  
15.4 10.8 0.0 15.4 5.6 0.6  
15.4 11.19 -10.76 15.4 -3.24  
20.24 5.0 -130.0 20.24 -1.4  
20.24 5.0 -178.0 20.24 0.0  
0.0 0.0 0.0 -130.0  
33.875 -130.0 40.75  
0.0

Gps. 11 and 12 - Coordinates of axles and wheels (inches)

0.0	0.0
33.875	-130.0
0.0	40.75
29.266	

0.0 -178.0  
29.266 40.75

Gp. 13 - Attachment points for bogie springs  
2 20.24

Gp. 18 - Non-linear damping force-velocity curves (lbs, in/sec)

-10000.	3	42000.	0.0	0.0	10000.	-82000.
-10000.	3	160000.	0.0	0.0	10000.	-320000.
-10000.	2	0.0	10000.	0.0		
-10000.	2	0.0	10000.	0.0		
-10000.	3	0.0	10000.	0.0		
-10000.	3	0.0	10000.	0.0		
-10000.	2	0.0	10000.	0.0		
-10000.	2	0.0	10000.	0.0		
-10000.	3	0.0	10000.	0.0		
-10000.	3	0.0	10000.	0.0		

Gp. 19 - Tire damping coefficients (lbs-sec/in)  
2.48 2.48

Gp. 20 - Non-linear spring force-displacement curves (lbs, inches)

-6.2	3	6243.	0.0	0.0	100.	-100700.
-6.2	2	0.0	100.	0.0		
-100.	2	0.0	100.	0.0		
-5.0	2	0.0	100.	0.0		
-5.0	2	0.0	100.	0.0		
-5.0	3	0.0	100.	0.0		
-6.2	3	7161.	0.0	0.0	100.	-115500.

Gp. 21 - Tire non-linear force-normal displacement data (lbs, inches)  
-8.5 26900. -1.125 80.0 0.0 0.0

Gp. 22 - Tire non-linear force-tangential displacement data (lbs, inches)  
0.0 3 0.0 1.125 32.5 10.0 12700.

Gp. 23 - Tire and gravity data (inches, in/sec<sup>2</sup>)  
20.575 1000. 386.0

Gp. 24 - Ground slope data (radians, inches)  
0.0 0.0 1000.

Gp. 25 - Response time and integration time step (seconds)  
1.0 .001

Gp. 26 - No. of time steps between printouts  
25

Gp. 27 - No. of rectangular boxes in aerodynamic model  
3

Gp. 28 - Code designating type of box  
1 1

Gp. 29 - No. of aerodynamic load points on surface (Box 1, Surface 1)  
4

Gps.	30	31	32
29.57	12.36	8.06	1285.9
26.02	37.07	78.06	12.36
29.57	37.07	8.06	1285.9
26.02	12.36	78.06	37.07
29.57	37.07	-43.98	1285.9
76.06	12.36	26.02	37.07
29.57	12.36	-43.98	1285.9
76.06	37.07	26.02	12.36

Gp. 29 - (Box 1, Surface 3)  
4

Gps.	30	31	32
21.25	15.89	54.08	1350.2
63.75	33.54	17.93	15.89
-21.25	15.89	54.08	1350.2
17.93	33.54	63.75	15.89

-14.79	40.60	34.08	521.9
14.79	8.83	44.36	40.59
14.79	40.60	34.08	521.9
44.36	8.83	14.79	40.59

Gp. 29 - (Box 1, Surface 4)  
1

Gps. 30 and 31  
0.0 46.71  
29.57 2.71

Gp. 29 - (Box 1, Surface 5)  
1

Gps. 30 and 31  
0.0 49.42  
BLANK CARD

Gp. 29 - (Box 1, Surface 6)  
1

Gps. 30 and 31  
0.0 0.0  
BLANK CARD

Gp. 29 - (Box 2, Surface 1)  
6

46.5	11.0	-200.5	1122.0
127.5	33.0	25.5	11.0
46.5	11.0	-149.5	1122.0
76.5	33.0	76.5	11.0
46.5	11.0	-98.5	1122.0
25.5	33.0	127.5	11.0
46.5	33.0	-98.5	1122.0
25.5	11.0	127.5	33.0
46.5	33.0	-149.5	1122.0
76.5	11.0	76.5	33.0

46.5	33.0	-209.5	1122.0
127.5	11.0	25.5	33.0

Gp. 29 - (Box 2, Surface 3)  
<sub>4</sub>

Gps. 30 and 31			
-44.5	15.89	-73.0	127.1
2.0	28.11	91.0	15.89
-36.04	37.89	-73.0	207.1
6.47	6.12	84.54	37.89
38.04	37.89	-73.6	207.1
64.54	6.12	8.47	37.89
44.5	15.89	-73.6	127.1
91.0	28.11	2.0	15.89

Gp. 29 - (Box 2, Surface 4)  
<sub>4</sub>

Gps. 30 and 31			
23.25	11.0	-226.0	1023.0
23.25	33.0	69.75	11.0
23.25	33.0	-226.0	1023.0
23.25	11.0	69.75	33.0
-23.25	33.0	-226.0	1023.0
69.75	11.0	23.25	33.0
-23.25	11.0	-226.0	1023.0
69.75	33.0	23.25	11.0

Gp. 29 - (Box 2, Surface 5)  
<sub>1</sub>

Gps. 30 and 31			
0.0	30.0	-149.5	14229.0
BLANK CARD			

Gp. 29 - (Box 2, Surface 6)  
<sub>1</sub>

Gps. 30 and 31      0.0      0.0      -149.5      14229.0  
BLANK CARD

Gp. 29 - (Box 3, Surface 1)  
6

Gps. 30 and 31      49.63      -198.5      431.81  
46.5      2.20      24.5      0.73  
122.5      49.63      -149.5      431.81  
46.5      2.20      73.5      0.73  
73.5      2.20      -100.5      431.81  
46.5      49.63      -122.5      0.73  
24.5      2.20      -100.5      431.81  
46.5      60.88      122.5      0.73  
24.5      2.20      149.5      431.81  
46.5      60.88      73.5      0.73  
73.5      2.20      -198.5      431.81  
46.5      60.88      24.5      0.73  
122.5      2.20

Gp. 29 - (Box 3, Surface 3)  
3

Gps. 30 and 31      55.25      -76.0      298.39  
36.04      2.20      6.47      0.73  
84.54      57.96      -76.0      817.91  
0.0      2.20      46.5      0.73  
46.5      55.25      -76.0      298.39  
-36.04      2.20      34.54      0.73  
8.47

Gp. 29 - (Box 3, Surface 4)  
4

Gps. 30 and 31      49.63      -76.0      409.78  
-23.25      2.20      23.25      0.73  
69.75      49.63      -76.0      409.78  
23.25      2.20      69.75      0.73  
23.25      60.88      -76.0      409.78  
23.25

23.25	2.20	69.75	0.73
-23.25	60.66	-76.0	409.78
69.75	2.20	23.25	0.73

Gp. 29 - (Box 3, Surface 5)  
0

Gp. 29 - (Box 3, Surface 6)  
0

Gp. 32 - Code for controlling iteration  
0 1

Gp. 33 - Blast data (psi, degrees, KT, feet)  
1. 0. 0.  
BLANK CARD  
END  
0250.

**APPENDIX B**

**INPUT DATA LIST FOR TRUCK CODE  
M35A2 TRUCK, LOADED, WITH CANVAS**

Gp. 1 - Identification  
**M55A2 WITH CANVAS TOP LOADED WITH CONCRETE BLOCKS**

Gp. 2 - Vehicle type  
 0

Gp. 3 - Configuration data  
 0 0 0 0

Gp. 4 - No. of tires on left end of each axle  
 1 2 2

Gp. 5 - No. of springs on left side of each axle  
 2 1 1

Gp. 7 - Masses and their locations (lbs-sec<sup>2</sup>/in, inches)

33.44	0.0	26.63	-100.54
3.705	0.0	1.0	0.0
4.483	0.0	0.3	-130.0
4.483	0.0	0.0	-178.0

Gp. 8 - Product of inertia of mass 1 (lbs-in-sec<sup>2</sup>)  
 -11020.

Gp. 9 - Mass moments of inertia (lbs-in-sec<sup>2</sup>)

195900.	199200.	19890.	0.0
312.0	2952.0	2844.0	-3.24
93.26	3381.0	3960.0	-1.4
93.26	3381.0	3960.0	0.0
			-150.0
			-178.0

Gp. 10 - Attachment points for axle springs (inches)

15.4	10.8	0.0	15.4	5.6
15.4	11.19	-10.76	15.4	-1.4
20.24	5.0	-130.0	20.24	0.0
20.24	5.0	-173.0	20.24	0.0

Gps. 11 and 12 - Coordinates of axles and wheels (inches)

0.0	0.0
33.875	
0.0	-130.0
29.266	40.75

0.0      -174.0  
 29.266      40.75

Gp. 13 - Attachment points for bogie springs  
 2<sup>2</sup>0<sub>2</sub>4<sup>2</sup>4

Gp. 18 - Non-linear damping force-velocity curves (lbs, in/sec)

-10000.	3	42000.	0.0	0.0	10000.	-12000.
-10000.	3	168000.	0.0	0.0	10000.	-326000.
-10000.	2	0.0	10000.	0.0		
-10000.	2	0.0	10000.	0.0		
-10000.	3	0.0	10000.	0.0		
-10000.	3	84000.	0.0	0.0	10000.	-164000.

Gp. 19 - Tire damping coefficients (lbs-sec/in)  
 2<sup>2</sup>48<sup>2</sup>48

Gp. 20 - Non-linear spring force-displacement curves (lbs, inches)

-6.2	3	6243.	0.0	0.0	190.	-100700.
-100.	2	0.0	100.	0.0		
-5.0	0.0	100.	0.0	0.0		
-5.0	2	0.0	100.	0.0		
-6.2	7161.	0.0	0.0	100.		-115500.

Gp. 21 - Tire non-linear force-normal displacement data (lbs, inches)  
 2<sup>2</sup>6900. -125 40.0 0.0 0.0

Gp. 22 - Tire non-linear force-tangential displacement data (lbs, inches)  
 3 0.0 0.0 32.5 16.0 12700.

Gp. 23 - Tire and gravity data (inches, in/sec<sup>2</sup>)  
20.375 1000.0  
350.0

Gp. 24 - Ground slope data (radians, inches)  
0.1 0.0  
1000.

Gp. 25 - Response time and integration time step (seconds)  
1.5 .001

Gp. 26 - No. of time steps between printouts  
25

Gp. 27 - No. of rectangular boxes in aerodynamic model  
3

Gp. 28 - Code designating type of box  
1 1

Gp. 29 - No. of aerodynamic load points on surface (Box 1, Surface 1)  
4

Gps. 30 and 31 - Loading information (inches, in<sup>2</sup>)  
24.57 12.36 9.06 1285.9  
26.52 37.07 78.06 12.36  
29.57 37.07 6.06 1285.9  
26.02 12.36 78.06 37.07  
29.57 37.07 -43.9A 1285.9  
76.06 12.36 26.02 37.07  
29.57 12.36 -43.9A 1285.9  
76.06 37.07 26.02 12.36

Gp. 29 - (Box 1, Surface 3)  
4

Gps. 30 and 31  
21.25 15.89 34.08 1350.2  
63.75 33.54 17.93 15.89  
-21.25 15.89 34.08 1350.2  
17.93 33.54 03.75 15.89

-14.79	40.60	54.95	121.4
14.79	8.45	41.56	40.59
14.79	40.60	53.08	521.9
34.56	8.43	14.79	40.54

Gp. 29 - (Box 1, Surface 4)  
6

Gp. 29 - (Box 1, Surface 5)  
1

Gps. 30 and 31  
0.0 49.42 -17.46 6846.6  
BLANK CARD

Gp. 29 - (Box 1, Surface 6)  
1

Gps. 30 and 31  
0.0 0.0 -17.46 9446.6  
BLANK CARD

Gp. 29 - (Box 2, Surface 1)  
6

46.5	11.3	-20.5	1122.0
127.5	77.24	25.5	11.0
46.5	11.0	-14.5	1122.0
76.5	77.24	79.5	11.0
46.5	11.0	-48.5	1122.0
25.5	77.24	127.5	11.0
46.5	33.0	-9.5	1122.0
25.5	55.24	127.5	33.0
46.5	33.0	-14.5	1122.0
76.5	75.24	75.5	33.0
46.5	33.0	-20.5	1122.0
127.5	55.24	25.5	33.0

Gp. 29 - (Box 2, Surface 3)  
4

Gps. 30 and 31			
-44.5	15.34	-74.6	127.1
2.0	72.35	91.0	15.89
-33.04	37.84	-73.0	207.1
4.47	50.36	84.54	37.49
50.04	37.89	-73.0	207.1
84.54	50.36	9.47	57.89
44.5	15.84	-73.0	127.1
91.0	72.35	2.0	15.89

Gp. 29 - (Box 2, Surface 4)  
4

Gps. 30 and 31			
25.25	11.0	-226.0	1023.0
23.25	77.24	69.75	11.0
23.25	33.0	-226.0	1023.0
23.25	55.24	69.75	53.0
-23.25	53.0	-226.0	1023.0
59.75	55.24	25.25	53.0
-23.25	11.0	-226.0	1023.0
69.75	77.24	25.25	11.0

Gp. 29 - (Box 2, Surface 5)  
0

Gp. 29 - (Box 2, Surface 6)  
1

Gps. 30 and 31			
0.0	0.0	-142.5	14224.0
41.42	41.42		

Gp. 29 - (Box 3, Surface 1)  
6

Gps. 30 and 31			
46.5	55.00	-144.5	1085.9

122.5	33.18	24.7	55.96
46.5	55.06	-140.5	1083.9
73.5	33.19	75.5	55.06
46.5	55.06	-130.5	1083.9
24.5	33.18	122.5	55.06
46.5	77.18	-100.5	1083.9
24.5	11.06	122.5	77.18
46.5	77.18	-149.5	1083.9
73.5	11.06	75.5	77.18
46.5	77.18	-198.5	1083.9
122.5	11.06	24.5	77.18

Gp. 29 - (Box 3, Surface 3)

Gps. 30 and 31			
38.04	66.12	-10.0	149.0
84.54	22.12	8.46	66.12
0.0	68.63	-75.0	2295.8
46.5	19.41	46.5	68.84
-38.04	66.12	-76.0	749.0
8.46	22.12	64.54	66.12

Gp. 29 - (Box 3, Surface 4)

Gps. 30 and 31			
-23.25	55.16	-224.1	1024.6
69.75	55.16	25.25	55.06
23.25	55.06	-225.0	1024.6
23.25	33.18	69.75	55.06
23.25	77.18	-225.0	1024.6
23.25	11.06	64.75	77.18
-23.25	17.18	-225.0	1024.6
69.75	11.06	25.25	77.18

Gp. 29 - (Box 3, Surface 5)

Gps. 30 and 31	0.0	08.24	-149.5	14229.0
BLANK CARD				

Gp. 29 - (Box 3, Surface 6)  
0

Gp. 32 - Code for controlling iteration

APPENDIX C

INPUT DATA LIST FOR TRUCK CODE  
M35A2 TRUCK, WITH S280 SHELTER

Gp. 1 - Identification  
**M35A2-S280 SHELLER, SHELTER AND HEAVY RACKS VISIBLY ATTACHED**

Gp. 2 - Vehicle type  
**0**

Gp. 3 - Configuration data  
**0**

Gp. 4 - No. of tires on left end of each axle  
**1 2 2**

Gp. 5 - No. of springs on left side of each axle  
**2 1 1**

Gp. 7 - Masses and their locations (lbs-sec<sup>2</sup>/in, inches)

<b>35.52</b>	<b>0.0</b>	<b>42.97</b>	<b>-103.59</b>
<b>3.705</b>	<b>0.0</b>	<b>1.0</b>	<b>0.0</b>
<b>4.483</b>	<b>0.0</b>	<b>0.9</b>	<b>-130.0</b>
<b>4.483</b>	<b>0.0</b>	<b>0.1</b>	<b>-178.0</b>

Gp. 8 - Product of inertia of mass 1 (lbs-in-sec<sup>2</sup>)  
**-38080.**

Gp. 9 - Mass moments of inertia (lbs-in-sec<sup>2</sup>)

<b>241400.</b>	<b>228200.</b>	<b>62750.</b>
<b>312.0</b>	<b>2952.0</b>	<b>2944.0</b>
<b>93.26</b>	<b>3381.0</b>	<b>3959.0</b>
<b>93.26</b>	<b>3381.0</b>	<b>5550.0</b>

90

Gp. 10 - Attachment points for axle springs (inches)

<b>15.4</b>	<b>10.8</b>	<b>0.0</b>	<b>15.4</b>	<b>5.6</b>	<b>0.0</b>
<b>15.4</b>	<b>11.19</b>	<b>-10.76</b>	<b>15.4</b>	<b>-1.4</b>	<b>-1.24</b>
<b>20.24</b>	<b>5.0</b>	<b>-131.0</b>	<b>20.24</b>	<b>0.0</b>	<b>-130.0</b>
<b>20.24</b>	<b>5.0</b>	<b>-173.0</b>	<b>20.24</b>	<b>0.0</b>	<b>-175.0</b>

Gps. 11 and 12 - Coordinates of axles and wheels (inches)

<b>0.0</b>	<b>0.0</b>
<b>33.875</b>	
<b>0.0</b>	<b>-150.0</b>
<b>29.264</b>	<b>40.75</b>

0.0	-178.0
29.266	40.75

Gp. 13 - Attachment points for bogie springs  
 $\begin{matrix} 2 \\ 20.24 \end{matrix}$

Gp. 18 - Non-linear damping force-velocity curves (lbs, in/sec)

-10000.	42000.	0..0	0.0	10000.	-20000.
-10000.	160000.	0..0	0.0	10000.	-320000.
-10000.	0..0	10000.	0.0		
-10000.	0..0	10006.	0.0		
-10000.	84000.	0..0	0.0	10000.	-164000.

Gp. 19 - Tire damping coefficients (lbs-sec/in)  
 $\begin{matrix} 2.48 \\ 2.48 \end{matrix}$

Gp. 20 - Non-linear spring force-displacement curves (lbs, inches)

-6.2	6243.	0..0	0..0	100.	-10.700.
-100.	0..0	100.	0..0		
-5..0	0..0	100.	0..0		
-5..0	0..0	100.	0..0		
-6..2	7161.	0..0	0..0	100.	-115500.

Gp. 21 - Tire non-linear force-normal displacement data (lbs, inches)  
 $\begin{matrix} 3 \\ -8.5 \end{matrix}$

26900.	-0.125	80.0	0..0	0..0
0..0	0..0	125	32.5	1..0..0
				12700.

Gp. 22 - Tire non-linear force-tangential displacement data (lbs, inches)

Gp. 23 - Tire and gravity data (inches, in/sec<sup>2</sup>)  
20.375 0.8 536.0

Gp. 24 - Ground slope data (radians, inches)  
0.0 0.6 100.0.

Gp. 25 - Response time and integration time step (seconds)  
1.5 .001

Gp. 26 - No. of time steps between printouts  
25

Gp. 27 - No. of rectangular boxes in aerodynamic model  
3

Gp. 28 - Code designating type of box  
1 1 1

Gp. 29 - No. of aerodynamic load points on surface (Box 1, Surface 1)  
4

Gps. 30 and 31 - Loading information (inches, in<sup>2</sup>)  
29.57 12.36 8.06 1285.9  
26.02 37.07 78.36 12.36  
29.57 37.07 6.06 1285.9  
26.02 12.36 78.96 37.07  
29.57 37.07 -43.98 1285.9  
78.06 12.36 26.02 37.07  
29.57 12.36 -43.98 1285.9  
78.06 37.07 26.02 12.36

Gp. 29 - (Box 1, Surface 3)  
4

Gps. 30 and 31  
21.25 15.89 34.09 1350.2  
63.75 33.54 17.93 15.89  
-21.25 15.89 33.98 1350.2  
17.93 33.54 63.75 15.89

-14.79	40.60	54.08	521.9
14.79	8.83	44.36	40.59
14.79	40.60	34.08	521.9
44.36	8.83	14.79	40.59

Gp. 29 - (Box 1, Surface 4)  
0

Gp. 29 - (Box 1, Surface 5)  
1

Gps. 30 and 31  
0.0  
BLANK CARD

Gp. 29 - (Box 1, Surface 6)  
1

Gps. 30 and 31  
0.0  
BLANK CARD

Gp. 29 - (Box 2, Surface 1)  
6

46.5	11.0	-200.5	1122.0
127.5	101.17	27.5	11.6
46.5	11.0	-149.5	1122.0
76.5	101.17	76.5	11.0
46.5	11.0	-93.5	1122.0
25.5	101.17	127.5	11.0
46.5	33.0	-94.5	1122.0
25.5	79.17	127.5	33.0
46.5	33.0	-149.5	1122.0
76.5	79.17	75.5	33.0
46.5	33.0	-200.5	1122.0
127.5	79.17	25.5	33.0

Gp. 29 - (Box 2, Surface 3)  
4

Gps. 30 and 31				
-44.5	15.89	-73.0	127.1	
2.0	96.28	91.0	15.69	
-38.04	37.89	-73.0	207.1	
8.47	74.29	44.54	37.89	
38.04	37.89	-73.0	207.1	
84.54	74.29	6.47	37.89	
44.5	15.89	-73.0	127.1	
91.0	96.28	2.0	15.89	

Gp. 29 - (Box 2, Surface 4)  
4

Gps. 30 and 31				
23.25	11.0	-226.0	1023.0	
23.25	101.17	69.75	11.0	
23.25	33.0	-226.0	1023.0	
23.25	79.17	69.75	33.0	
-23.25	33.0	-226.0	1023.0	
69.75	79.17	23.25	33.0	
-23.25	11.0	-226.0	1023.0	
69.75	101.17	23.25	11.0	

Gp. 29 - (Box 3, Surface 5)  
4

Gps. 30 and 31				
44.65	30.0	-149.5	566.87	
BLANK CARD				
0.0	30.0	-73.73	466.47	
BLANK CARD				
-44.65	30.0	-149.5	566.87	
BLANK CARD				
0.0	30.0	-225.24	466.47	
BLANK CARD				

Gp. 29 - (Box 2, Surface 6)  
1

Gps. 30 and 31  
0.0  
BLANK CARD

Gp. 29 - (Box 3, Surface 1)

6

Gps. 30 and 31			
42.80	61.04	-149.87	1614.49
118.42	51.13	23.55	61.04
42.80	61.04	-143.50	1614.49
71.05	51.13	71.05	61.04
42.80	61.04	-112.15	1614.49
23.68	51.13	113.42	61.04
42.80	95.13	-102.15	1614.49
23.68	17.04	113.42	95.13
42.80	95.13	-149.50	1614.49
71.05	17.04	71.05	95.13
42.80	95.13	-136.87	1614.49
118.42	17.04	23.55	95.13

Gp. 29 - (Box 3, Surface 3)

Gps. 30 and 31			
36.18	74.09	-13.45	901.55
78.96	34.08	5.02	74.09
0.0	80.80	-73.45	3711.04
42.80	31.37	42.30	89.90
-36.18	79.09	-73.45	901.55
6.62	34.06	76.38	78.09

Gp. 29 - (Box 3, Surface 4)

Gps. 30 and 31			
-21.40	61.04	-229.55	1458.67
64.19	51.13	21.40	61.04
21.40	61.04	-220.55	1458.67

21.40	51.13	64.19	61.04
21.40	95.13	-220.55	1458.67
21.40	17.04	64.19	95.13
-21.40	95.13	-220.55	1458.67
64.19	17.04	21.40	95.13

Gp. 29 - (Box 3, Surface 5)  
<sub>1</sub>

Gps. 30 and 31  
<sub>0.0</sub> 112.17 -149.5 12162.34  
 BLANK CARD

Gp. 29 - (Box 3, Surface 6)  
<sub>0</sub>

Gp. 32 - Code for controlling iteration  
<sub>0</sub> 1

Gp. 33 - Blast data (psi, degrees, KT, feet)  
<sub>1.</sub> 0. 0. 0.  
 BLANK CARD  
 END

APPENDIX D

INPUT DATA LIST FOR TRUCK CODE  
M38A1 JEEP

Gp. 1 - Identification  
**438A1 JEEP**

Gp. 2 - Vehicle type  
**0**

Gp. 3 - Configuration data

0	0	0	0
---	---	---	---

Gp. 4 - No. of tires on left end of each axle  

1	1
---	---

Gp. 5 - No. of springs on left side of each axle  

2	2
---	---

Gp. 7 - Masses and their locations ( $\text{lbs-sec}^2/\text{in, inches}$ )

4.54	0.0	11.37	-32.22
0.98	0.0	0.07	0.08
1.00	0.0	1.03	-80.86

Gp. 8 - Product of inertia of mass 1 ( $\text{lbs-in-sec}^2$ )  
**20.46**

Gp. 9 - Mass moments of inertia ( $\text{lbs-in-sec}^2$ )

18908.	10908.	1119.
0.0	515.8	515.8
0.0	555.2	555.2

Gp. 10 - Attachment points for axle springs (inches)

12.5	1.25	0.0	12.5	0.0
15.0	9.5	6.5	15.0	2.0
12.5	1.5	-21.0	12.5	-4.0
15.0	10.0	-70.5	15.0	-81.0

Gps. 11 and 12 - Coordinates of axles and wheels (inches)

0.0	0.0	0.0
24.56		
0.0		-81.0
24.6		

Gp. 18 - Non-linear damping force-velocity curves (lbs, in/sec)

	5	5	5	5	5	5
-10000.	10014.	-55.0	19.0	0.0	0.0	0.0
5.0	-38.0	10000.	-12531.			
-10000.	40055.	-55.0	75.	0.0	0.0	0.0
5.0	-150.	10000.	-50125.			
-10000.	8766.	-10.	25.	0.0	0.0	0.0
10.0	-38.	10000.	-12525.			
-10000.	35065.	-10.	100.	0.0	0.0	0.0
10.	-150.	10000.	-50100.			

Gp. 19 - Tire damping coefficients (lbs-sec/in)

	4	4	4	4	4	4
-3.5	976.0	-125	100.	0.0	0.0	0.0
100.	-10000.					
2						
-100.	0.0	100.	0.0			
5						
-6.74	1929.	-3.0	732.	-1114	110.	
0.0	0.0	100.0	-900.0			
2						
-100.	0.0	100.	0.0			

Gp. 21 - Tire non-linear force-normal displacement data (lbs, inches)

	3	3	3	3	3	3
-8.5	15960.	-125	47.5	0.0	0.0	0.0

Gp. 22 - Tire non-linear force-tangential displacement data (lbs, inches)

	3	3	3	3	3	3
0.0	0.0	125	10.75	10.0	10.0	10.0

Gp. 23 - Tire and gravity data (inches, in/sec<sup>2</sup>)

	2	2	2	2	2	2
15.0	1000.	545.0	1000.	545.0	1000.	545.0

Gp. 24 - Ground slope data (radians, inches)  
0.0 0.0 1.009.

Gp. 25 - Response time and integration time step (seconds)  
1.0 0.005 .0005

Gp. 26 - No. of time steps between printouts  
50

Gp. 27 - No. of rectangular boxes in aerodynamic model  
4

Gp. 28 - Code designating type of box  
1 1 1

Gp. 29 - No. of aerodynamic load points on surface (Box 1, Surface 1)  
4

Gps. 30 and 31 - Loading information (inches, in<sup>2</sup>)  
30.44 8.19 33 426.55  
13.01 24.59 39.04 8.19  
30.44 24.59 33 426.55  
13.01 8.19 39.04 24.59  
30.44 24.59 25.70 426.55  
39.04 8.19 13.01 24.59  
30.44 8.19 25.70 426.55  
39.04 24.59 13.01 8.19

Gp. 29 - (Box 1, Surface 3)  
2

Gps. 30 and 31  
-15.22 16.39 13.54 997.82  
15.22 16.39 12.65 16.39  
15.22 16.39 15.54 997.82  
45.66 16.39 15.22 16.39

Gp. 29 - (Box 1, Surface 4)  
2

Gps. 30 and 31				
15.22	16.39	-36.71	997.82	
15.22	16.39	45.66	16.39	
-15.22	16.39	-38.71	997.82	
45.66	16.39	15.22	16.39	

Gp. 29 - (Box 1, Surface 5)  
1

Gps. 30 and 31				
0.0	32.78	-12.69	3168.8	
BLANK CARD				

Gp. 29 - (Box 1, Surface 6)  
1

Gps. 30 and 31				
0.0	0.0	-12.69	3168.8	
BLANK CARD				

Gp. 29 - (Box 2, Surface 1)  
1

Gps. 30 and 31				
30.44	6.72	-44.28	284.12	
10.57	6.72	10.57	6.72	

Gp. 29 - (Box 2, Surface 3)  
0

Gp. 29 - (Box 2, Surface 4)  
0

Gp. 29 - (Box 2, Surface 5)  
1

Gps. 30 and 31				
0.0	0.0	-44.28	1287.	
BLANK CARD				

Gp. 29 - (Box 2, Surface 6)

1

Gps. 30 and 31  
0.0 0.0

BLANK CARD

1287.

Gp. 29 - (Box 3, Surface 1)

4

Gps. 30 and 31			
30.44	6.56	-73.43	356.13
15.58	19.67	40.75	6.56
30.44	19.67	-73.43	356.13
15.58	6.56	40.75	19.67
30.44	19.67	-100.64	356.13
40.75	6.56	13.58	19.67
30.44	6.56	-100.64	356.13
40.75	19.67	13.58	6.56

Gp. 29 - (Box 3, Surface 3)

2

Gps. 30 and 31			
-15.22	13.11	-59.95	798.13
15.22	13.11	42.66	13.11
15.22	13.11	-39.95	798.13
45.66	13.11	13.22	13.11

Gp. 29 - (Box 3, Surface 4)

3

Gps. 30 and 31			
21.65	13.11	-114.18	450.72
8.60	13.11	32.28	13.11
0.0	6.49	-114.18	343.71
30.44	19.75	59.44	6.49
-21.45	13.11	-114.18	450.72
52.29	13.11	5.00	13.11

Gp. 29 - (Box 3, Surface 5)  
1

Gps. 30 and 31  
0.0 0.0  
BLANK CARD

Gp. 29 - (Box 3, Surface 6)  
1

Gps. 30 and 31  
0.0 0.0  
BLANK CARD

Gp. 29 - (Box 4, Surface 1)  
2

Gps. 30 and 31  
13.25 32.85  
3.12 6.65  
13.25 19.59  
7.32 19.86

Gp. 29 - (Box 4, Surface 3)  
1

Gps. 30 and 31  
0.0 32.65  
13.25 6.63

Gp. 29 - (Box 4, Surface 4)  
1

Gps. 30 and 31  
0.0 26.22  
13.25 13.25

Gp. 29 - (Box 4, Surface 5)  
1

Gps. 30 and 31  
0.0 39.47 -117.30 165.10  
BLANK CARD

Gp. 29 - (Box 4, Surface 6)  
1

Gps. 30 and 31  
0.0 12.97 -117.30 165.10  
BLANK CARD

Gp. 32 - Code for controlling iteration  
0 1

Gp. 33 - Blast data (psi, degrees, KT, feet)  
1.0 0.0 0.0 0.0 1.0 4250.  
BLANK CARD  
END

APPENDIX E

INPUT DATA LIST FOR TRUCK CODE  
M35A2 TRUCK, LOADED, WITHOUT CANVAS

Gp. 1 - Identification  
**M35A2 WITH CANVAS TUP BUT LOADED WITH CURRENT BLOCKS**

Gp. 2 - Vehicle type  
**0**

Gp. 3 - Configuration data  
**0 0 0 0 0 0 0 0**

Gp. 4 - No. of tires on left end of each axle  
**1 2 2**

Gp. 5 - No. of springs on left side of each axle  
**1 2 1**

Gp. 7 - Masses and their locations (lbs-sec<sup>2</sup>/in, inches)

33.16	0.0	26.42	-100.16
3.705	0.0	1.0	0.0
4.483	0.6	0.0	-130.0
4.483	0.0	0.7	-178.0

Gp. 8 - Product of inertia of mass 1 (lbs-in-sec<sup>2</sup>)  
**-11020.**

Gp. 9 - Mass moments of inertia (lbs-in-sec<sup>2</sup>)

193600.	196600.	19160.
312.0	2952.0	2844.0
93.26	3381.0	3960.0
93.26	3381.0	3960.0

Gp. 10 - Attachment points for axle springs (inches)

15.4	10.8	9.0	15.4	5.6	0.6
15.4	11.19	-10.76	15.4	-1.4	-3.24
20.24	5.0	-1.59.0	20.24	0.0	-130.0
20.24	5.0	-178.0	20.24	0.0	-178.0

Gps. 11 and 12 - Coordinates of axles and wheels (inches)

0.0	0.0	0.0
33.875		-130.0
0.0		40.75
23.266		

0.0	-178.0
29.266	40.75

Gp. 13 - Attachment points for bogie springs

2 20.24

Gp. 18 - Non-linear damping force-velocity curves (lbs, in/sec)

3	0.0	0.0	10000.	-82000.
3	42000.	0.0	0.0	-32000.
168000.	0.0	0.0	10000.	
2	10000.	0.0	0.0	
2	0.0	10000.	0.0	
2	0.0	10000.	0.0	
3	84000.	0.0	10000.	-164000.

Gp. 19 - Tire damping coefficients (lbs-sec/in)

2.4b 2.48

Gp. 20 - Non-linear spring force-displacement curves (lbs, inches)

5	6243.	0.0	0.0	100.	-100700.
2	0.0	100.	0.0		
2	0.0	100.	0.0		
2	0.0	100.	0.0		
3	1161.	0.0	0.0	100.	-115500.

Gp. 21 - Tire non-linear force-normal displacement data (lbs, inches)

3	26900.	-0.125	80.0	0.0	0.0
---	--------	--------	------	-----	-----

Gp. 22 - Tire non-linear force-tangential displacement data (lbs, inches)

3	0.0	-125	52.5	10.0	17700.
---	-----	------	------	------	--------

Gp. 23 - Tire and gravity data (inches, in/sec<sup>2</sup>)  
 20.575 0.8 545.0

Gp. 24 - Ground slope data (radians, inches)  
 0.4 0.0 100.0

Gp. 25 - Response time and integration time step (seconds)  
 1.5 .001

Gp. 26 - No. of time steps between printouts  
 25

Gp. 27 - No. of rectangular boxes in aerodynamic model  
 3

Gp. 28 - Code designating type of box  
 1 1

Gp. 29 - No. of aerodynamic load points on surface (Box 1, Surface 1)  
 4

Gps. 30 and 31 - Loading information (inches, in<sup>2</sup>)  
 29.57 12.36 8.06 1285.9  
 26.02 37.07 73.06 12.36  
 29.57 37.07 5.06 1285.9  
 26.02 12.36 78.06 57.07  
 29.57 37.07 -43.98 1285.9  
 78.06 12.36 26.02 37.07  
 29.57 12.36 -3.93 1285.9  
 78.06 37.07 26.02 12.36

Gp. 29 - (Box 1, Surface 3)  
 4

Gps. 30 and 31  
 21.25 15.89 34.09 1350.2  
 63.75 33.54 17.93 15.89  
 -21.25 15.89 34.09 1350.2  
 17.93 33.54 05.75 15.89

-14.79	40.60	34.98	521.9
14.79	8.83	44.36	40.59
14.79	40.60	34.08	521.9
44.36	9.83	14.79	40.59

Gp. 29 - (Box 1, Surface 4)  
1

Gps. 30 and 31	4.71	-70.0	96.17
0.0	2.71	29.57	46.71
29.57			

Gp. 29 - (Box 1, Surface 5)  
1

Gps. 30 and 31	49.42	-17.95	8846.8
0.0	BLANK CARD		

Gp. 29 - (Box 1, Surface 6)  
1

Gps. 30 and 31	0.0	-17.96	8846.8
0.0	BLANK CARD		

Gp. 29 - (Box 2, Surface 1)  
6

Gps. 30 and 31	11.0	-200.5	1122.0
46.5	33.0	25.5	11.0
127.5	11.0	-149.5	1122.0
46.5	33.0	76.5	11.0
76.5	11.0	-98.5	1122.0
46.5	33.0	127.5	11.0
25.5	33.0	-98.5	1122.0
46.5	11.0	127.5	33.0
25.5	33.0	-149.5	1122.0
46.5	11.0	76.5	33.0
76.5	33.0	-98.5	1122.0

46.5	33.0	-2109.5	1122.0
127.5	11.0	25.5	33.0

Gp. 29 - (Box 2, Surface 3)

Gps. 30 and 31			
-44.5	15.89	-73.0	127.1
2.0	28.11	91.0	15.89
-38.04	37.69	-75.0	207.1
6.47	6.12	44.54	57.89
38.04	37.69	-75.0	207.1
84.54	6.12	3.47	37.89
44.7	15.89	-73.0	127.1
91.0	26.11	2.0	15.89

Gp. 29 - (Box 2, Surface 4)

Gps. 30 and 31			
23.25	11.0	-226.0	1023.0
23.25	33.0	69.75	11.0
23.25	33.0	-226.0	1023.0
23.25	11.0	69.75	33.0
-23.25	33.0	-226.0	1023.0
69.75	11.0	23.25	33.0
-23.25	11.0	-226.0	1023.0
69.75	33.0	23.25	11.0

Gp. 29 - (Box 2, Surface 5)

Gps. 30 and 31			
0.0	30.0	-149.5	14229.0
BLANK CARD			
Gp. 29 - (Box 2, Surface 6)			
1			

Gps. 30 and 31  
0.0 0.0

BLANK CARD

Gp. 29 - (Box 3, Surface 1)  
6

Gps. 30 and 31				
46.5	49.63	-198.5	431.81	
122.5	2.20	24.5	0.73	
46.5	49.63	-149.5	431.81	
73.5	2.20	73.5	0.73	
46.5	49.63	-100.5	431.81	
24.5	2.20	122.5	0.73	
46.5	60.88	-100.5	431.81	
24.5	2.20	122.5	0.73	
46.5	60.88	-149.5	431.81	
73.5	2.20	73.5	0.73	
46.5	60.88	-198.5	431.81	
122.5	2.20	24.5	0.73	

Gp. 29 - (Box 3, Surface 3)  
3

Gps. 30 and 31				
36.04	55.25	-76.0	298.39	
84.54	2.20	8.47	0.73	
0.0	57.96	-76.0	617.91	
46.5	2.20	46.5	0.73	
-38.04	55.25	-76.0	298.39	
8.47	2.20	34.54	0.73	

Gp. 29 - (Box 3, Surface 4)  
4

Gps. 30 and 31				
-23.25	49.63	-72.0	409.78	
69.75	2.20	25.25	0.73	
23.25	49.63	-70.0	409.78	
23.25	2.20	59.75	0.75	
23.25	60.88	-76.0	409.78	

23.25 2.20 69.75 0.73  
-23.25 60.88 -76.0 409.78  
69.75 2.20 23.25 0.73

Gp. 29 - (Box 3, Surface 5)

Gp. 29 - (Box 3, Surface 6)

Gp. 32 - Code for controlling iteration

0 1

Gp. 33 - Blast data (psi, degrees, KR, feet)  
1. 0. 0.  
BLANK CARD  
END

4250.

1.

DISTRIBUTION LIST

<u>No. of Copies</u>	<u>Organization</u>	<u>No. of Copies</u>	<u>Organization</u>
12	<p>Commander            Defense Technical Info Center            ATTN: DDC-DDA            Cameron Station            Alexandria, VA 22314</p>	1	<p>Director            Weapons Systems Evaluation Gp            ATTN: Document Control            Washington, DC 20305</p>
4	<p>Director of Defense            Research and Engineering            ATTN: DD/TWP            DD/S&amp;SS            DD/I&amp;SS            AD/SW            Washington, DC 20301</p>	1	<p>Director            National Security Agency            ATTN: E.F. Butala, R15            Ft. George G. Meade, MD 20755</p>
2	<p>Asst to the Secretary of            Defense (Atomic Energy)            ATTN: Document Control            Donald R. Cotter            Washington, DC 20301</p>	3	<p>Director            Joint Strategic Target            Planning Staff JCS            ATTN: Sci &amp; Tech Info Lib            JLTW-2            DOXT            Offut AFB            Omaha, NM 68113</p>
3	<p>Director            Defense Advanced Research            Projects Agency            ATTN: Tech Lib            NMRO            PMO            1400 Wilson Boulevard            Arlington, VA 22209</p>	1	<p>Director            Defense Communications Agency            ATTN: Code 930            Washington, DC 20305</p>
2	<p>Director            Defense Civil Preparedness            Agency            ATTN: Mr. George Sisson/RF-SR            Technical Library            Washington, DC 20301</p>	5	<p>Director  <del>Defense Nuclear Agency</del>  <del>ATTN: STSI/Archives</del>  <del>SPAS/Mr. J. Moulton</del>  <del>STSP</del>  <del>STVL/Dr. La Vier</del>  <del>RATN</del>            Washington, DC 20305</p>
4	<p>Director            Defense Intelligence Agency            ATTN: DT-1B            DB-4C/E. O. Farrell            DT-2/Wpns &amp; Sys Div            RDS-3A4            Washington, DC 20301</p>	6	<p>Director            Defense Nuclear Agency            ATTN: DDST/Dr. Conrad            DDST/Dr. Oswald            STTL/Tech Lib (2 cys)            SPSS (2 cys)            Washington, DC 20305</p>
		2	<p>Commander            Field Command, DNA            ATTN: FCPR            PCTMOF            Kirtland AFB, NM 87115</p>

DISTRIBUTION LIST

<u>No. of Copies</u>	<u>Organization</u>	<u>No. of Copies</u>	<u>Organization</u>
1	Commander Field Command, DNA Livermore Branch ATTN: FCPRL P.O. Box 808 Livermore, CA 94550	2	Office, Chief of Engineers Department of the Army ATTN: DAEN-MCE-D DAEN-RDM 890 South Pickett Street Alexandria, VA 22304
1	Director Institute for Defense Analyses ATTN: IDA Librarian, Ruth S. Smith 400 Army-Navy Drive Arlington, VA 22202	1	Commander US Army Engineering Center ATTN: ATSEN-SY-L Fort Belvoir, VA 22060
1	HQDA (DAMA-AR; NCL Div) Washington, DC 20310	1	Division Engineer US Army Engineering Division ATTN: HNDSB-R/M. M. Dembo Huntsville Box 1600 Huntsville, AL 35804
1	Program Manager US Army BMD Program Office ATTN: John Shea Alexandria, VA 22333	1	Division Engineer US Army Engineering Division Ohio River ATTN: Docu Cen P.O. Box 1159 Cincinnati, OH 45201
2	Director US Army BMD Advanced Technology Center ATTN: CRDABH-X CRDABH-S Huntsville, AL 35807	5	Commander US Army Engineer Waterways Experiment Station ATTN: Technical Library William Flathau John N. Strange Guy Jackson Leo Ingram P.O. Box 631 Vicksburg, MS 39180
1	Commander US Army BMD System Command ATTN: BDMSC-TFN/N.J. Hurst P.O. Box 1500 Huntsville, AL 35807	1	Commander US Army Materiel Development and Readiness Command ATTN: DRCDMD-ST 5001 Eisenhower Avenue Alexandria, VA 22333
2	Deputy Chief of Staff for Operations and Plans ATTN: Technical Library Director of Chemical and Nuclear Operations Department of the Army Washington, DC 20310		

DISTRIBUTION LIST

<u>No. of Copies</u>	<u>Organization</u>	<u>No. of Copies</u>	<u>Organization</u>
1	Commander US Army Materiel Development and Readiness Command ATTN: Technical Library 5001 Eisenhower Avenue Alexandria, VA 22333	6	Commander US Army Electronics Research and Development Command ATTN: DELSD-L DELEW-E W.S. McAfee R. Frieberg DELSD-EI, J. Roma DELSD-EM A. Sigismondi C. Goldy Fort Monmouth, NJ 07703
3	Commander US Army Armament Research and Development Command ATTN: DRDAR-LCN-F, W. Reiner DRDAR-TSS (2 cys) Dover, NJ 07801	5	Commander US Army Harry Diamond Labs ATTN: Mr. James Gaul Mr. L. Belliveau Mr. J. Gwaltney Mr. F.N. Wimenitz Mr. Bill Vault 2800 Powder Mill Road Adelphi, MD 20783
1	Director US Army ARRADCOM Benet Weapons Laboratory ATTN: DRDAR-LCB-TL Watervliet, NY 12189	5	Commander US Army Harry Diamond Labs ATTN: DRXDO-TI DRXDO-TI/012 DRXDO-NP DRXDO-RBH/P. Caldwell DEIHD-RBA/J. Rosado 2800 Powder Mill Road Adelphi, MD 20783
1	Commander US Army Armament Materiel Readiness Command ATTN: DRSAR-LEP-L, Tech Lib Rock Island, IL 61299	3	Commander US Army Missile Command ATTN: DRDMI-R DRDMI-YDL Chief Scientist Redstone Arsenal, AL 35809
1	Commander US Army Aviation Research and Development Command ATTN: DRSAV-E P.O. Box 209 St. Louis, MO 63166	1	Commander US Army Natick Research and Development Command ATTN: DRXRE/Dr. D. Sieling DRXNM-UE, Arthur Johnson Natick, MA 01762
1	Director US Army Air Mobility Research and Development Laboratory Ames Research Center Moffett Field, CA 94035	2	
1	Commander US Army Communications Research and Development Command ATTN: DRDCO-PPA-SA Fort Monmouth, NJ 07703	2	

DISTRIBUTION LIST

<u>No. of Copies</u>	<u>Organization</u>	<u>No. of Copies</u>	<u>Organization</u>
1	Commander US Army Tank Automotive Rsch and Development Command ATTN: DRDTA-UL Warren, MI 48090	2	Director US Army TRADOC Systems Analysis Activity ATTN: LTC John Hesse ATAA-SL (Tech Lib) White Sands Missile Range, New Mexico 88002
1	Commander US Army Foreign Science and Technology Center ATTN: Rsch & Concepts Branch 220 7th Street, NE Charlottesville, VA 22901	1	Commander Combined Arms Combat Developments Activity ATTN: ATCA-CO/Mr. L.C. Pleger Fort Leavenworth, KS 66027
1	Commander US Army Logistical Center ATTN: ATCL-SCA Mr. Robert Cameron Fort Lee, VA 23801	1	Chief of Naval Research ATTN: N. Perrone Department of the Navy Washington, DC 20360
3	Commander US Army Materials and Mechanics Research Center ATTN: Technical Library John Mescall Richard Shea Watertown, MA 02172	2	Chief of Naval Operations ATTN: OP-03EG OP-985F Department of the Navy Washington, DC 20350
2	Commander US Army Nuclear Agency ATTN: ACTA-NAW Technical Library 7500 Backlick Road, Bldg. 2073 Springfield, VA 22150	1	Chief of Naval Material ATTN: MAT 0323 Department of the Navy Arlington, VA 22217
1	Commander US Army Research Office P.O. Box 12211 Research Triangle Park NC 27709	3	Director Strategic Systems Projects Ofc ATTN: NSP-43, Tech Lib NSP-273 NSP-272 Department of the Navy Washington, DC 20360
1	Commander USA Training & Doctrine Command ATTN: ATCD-SA/Mr. Oscar Wells Fort Monroe, VA 23351	1	Commander Naval Electronic Systems Command ATTN: PME 117-21A Washington, DC 20360

DISTRIBUTION LIST

<u>No. of Copies</u>	<u>Organization</u>	<u>No. of Copies</u>	<u>Organization</u>
3	<p>Commander Naval Facilities Engineering Command ATTN: Code 03A Code 04B Technical Library Washington, DC 20360</p>	3	<p>Commander Naval Surface Weapons Center ATTN: Code W501/Navy Nuclear Programs Office Code WX21/Tech Lib Code 240/C.J. Aronson Silver Spring, MD 20910</p>
2	<p>Commander Naval Sea Systems Command ATTN: ORD-91313 Library Code 03511 Department of the Navy Washington, DC 20362</p>	2	<p>Commander Naval Weapons Center ATTN: Code 533/Tech Lib Code 40701/M. Keith China Lake, CA 94555</p>
4	<p>Officer-in-Charge Civil Engineering Laboratory Naval Constr Ptn Ctr ATTN: Stan Takahashi R.J. Odello John Crawford Technical Library Port Hueneme, CA 93041</p>	2	<p>Commander Naval Ship Research and Development Center Facility Underwater Explosions Research Division ATTN: Code 17/W.W. Murray Technical Library Portsmouth, VA 23709</p>
2	<p>Commander Naval Ship Engineering Center ATTN: Technical Library NSEC 6105G Hyattsville, MD 20782</p>	2	<p>Commander Naval Weapons Evaluation Facility ATTN: Document Control R. Hughes Kirtland AFB Albuquerque, NM 87117</p>
1	<p>Commander David W. Taylor Naval Ship Research &amp; Development Center ATTN: Lib Div, Code 522 Bethesda, MD 20084</p>	2	<p>Commander Naval Research Laboratory ATTN: Code 2027/Tech Lib Code 8440/F. Rosenthal Washington, DC 20375</p>
1	<p>Commander Naval Surface Weapons Center ATTN: DX-21, Library Br. Dahlgren, VA 22448</p>	1	<p>Superintendent Naval Postgraduate School ATTN: Code 2124/Tech Rpts Lib Monterey, CA 93940</p>
		1	<p>HQ USAF (IN) Washington, DC 20330</p>

DISTRIBUTION LIST

<u>No. of Copies</u>	<u>Organization</u>	<u>No. of Copies</u>	<u>Organization</u>
1	HQ USAF (PRE) Washington, DC 20330	1	PTD (TD-BTA/Lib) Wright-Patterson AFB Ohio 45433
2	AFSC (DLCAW; Tech Lib) Andrews AFB Washington, DC 20331	1	AFIT (Lib Bldg. 640, Area B) Wright-Patterson AFB Ohio 45433
2	AFATL (DLYV, P. Nash) Eglin AFB, FL 32542	1	Director US Bureau of Mines ATTN: Technical Library Denver Federal Center Denver, CO 80225
1	AFATL (DLYV, Jim Flint) Eglin AFB, FL 32542		
2	ADTC (ADBRL-2; Tech Lib) Eglin AFB, FL 32542	1	Director US Bureau of Mines Twin Cities Research Center ATTN: Technical Library P.O. Box 1660 Minneapolis, MN 55111
2	RADC (EMTLD/Docu Lib; EMREC/ R.W. Mair) Griffis AFB, NY 13440		
1	AFWL/DE-I Kirtland AFB, NM 87117	1	US Energy Research and Development Administration Albuquerque Operations Office ATTN: Doc Control for Tech Lib P.O. Box 5400 Albuquerque, NM 87115
1	AFWL/DEX Kirtland AFB, NM 87117		
1	AFWL/SUL Jimmie L. Bratton Kirtland AFB, NM 87117	1	US Energy Research and Development Administration Nevada Operations Office ATTN: Doc Control for Tech Lib P.O. Box 14100 Las Vegas, NV 89114
1	AFWL/R. Henny Kirtland AFB, NM 87117		
1	AFWL/SUL M.A. Piiamondon Kirtland AFB, NM 87117	1	Director Lawrence Livermore Laboratory ATTN: L.W. Woodruff/L-96 P.O. Box 808 Livermore, CA 94550
1	Interservice Nuclear Weapons School ATTN: Technical Library Kirtland AFB, NM 87115		
2	Commander-in-Chief Strategic Air Command ATTN: NRI-STINFO Lib XPPS Offutt AFB, NB 68113	1	Director Lawrence Livermore Laboratory ATTN: Jack Kahn/L-7 P.O. Box 808 Livermore, CA 94550

DISTRIBUTION LIST

<u>No. of Copies</u>	<u>Organization</u>	<u>No. of Copies</u>	<u>Organization</u>
1	Director Lawrence Livermore Laboratory ATTN: Tech Info Dept L-3 P.O. Box 808 Livermore, CA 94550	6	Sandia Laboratories ATTN: Doc Control for 3141 Sandia Rpt Collection A.M. Chaban M.L. Merritt L.J. Vortman W. Roherty L. Hill Albuquerque, NM 87115
1	Director Lawrence Livermore Laboratory ATTN: R.G. Dong/L-90 P.O. Box 808 Livermore, CA 94550	1	Sandia Laboratories Livermore Laboratory ATTN: Doc Control for Tech Lib P.O. Box 969 Livermore, CA 94550
1	Director Lawrence Livermore Laboratory ATTN: Ted Butkovich/L-200 P.O. Box 808 Livermore, CA 94550	1	Director National Aeronautics and Space Administration Scientific and Technical Information Facility P.O. Box 8757 Baltimore/Washington International Airport, MD 21240
1	Director Lawrence Livermore Laboratory ATTN: Robert Schock/L-437 P.O. Box 808 Livermore, CA 94550	3	Aerospace Corporation ATTN: Tech Info Services (2 cys) P.N. Mathur P.O. Box 92957 Los Angeles, CA 90009
1	Director Lawrence Livermore Laboratory ATTN: J.R. Hearst/L-205 P.O. Box 808 Livermore, CA 94550	1	Agbabian Associates ATTN: M. Agbabian 250 North Nash Street El Segundo, CA 90245
4	Director Los Alamos Scientific Laboratory ATTN: Doc Control for Rpts Lib R.A. Gentry G.R. Spillman Al Davis P.O. Box 1663 Los Alamos, NM 87544	1	Applied Theory, Inc. ATTN: John G. Trulio 1010 Westwood Blvd. Los Angeles, CA 90024
		1	Artec Associates, Inc. ATTN: Steven Gill 26046 Eden Landing Road Hayward, CA 94545

DISTRIBUTION LIST

<u>No. of Copies</u>	<u>Organization</u>	<u>No. of Copies</u>	<u>Organization</u>
1	AVCO ATTN: Res Lib A830, Rm 7201 201 Lowell Street Wilmington, MA 01887	1	The Franklin Institute ATTN: Zemons Zudans 20th Street and Parkway Philadelphia, PA 19103
1	The BDM Corporation ATTN: Richard Hensley P.O. Box 9274 Albuquerque International Albuquerque, NM 87119	1	General American Trans Corporation General American Research Division ATTN: G.L. Neidhardt 7449 N. Natchez Avenue Niles, IL 60648
2	The Boeing Company ATTN: Aerospace Library R.H. Carlson P.O. Box 3707 Seattle, WA 98124	1	General Electric Company-TEMPO ATTN: DASIAC P.O. Drawer QQ Santa Barbara, CA 93102
1	Brown Engineering Co., Inc. ATTN: Manu Patel Cummings Research Park Huntsville, AL 35807	1	General Electric-TEMPO ATTN: E. Bryant 220 S. Main Street, Rm 206 Bel Air, MD 21014
2	California Research and Technology, Inc. ATTN: Ken Kreyenhagen Technical Library 6269 Variel Avenue Woodland Hills, CA 91364	2	Hazeltine Corp. ATTN: Cai' Meinen Greenlawn, NY 11740
1	Calspan Corporation ATTN: Technical Library P.O. Box 235 Buffalo, NY 14221	1	J.H. Wiggins Co., Inc. ATTN: John Collins 1650 South Pacific Coast Highway Redondo Beach, CA 90277
1	Civil/Nuclear Systems Corporations ATTN: Robert Crawford 1200 University N.E. Albuquerque, NM 87102	5	Kaman Avidyne ATTN: Dr. N.P. Hobbs (4 cys) Mr. S. Criscione 83 Second Avenue Northwest Industrial Park Burlington, MA 01830
1	EG&G, Incorporated Albuquerque Division ATTN: Technical Library P.O. Box 10218 Albuquerque, NM 87114	3	Kaman Sciences Corporation ATTN: Library P.A. Ellis F.H. Shelton 150C Garden of the Gods Road Colorado Springs, CO 80907

DISTRIBUTION LIST

<u>No. of Copies</u>	<u>Organization</u>	<u>No. of Copies</u>	<u>Organization</u>
1	Lockheed Missiles & Space Co. ATTN: Technical Library P.O. Box 504 Sunnyvale, CA 94088	2	Pacifica Technology ATTN: G. Kent R. Bjork P.O. Box 148 Del Mar, CA 92014
2	Martin Marietta Aerospace Orlando Division ATTN: G. Fotieo Mail Point 505, Craig Luongo P.O. Box 5837 Orlando, FL 32805	4	Physics International Corp. ATTN: B.T. Moore Dennis Orphal Coye Vincent F.M. Sauer 2700 Merced Street San Leandro, CA 94577
3	McDonnell Douglas Astronautics Corporation ATTN: Robert W. Halprin Mr. C. Gardiner Dr. P. Lewis 5301 Bolsa Avenue Huntington Beach, CA 92647	4	Physics International Corp. ATTN: Robert Swift Charles Godfrey Larry A. Behrman Technical Library 2700 Merced Street San Leandro, CA 94577
2	Merritt Cases, Inc. ATTN: J.L. Merritt Technical Library P.O. Box 1206 Redlands, CA 92373	1	Radkowski Associates ATTN: Peter P. Radkowski P.O. Box 5474
1	Meteorology Research, Inc. ATTN: W.D. Green 454 West Woodbury Road Altadena, CA 91001	2	R&D Associates ATTN: Dr. Albert L. Latter William B. Wright P.O. Box 9695 Marina del Rey, CA 90291
1	The Mitre Corporation ATTN: Library P.O. Box 208 Bedford, MA 01730	4	R&D Associates ATTN: Jerry Carpenter Sheldon Schuster J.G. Lewis Technical Library P.O. Box 9695 Marina del Rey, CA 90291
1	Pacific Sierra Research Corp ATTN: Dr. Harold Brode 1456 Cloverfield Boulevard Santa Monica, CA 90404	1	R&D Associates ATTN: Henry Cooper Suite 500 1401 Wilson Boulevard Arlington, VA 22209

DISTRIBUTION LIST

<u>No. of Copies</u>	<u>Organization</u>	<u>No. of Copies</u>	<u>Organization</u>
1	The Rand Corporation ATTN: C.C. Mow 1700 Main Street Santa Monica, CA 90406	1	TRW Systems Group ATTN: Greg Hulcher San Bernardino Operations P.O. Box 1310 San Bernardino, CA 92402
1	Science Applications, Inc. 2450 Washington Avenue Suite 120 San Leandro, CA 94577	2	Union Carbide Corporation Holifield National Laboratory ATTN: Doc Control for Tech Lib Civil Defense Research Proj P.O. Box X Oak Ridge, TN 37830
2	Science Applications, Inc. ATTN: Technical Library Michael McKay P.O. Box 2351 La Jolla, CA 92038	1	Universal Analytics, Inc. ATTN: E.I. Field 7740 W. Manchester Blvd. Playa del Rey, CA 90291
4	Systems, Science & Software ATTN: Donald R. Grine Ted Cherry Thomas D. Riney Technical Library P.O. Box 1620 La Jolla, CA 92037	1	Weidlinger Assoc. Consulting Engineers ATTN: M.L. Baron 110 East 59th Street New York, NY 10022
3	Terra Tek, Inc. ATTN: Sidney Green A.H. Jones Technical Library 420 Wakara Way Salt Lake City, UT 84108	1	Westinghouse Electric Company Marine Division ATTN: W.A. Voltz Hendy Avenue Sunnyvale, CA 94008
2	Terra Tech, Inc. ATTN: Li-San Hwang Technical Library 630 North Rosemead Blvd. Pasadena, CA 91107	2	Battelle Memorial Institute ATTN: Technical Library R.W. Klingesmith 505 King Avenue Columbus, OH 43201
7	TRW Systems Group ATTN: Paul Lieberman Benjamin Sussholtz Norm Lipner William Rowan Jack Farrell Pravin Bhutta Tech Info Ctr/S-1930 One Space Park Redondo Beach, CA 92078	1	California Institute of Technology ATTN: T.J. Ahrens 1201 E. California Blvd. Pasadena, CA 91109
		2	Denver Research Institute University of Denver ATTN: Mr. J. Wisotski Technical Library P.O. Box 10127 Denver, CO 80210

DISTRIBUTION LIST

<u>No. of Copies</u>	<u>Organization</u>	<u>No. of Copies</u>	<u>Organization</u>
3	IIT Research Institute ATTN: Milton R. Johnson R.E. Welch Technical Library 10 West 35th Street Chicago, IL 60616	1	University of Illinois Consulting Engineering Services ATTN: Nathan M. Newmark 1211 Civil Engineering Building Urbana, IL 61801
2	Lovelace Foundation for Medical Education ATTN: Asst. Dir of Research/ Robert K. Jones Technical Library P.O. Box 5890 Albuquerque, NM 87115	2	The University of New Mexico The Eric H. Wang Civil Engineering Research Facility ATTN: Larry Bickle Neal Baum University Station Box 188 Albuquerque, NM 87131
1	Massachusetts Institute of Technology Aeroelastic and Structures Research Laboratory ATTN: Dr. E.A. Witmer Cambridge, MA 02139	2	Washington State University Administration Office ATTN: Arthur Miles Hohorf George Duval Pullman, WA 99163
2	Southwest Research Institute ATTN: Dr. W.E. Baker A.B. Wenzel 8500 Culebra Road San Antonio, TX 78206	<u>Aberdeen Proving Ground</u>	
2	SRI International ATTN: Dr. G.R. Abrahamson Carl Peterson 333 Ravenswood Avenue Menlo Park, CA 94025	Dir, USAMSA ATTN: DRXSY-D DRXSY-MP, H. Cohen B. E. Cummings M. Reches	Cdr, USATECOM ATTN: DRSTE-T0-F
1	University of Dayton Industrial Security Super. KL-505 ATTN: H.F. Swift 300 College Park Avenue Dayton, OH 45409	Dir, Wpns Sys Concepts Team, Bldg. E3516, EA ATTN: DRDAR-ACW	Cmdt, USAOCGS ATTN: ATSL-CD-CS, LT C.E. Tate

### USER EVALUATION OF REPORT

Please take a few minutes to answer the questions below; tear out this sheet and return it to Director, US Army Ballistic Research Laboratory, ARRADCOM, ATTN: DRDAR-TSB, Aberdeen Proving Ground, Maryland 21005. Your comments will provide us with information for improving future reports.

1. BRL Report Number \_\_\_\_\_

2. Does this report satisfy a need? (Comment on purpose, related project, or other area of interest for which report will be used.)  
\_\_\_\_\_  
\_\_\_\_\_  
\_\_\_\_\_

3. How, specifically, is the report being used? (Information source, design data or procedure, management procedure, source of ideas, etc.)  
\_\_\_\_\_  
\_\_\_\_\_  
\_\_\_\_\_

4. Has the information in this report led to any quantitative savings as far as man-hours/contract dollars saved, operating costs avoided, efficiencies achieved, etc.? If so, please elaborate.  
\_\_\_\_\_  
\_\_\_\_\_  
\_\_\_\_\_

5. General Comments (Indicate what you think should be changed to make this report and future reports of this type more responsive to your needs, more usable, improve readability, etc.)  
\_\_\_\_\_  
\_\_\_\_\_  
\_\_\_\_\_

6. If you would like to be contacted by the personnel who prepared this report to raise specific questions or discuss the topic, please fill in the following information.

Name: \_\_\_\_\_

Telephone Number: \_\_\_\_\_

Organization Address: \_\_\_\_\_  
\_\_\_\_\_  
\_\_\_\_\_